THE ROLES OF *Ly108*, THE GENETIC SUSCEPTIBILITY LOCI *Sle3*, AND CXCR4/CXCL12 IN SYSTEMIC LUPUS ERYTHEMATOSUS

APPROVED BY SUPERVISORY COMMITTEE

Edward K. Wakeland, Ph.D

Chandra Mohan, M.D., Ph.D

Christopher Lu, M.D., Ph.D

Christoph Wuelfing, Ph.D

Nancy Olsen, M.D.

Michael Carroll, Ph.D

THE ROLES OF *Ly108*, THE GENETIC SUSCEPTIBILITY LOCI *Sle3*, AND CXCR4/CXCL12 IN SYSTEMIC LUPUS ERYTHEMATOSUS

by

ANDREW WANG

DISSERTATION

Presented to the Faculty of the Graduate School of Biomedical Sciences

The University of Texas Southwestern Medical Center at Dallas

In Partial Fulfillment of the Requirements

For the Degree of

DOCTOR OF PHILOSOPHY

The University of Texas Southwestern Medical Center at Dallas

Dallas, Texas

July, 2008

Acknowledgments

L'homme absurde dit oui et son effort n'aura plus de cesse. S'il y a un destin personnel, il n'y a point de destinée supérieure ou du moins il n'en est qu'une dont il juge qu'elle est fatale et méprisable. Pour le reste, il se sait le maitre de ses jours. La lutte elle-même vers les sommets suffit à remplir un cœur d'homme. Il faut imaginer Sisyphe heureux.

My path on the mountain was laid out by giants. My work would not have been possible without former Wakeland and Mohan personnel, on whose backs my work is built. These are Drs. Alice Chan, Nisha Limaye, Charles Nguyen, who, together, paved the road for my studies in Ly108 and the SLAM/CD2 family; Dr. Srividya Subramanian, who unlocked the mystery of TLR7; Drs. Kui Liu and Jiankun Zhu, who made key contributions in *Sle3*; and Dr. Yang Liu, who identified CXCR4 as a gene which warranted further study.

My progress was the boon of master sherpas and consummate team members. My Tenzing Norgays are Ward Wakeland and Chandra Mohan. Ward is my mentor and friend. With his erudite grasp of all things immunogenetic, his remarkable vision, and his fearlessness of the unknown, Ward granted me unlimited scientific freedom, gave me guidance through the many dark scientific and personal labyrinths, and has inspired me in my scientific, musical and mountaineering life. Chandra has been my guide, friend, and a steady hand on sometimes treacherous terrain. His masterful attention to both the bench and the bed is exceptional and instructive, and, indeed, it is to Chandra that I owe my first venture into translational research. He has been ever supportive and understanding of my various scientific and extra-scientific ventures. I thank them both deeply for their priceless mentorship and friendship over the years.

My assistant sherpas, my committee members, Drs. Chris Liu, Christoph Wuelfing, and Nancy Olsen, have been voices of invaluable counsel, and all to whom I am indebted. Last, but certainly not least of all, I thank all of my former master sherpas, Drs. Frank Arnett, Mike Brenner, Joel Taurog, Hidde Ploegh, and Mike Carroll, who taught me everything I knew prior to my Ph.D. years.

I thank my consummate team, the *sine qua non* of my work. Ferdicia Carr-Johnson and Li Li, the lab managers of the Wakeland and Mohan labs, respectively, are the people who turn the wheel of scientific industry. Dr. Jose Casco, the mouse colony manager, and his competent animal team, are the people who make work in mice possible. The Center for Immunology office staff, Karen Elison, Renee Gugino, Bettye Puryear, and Cathy Smith, are single-handedly responsible for the often under-appreciated massive logistical coordination which underlies our enormous scientific operations. I owe Angie Mobley and her team in Flow Cytometry core, who made possible my technique *du jour*, a deep gratitude. Drs. Joseph Zhou, Fangming Lin, Peter Igarashi and his consummate staff, and Borna Mehrad, are solely responsible for all of my work in the kidney. Dr. Quan Li and his staff at the Microarray Core made gene expression studies possible. I thank the Immunology Graduate Program, and specifically Karen Kazemzadeh, Dr. Nicolai van Oers, and Dr. David Farrar for the education, opportunities, and advice they have given me. I thank Katie Belobrajdic, Drs. Sunhee Hwang, Chandra Pasare, Kirthi Raman, and Felix Yarovinsky, Jennifer Young for insightful discussions and personal support.

I will take the longest moment for my fellow front-line mountaineers, musical pedagogues, my friends, and my family—those who have, in their own rights, *irreplaceably* and *irrevocably* fashioned me into who I am today.

The front-line mountaineers: Drs. Anna-Marie Fairhurst, John Scahtzle, Srividya Subramanian, Dr. Katalin Tus and family, and Jill Wescott.

My musical pedagogues: Emmanuel Borok, Fredell Lack, Robert Levin, Josephine McAndrews, Donald Weilerstein, and Patricia Zander.

My colleagues and friends in music, humanitarian endeavors, science, and medicine: Joanna Cartwright, Helen Chou, Oshri Hakak, Jessica Kinloch, Rebecca Racusin, Sean Rosario, and Tzu-Yuan Su.

I must take a special moment to acknowledge my friends and family in France. I thank deeply Dr. Frédéric Batteux and family who arranged the extraordinary opportunity to learn medicine at the Université de Paris Descartes at the hospitals of Cochin and St. Vincent de Paul. I thank all those who have participated in the CXCR4 project in the human there: Drs. Phillipe Guillpan and Frédéric Batteux and the flow-core director, Sandrine Chouzenoux. I thank my mentors in France, who have taught me medicine: Drs. Dominique Cabrol, Martin Chalemeau, Dominique Gendrel, Loic Guillevan, Phillipe Guillpan, Luc Mouthon, and Bernard Weill.

I thank deeply my friends in Paris, Geneva, and Dusseldorf: Drs. and future Drs. Astrid Petit de Bantel, Caroline Boge, Julia Caudron, Dan Goldstein, Lisa Haushofer, Niloufar Kavian, Celine Quach, Antoine Monsel, and Eimad Shotar.

I thank my families and friends in Sierra Leone, Tanzania, India, and Cambodia.

I thank Mt. Kilimanjaro, Mt. Blanc and *le Mur de la Mort* in Fountainbleau.

My family: Ann, Chia, and Jean.

Thank all of you. I have no other words that would be appropriate for such a journey as we have taken together.

I know now that mountains cannot be conquered—only climbed. I take respite in the glimmer of truth, the shred of beauty, the glimpse of humanity that is revealed, if only for a moment, if only as a memory, in our struggle to the heights. It should be enough to fill a man's heart.

Deum et animam scire cupio.

Andrew Wang

Paris, 18/07/2008

THE ROLES OF *Ly108*, THE GENETIC SUSCEPTIBILITY LOCI *Sle3*, AND CXCR4/CXCL12 IN SYSTEMIC LUPUS ERYTHEMATOSUS

Publication No._____

Andrew Wang

The University of Texas Southwestern Medical Center at Dallas, 2007

Supervising Professors: Edward K. Wakeland, Ph.D and Chandra Mohan, M.D. Ph.D

Ly108, in the NZM2410-derived *Sle1b* locus, was identified to play a key role in thymic selection. B6.*Sle1b* thymocytes displayed aberrant cell-surface Ly108 expression and decreased sensitivity to CD3-induced cell-death. Significant V-β usage was found in B6.*Sle1b* versus B6 thymocytes. Simultaneous administration of OVA and anti-Ly108 antibody led to complete protection of OVA-induced deletion in B6.*Sle1b*.OTII mice but not in B6.OTII controls. Significant differences between B6 and B6.*Sle1b* were found in the amount of Ly108 phosphorylation and subsequent SAP-binding. *Calm2* was found to be differentially expressed in B6.*Sle1b* thymocytes following Ly108 cross-linking.

B6.*Sle1b* thymocytes were shown to flux less calcium, as result of modulated intracellular stocks of calcium, and, be more arrested in G1-phase following Ly108 engagement compared to B6, leading to an overall reduction in thymic apoptosis. These data suggest that the autoimmune form of Ly108 impairs thymic tolerance by dampening CD3-signaling and disrupting a G1-S cell-cycle checkpoint.

Sle3, an NZM2410-derived susceptibility locus, mediates transition from benign to fatal autoimmunity. *Sle3* was mapped to two main sub-loci, *Sle3a* and *Sle3b*. *Sle3b* was mapped to a 3.4 Mb interval containing *Klf13*, which has a known role in regulating RANTES. We found that *Klf13* mRNA expression was significantly increased and that B6.*Sle3* macrophages secreted roughly 2-fold more RANTES compared to B6. Co-culture of B6.*Sle3* macrophages with blocking antibody to RANTES reversed the hyperactivation phenotype to B6 levels, indicating that increased RANTES secretion due to a genetic lesion in *Klf13* could be responsible for the hyperactivation of macrophages seen in B6.*Sle3*. Polymorphisms in *Klf13* were shown to be associated with human SLE.

A significant dysregulation of the CXCR4/CXCL12 axis was observed in multiple murine models of spontaneous lupus. Increased CXCR4 expression in lupus mice led to functional differences, including increased migration to positive CXCL12 gradients. Simultaneously, the ligand for CXCR4, CXCL12, was significantly upregulated in the nephritic kidneys. To assess the contribution of CXCR4/CXCL12 upregulation on lupus pathogenesis, mice were treated with a peptide antagonist of CXCR4. Both preventive and therapeutic administration of CXCR4 blockade resulted in reduced renal infiltration by inflammatory myeloid cells and prolonged survival. Finally, increased renal CXCL12 expression and increased immune-cell CXCR4 expression was also observed in human

SLE. These findings underscore the pathogenic role of CXCR4/CXCL12 in lupus nephritis and highlight this axis as a new and promising therapeutic target in this disease.

TABLE OF CONTENTS

Publications

Wang A, et al. CXCR4/CXCL12 dysregulation plays a pivotal role in murine lupus nephritis. J Immunol. Accepted with revision. 2007.

Wang A, et al. CXCR4/CXCL12 dysregulation plays a pivotal role in human lupus. In preparation. 2008.

Wang A, et al. Modification of Thymocyte Development by the Lupus Susceptibility Gene *Ly108*. J Ex Med. Accepted with revision. 2008.

Wang A, et al. A novel technique for renal leukocyte delineation and enumeration. In preparation. 2008.

Wang A, Mohan C. Identification of the Yaa lupus gene as a Tlr-7 gene duplication event. Future Rheumatology. 2006 Oct: 1(5): 563-565.

Wang A, Wakeland W, Mohan C. Genetic susceptibility to kidney disease as a consequence of systemic autoimmunity. In press. 2007.

Fairhurst AM, Hwang S, **Wang A**, Tian X, Boudreaux C, Zhou XJ, Casco J, Li QZ, Connolly JE, Wakeland EK. Yaa autoimmune phenotypes are conferred by overexpression of TLR7. Eur J Immunol. 2008 Jun 28; 38(7):1971-1978.

Fairhurst AM, Mathian A, Connoly JE, **Wang A**, Gray HF, George TA, Boudreaux C, Zhou XJ, Li QZ, Koutouzov S, Banchereau J, Wakeland EK . Systemic IFNa drives kidney nephritis in B6.Sle123 mice. Eur J Immunol. 2008 Jun 28; 38(7):1948-1960.

Subramanian S, Tus K, Li QZ, **Wang A**, Tian XH, Zhou J, Liang C, Bartov G, McDaniel LD, Zhou XJ, Schultz RA, Wakeland EK. A Tlr7 translocation accelerates systemic autoimmunity in murine lupus. Proc Natl Acad Sci U S A. 2006 Jun 27;103(26):9970-5.

Tran TM, Satumtira N, Dorris ML, May E, **Wang A**, Furuta E, Taurog JD. HLA-B27 in Transgenic Rats Forms Disulfide-Linked Heavy Chain Oligomers and Multimers that Bind to the Chaperone BiP. J. Immunol. 2004 Apr 15;172(8):5110-9.

Vallet C, Pons-Catalano C, Guedj R, Moulin F, Mandelcwajg A, Chalumeau M, Raymond J, Rozenberg F, Lebon P, **Wang A**, Gendrel D. Bocavirus is a Frequent Cause of Severe Asthma Exacerbation in Children. Submitted. 2008.

Zhou X, Tan FK, Reveille JD, Wallis D, Milewicz DM, Ahn C, **Wang A**, Arnett FC. Association of novel polymorphisms with the expression of SPARC in normal fibroblasts and with susceptibility to scleroderma. Arthritis Rheum. 2002 Nov: 46(11): 2990-9.

Wang A. The Role of Complement C4 in SLE. Awarded Magna Cum Laude. Available through Harvard Press. 2004.

List of Figures

List of Tables

List of Abbreviations

SLE – Systemic Lupus Erythematosus
GN – glomerulonephritis
ANA – anti-nuclear antibodies
WHO – world health organization
NZB – New England Black
NZW – New England White
TLR – toll-like receptor
CD – cluster of differentiation
B6 – C57/Black 6
IC – immune complex
FITC - fluoresceine isothiocyanate
PE – phycoerythrin
APC - allophycocyanin
Cy - cyanine
QDot – quantum dot
IV - intravenous
IHC - immunohistochemistry
NTS – nephrotoxic rabbit serum
BUN – blood urea nitrogen
OVA - ovalbumin
CDK – cyclin-dependent kinase
ITSM – intracellular tyrosine stimulating motif
SAP – SLAM-associated protein
ER – endoplasmic reticulum
APC – antigen-presenting cell
LPS - lipopolysacharide
SDF-1 – stromal-derived factor 1
PBSF – pre-b-cell stimulating factor
ESR – erythrocyte sedimentation rate
ACR – American College of Rheumatology
VDRL – Venereal Disease Research Lab
RBC – red blood cell
AML – acute myeloid leukemia
CMML – chronic myelomonocytic leukemia
RT-PCR – reverse-transcription polymerase chain reaction

CHAPTER ONE: Introduction

ORGANIZATION OF THESIS

The following work summarizes the research I performed in the laboratories of Drs. Edward Wakeland and Chandra Mohan from June 2005 to December 2007. The thesis is organized by the pathways model described below and illustrated in Figure 2.

The work I have done with Dr. Frederic Batteux and Jill Wescott on *Ly108*, a Pathway One gene responsible for the initial breach in tolerance, and its role in thymic selection, is described in Chapter Three.

My work on identifying *Sle3*, a Pathway Two locus which epistatically interacts with *Ly108* and subsequently drives fatal lupus, is described in Chapter Four. Admittedly, this is the weakest aspect of my thesis, is yet a work in process, and is only included for purposes of documenting my work during my PhD years.

Finally, my work in identifying and characterizing a novel mechanism of end-organ targeting which drives fatal lupus nephritis, the CXCR4/CXCL12 axes, is described in Chapter Five.

I begin with a general discussion on lupus in mouse and man, with a specific focus on how epistatic interactions drive fatal nephritis. Subsequently, each chapter will contain its own introduction on its specific subject matter.

The materials and methods section will be organized by chapter. Since a critical portion of my research required the development of a novel method for isolating renal leukocytes, a discussion detailing the technique and its validation, and why such a technique, was required appears under “Isolation of Renal Leukocytes” in the Chapter Five section of the “Materials and Methods” chapter.

All figures relevant to a particular chapter will appear at the end of that chapter. Each chapter will contain its own discussion, and a general discussion follows at the end.

SYSTEMIC LUPUS ERYTHEMATOSUS

Systemic lupus erythematosus (SLE) is a chronic autoimmune disease that is classically associated with the production of pathogenic autoantibodies to a spectrum of nuclear antigens [1-3]. SLE is fairly common in the general population, affecting roughly 1 in 150 people in the United States, of whom 90% are women between the ages of 15 and 45. SLE presents with a diverse array of clinical symptoms, which often reflect the consequences of injury to multiple organ systems. This clinical heterogeneity results from tissue damage targeted by autoantibody and inflammatory processes initiated as a consequence of deposition of complement-fixing immune complexes. Severe complications, which ultimately develop in about 50% of lupus patients, can manifest as a variety of clinical problems, including nephritis, central nervous system vasculitis, pulmonary hypertension, interstitial lung disease, and stroke. Current treatments for SLE involve a variety of immunosuppressive drug therapies, including hydroxychloroquine, steroids, and cytotoxic drugs. Although these therapies allow management of disease severity for many patients, a variety of deleterious drug side effects and therapy-resistant disease symptoms significantly diminish the quality of life for many SLE patients.

The renal manifestations of SLE, termed lupus nephritis, occur in approximately 50% of patients [4], and pose the greatest risk to the patient as it is the leading cause of morbidity and mortality [5]. The pathogenesis of lupus nephritis is poorly understood given the complex nature of the disease and its highly heterogeneous presentation. It is

thought that autoantibodies are critical in the initiation of lupus nephritis. These autoantibodies include anti-nuclear antibodies (ANA), a diagnostic hallmark of SLE present in over 98 percent of patients, and non-anti-nuclear antibodies such as anti-glomerular basement membrane autoantibodies. It has been postulated that the deposition of these antibodies as well as their immune complexes in the glomeruli are required for the development of glomerulonephritis [6]. Recent work has also implicated a role for various innate stimuli and other antibody-independent factors. Moreover, genetic studies in both humans and mouse models of SLE have revealed kidney-intrinsic factors that may also play an important role in lupus nephritis.

LUPUS NEPHRITIS: A CLINICAL OVERVIEW

The renal manifestations of SLE are highly heterogeneous. The disease may affect glomeruli, tubules, interstitium, and blood vessels with varying degrees of chronicity, severity, and kinetics, and has the ability to transform from one morphological form to another in a spontaneous or treatment-induced fashion. Subsequently, clinical presentation of lupus nephritis is also highly varied, ranging from asymptomatic hematuria and proteinuria to nephrotic syndrome and renal failure. Given the wide spectrum of disease, the World Health Organization (WHO) classification of lupus nephritis was devised to help standardize interpretation of renal biopsies [7, 8]. It is the most widely used and accepted classification of disease status by clinicians and pathologists.

There are six classes of lupus nephritis defined by WHO guidelines that essentially describe a continuum of disease. Figure 1presents the most salient features of

the different WHO classes of lupus nephritis. Importantly, Figure 1 highlights two distinct stages of lupus of relevant to kidney function—a "benign" stage in which patients are seropositive for autoantibodies but lack renal manifestations, and a "pathogenic" stage where renal disease is active with or without seropositivity [9]. Class I and II nephritis belong to the "benign" category. Class I lupus nephritis is limited to the early course of SLE and is characterized by an absence of glomerular abnormalities and the lack of detectable renal manifestations. Class II is defined as glomerular disease limited to the mesangium, and is further subdivided based on the presence or absence of mesangial hypercellularity. These patients have detectable ANAs and hypocomplementemia, indicative of active disease, but typically have no renal manifestations. Indeed, these patients typically have no clinical symptoms of renal disease and exhibit normal renal function by all conventional measures, although some may exhibit mild hematuria, proteinuria, or leukocyturia.

Class I and II patients highlight the fact that a dysregulation of the immune system, and specifically the formation of ANAs, typically precedes renal disease but may not precipitate it [10]. This observation is consistent with the fact that about 5 percent of the normal population exhibit positive ANAs titers without ever developing lupus [11, 12]. There are two important implications from these observations. First, it indicates that the progression of lupus from benign to severe pathology involves a transitional threshold. That is, an accumulation of molecular events, dictated by a combination of genetic predisposition and environmental stimuli, is needed to transition to severe pathology. Second, ANAs may not be in themselves pathogenic. Thus, there appears to

be a qualitative difference between antibodies which can and cannot precipitate renal disease. Class V lupus patients exemplify this interpretation.

Class V lupus nephritis is defined as membranous proliferative glomerulonephritis. Interestingly, these patients are typically negative for or have low titers of ANA, and often present with renal manifestations well before the development of other SLE clinical features. Class V disease is characterized by widespread epimembranous immune deposits in the absence of endocapillary proliferation and a thickening of the glomerular basement membrane. This subset of patients provide anecdotal demonstration that other autoantibodies, such as anti-glomerular antibodies or other kidney-specific antibodies, and not ANAs, may be the key players in disease pathogenesis. Rephrased, ANAs, or at least those screened for by conventional methods, may be dispensable in the development of severe kidney disease. Class V patients provide a case wherein genetic and environmental factors can "short-circuit" the "benign" phase of the disease, or at least have benign autoantibodies which are unconventional and therefore missed by routine diagnostics. A more thorough discussion on the pathogenicity of autoantibodies is found later in the text.

Class III and IV lupus have transitioned to pathogenic autoimmunity. Class III and IV nephritis are both defined as endocapillary proliferative glomerulonephritis, and are distinguished based on the distribution of endocapillary proliferation. The glomerular capillary lumina are narrowed or obstructed by hyperprofileration of endothelial and mesangial cells and infiltrated by mononuclear and polymorphonuclear cells. There is a varying degree of tubular atrophy, interstitial fibrosis, and inflammation. Up to two-thirds of class III and IV patients are positive for SLE serologies, and typically have

hematuria, leukocyturia, cellular casts, and proteinuria, as well as renal hypertension. At this stage of disease, patients typically have impaired renal function as assessed by serum creatinine and measures of glomerular filtration rates. Finally, the WHO classifies patients with advanced, chronic disease, extensive glomerular scarring, and renal insufficiency as Class VI lupus nephritis.

GENETIC PREDISPOSITION TO SLE: MOUSE AND MAN

Since renal manifestations are a sequellae of SLE, genetic predisposition to lupus nephritis is intertwined with the genetics of susceptibility to SLE. It is clear from studies of both man and mouse that genetic factors play a dominant role in dictating predisposition to SLE. The high concordance rate of SLE in monozygotic twins (30-57%) and increased familial incidence provide strong evidence for genetic predisposition as a major factor in disease susceptibility [13, 14]. Moreover, the occurrence of spontaneous lupus in specific inbred mouse strains, such as the F1 hybrid of the New Zealand Black (NZB) and New Zealand White (NZW) strains, the MRL.*lpr* strain, and BXSB.*yaa* mice further point to the importance of predisposing disease alleles.

Genetic analysis of SLE susceptibility in humans has progressed significantly over the past few years and several disease alleles have been identified. The most robust associations detected in genetic analyses have been with deficiencies in the C2, C4, and C1q components of the complement system [15]. However, the disease-associated alleles of these complement components are relatively rare in human populations and thus, only account for a small portion of disease incidence. Nonetheless, genetic studies indicate that 45% of all white SLE patients are homozygous or heterozygous for defective alleles

of complement component C4a, indicating that even small deficiencies in this component may be an important component of disease progression. Furthermore, >90% of individuals deficient for the expression of C1q develop severe lupus-like disease [16, 17]. Although this genetic deficiency mediates SLE susceptibility in a highly penetrant fashion, the C1q-deficient allele is extremely rare in the human population and thus this genetic system only accounts for a very small proportion of affected individuals. The precise roles that any of these complement deficiencies play in the development of SLE remains unclear, although they are thought to cause impaired clearance of immune complexes and apoptotic blebs, which may lead to a breach in immune tolerance due to the accumulation of an excess of these self-antigens in regions of immune activation [18, 19]

Linkage and/or association analyses in humans also have associated alleles of HLA-DR (DR2 and DR3) [20], PDCA [21], PTPN22 [22], Fc receptors [23, 24], and IRF5 [25] with susceptibility to SLE. In this instance, the disease alleles associated with SLE are often quite common in human populations, consistent with the multifactorial nature of genetic predisposition in this disease. Thus, although these disease alleles are relatively common in SLE patients, they are also quite frequent in unaffected individuals as well. This is consistent with the possibility that complex epistatic interactions between these disease alleles and a multitude of other susceptibility and/or suppressive allelic modifiers and environmental factors are essential for the development of severe autoimmunity. As will be discussed below, these types of interactions have been clearly delineated in animal models of systemic autoimmunity [26]. Finally, the roles that these disease alleles play in SLE pathogenesis are either unknown or very poorly characterized,

which represents a major deficiency in our understanding of genetic predisposition to SLE in humans.

Genetic linkage studies in murine models of lupus, on the other hand, have been particularly fruitful in defining the roles that individual susceptibility alleles play in disease progression. Most notably, congenic dissection, in which genomic segments containing known susceptibility/resistant loci are introgressed between defined genetic backgrounds, has been a valuable tool. This genetic strategy, which was pioneered by George Snell more than 50 years ago for the analysis of histocompatibility alleles, involves the production of a series of strains with identical genomes that only differ by the incorporation of a small genomic segment known to contain a specific susceptibility locus. These strains can be used to characterize the phenotypes mediated by individual susceptibility loci, even before the causative genetic variation has been identified [27]. Studies employing these strategies to analyze NZB/NZW-derived, MRL.*lpr* and BXSB.*yaa* strains have been fruitful in identifying candidate genes and understanding disease mechanisms. The inhibitory Fc receptor gamma IIb [28], complement components [29], the pro-apoptotic Fas receptor and Fas ligand [30], members of the SLAM family of receptors [31], and Toll-like receptors (TLR) 7 [32, 33] and 9 [34] are but a handful of genes that have been implicated from studies in the mouse. Importantly, this strategy has been invaluable in delineating the roles that individual disease loci play in the development of nephritis in lupus-prone mice.

A PATHWAYS APPROACH TO SLE

We have utilized congenic dissection to define the roles that individual susceptibility loci play in disease progression in the NZB/NZW-derived NZM2410 strain [26]. An initial linkage analysis in crosses with the autoimmune-resistant C57/BL6 (B6) strain identified three susceptibility loci, termed *Sle1, Sle2,* and *Sle3*, that contributed to disease in the NZM2410 lupus-prone mouse strain. These loci were introgressed individually onto the B6 genetic background, which produced a series of B6-congenic strains, each carrying a single susceptibility locus in isolation on the B6 background. Over the past 10 years, we have performed detailed characterizations of the autoimmune phenotypes expressed by these congenic intervals, both individually and in various combinations [31, 32, 35-43]. These studies have led to a model of lupus pathogenesis that is presented in Figure 2 (adapted from [10, 26]). In this model, lupus susceptibility genes are postulated to modulate two separate immunologic pathways, the first mediating a breach in immune tolerance leading to benign autoimmunity (Pathway One) and the second driving the transition from benign to pathogenic autoimmunity (Pathway Two). Genes that confer susceptibility to nephritis, some of which may be kidney-intrinsic, belong to the second category.

The experimental observations that have led to this model can be illustrated by the genetic interactions that lead to fatal disease among some of the B6-congenic strains that we have developed. The most potent susceptibility locus identified in our original linkage analysis was *Sle1*, which is the best developed example of a gene in the first pathway. B6.*Sle1* mice develop high-titer IgG ANAs in the absence of significant renal disease and thus are reminiscent of the "benign" autoimmunity described above. This

mouse illustrates the concept that genes predisposing to ANAs may not in themselves be capable of mediating a transition to lupus nephritis. Our ongoing analysis of this locus has determined that it contains a linked cluster of four loci that impact susceptibility to autoimmunity and that polymorphisms in a cluster of 7 SLAM/CD2 genes play a predominant role in the development of ANAs. To date, *Ly108* within the SLAM/CD2 gene cluster has been implicated as the strongest candidate gene in this interval [31, 35]. The disease allele of *Ly108* has been demonstrated to impair the induction of immune tolerance in the immature B cell compartment, leading to an increased frequency of autoreactive B cells in the spleen and lymph nodes. As a result of this lesion in an early checkpoint in B cell tolerance, these mice are highly predisposed to spontaneously develop ANAs by about 7 months of age (penetrance >90%). As discussed above, a similar phenotype develops in roughly 5% of the aging human population, suggesting that a lesion in B cell tolerance may be a relatively common occurrence. Ly108 will be covered in greater detail in Chapter Three.

As shown in Figure 2, the second pathway contains a series of disease alleles or susceptibility loci that drive chronic immune activation. The phenotypes mediated by *Sle3* and *yaa* have been thoroughly investigated and their properties provide important insights into the types of genetic interactions that can lead to severe autoimmunity. Both B6.*Sle3* and B6.*yaa* mice have mild autoimmune phenotypes that lead to little or no autoantibody production. This characteristic is shared with the other disease alleles and susceptibility loci included in this pathway, all of which exhibit variable but generally minimal propensity to cause autoimmunity when isolated on an otherwise normal genome. Interestingly, B6.*Sle3* mice may develop low levels of GN, despite the absence

of significant levels of IgG ANAs [39]. The lack of high titered ANAs but presence of GN seen in the B6.*Sle3* mouse may be similar to Class V GN observed in the Class V subset of SLE patients and points to the importance of kidney-intrinsic genes and/or genes that predispose to the production of non-anti-nuclear autoantibodies or other nephrotoxic factors. B6.*yaa* mice have virtually no autoimmune phenotypes, although a careful analysis of their serum IgM reveals the presence of autoantibodies preferentially recognizing RNA containing antigens [32]. *Sle3* will be covered in greater detail in Chapter Four.

The combination of either of these Pathway Two loci with *Sle1* in the bi-congenic B6.*Sle1Sle3* and B6.*Sle1yaa* strains results in the development of a potent systemic autoimmunity, leading to severe levels of GN and highly penetrant fatal disease by 9 months of age [32, 38]. Thus, although none of these disease alleles are capable of driving severe pathology individually, a combination of *Sle1* with either *Sle3* or *yaa* results in the transition of the benign autoimmunity mediated by *Sle1* into a potent systemic autoimmunity culminating in lupus nephritis and kidney failure. These analyses clearly illustrate the dramatic impact of epistatic interactions between genes in Pathways One and Two on the development of fatal disease in this mouse model of lupus nephritis.

Recent work on the role of the innate immune compartment in SLE has provided new insights into at least one type of disease allele within Pathway Two. Genes in the toll-like receptor (TLR) family have been recently implicated in playing a critical role in SLE. TLRs normally function within the innate immune system to recognize pathogen-derived molecules, serving to initiate immediate host responses to infection and to drive the activation of the adaptive immune system against invading pathogens [44, 45]. The

TLR9, TLR7, and TLR3 molecules bind specifically with dsDNA, ssRNA, and dsRNA, respectively, but have also been shown to recognize self-derived nuclear antigens [46, 47]. A clear role for TLR7 and TLR9 in dictating humoral response to RNA and DNA-containing antigens, respectively, has been demonstrated by a number of investigators [32-34]. We and others have recently demonstrated that a two-fold increase in the level of expression of TLR7 is the genetic lesion underlying the potent autoimmune accelerating phenotype of *yaa* [32, 33]. These studies demonstrate that an incremental increase in the signaling of the TLR7 pathway is sufficient to drive the development of fatal lupus nephritis, when coupled with breach in B cell tolerance mediated by *Sle1*. In addition, we have shown that *Sle3* mediates increased responsiveness of myeloid cells to TLR4 ligands, suggesting that the synergistic interactions of *Sle3* with *Sle1* may also involve increased signaling by the Toll receptor pathway [32, 47]. These and other studies demonstrate that dysregulation of the innate immune system is a potent driver of the transition from benign to pathogenic autoimmunity, thus suggesting that simultaneous dysregulation of the adaptive and innate immune systems may be a common feature in autoimmune-prone genomes. Since TLRs have an impact both in dictating autoantibody repertoire as well as in activating effector cells such as macrophages, dendritic cells, and granulocytes, they thus straddle the two categories of genes. As will be discussed later, TLRs have also been shown to be expressed on renal cells, and it remains to be seen what effect TLR dysregulation has on the kidney intrinsically.

In a similar fashion, defects in complement components and apoptosis affect both the development of benign autoimmunity and also the transition and perpetuation of pathogenic autoimmunity. Complement is thought to play two important roles in lupus

pathogenesis. First, complement modulates adaptive immunity. C3b can bind foreign or self-antigen and signal via the complement receptor complex CD21/35 on B-cells [48]. The simultaneous co-ligation of the BCR and CD21/35 with antigen complexed with complement leads to enhanced signaling in B cells [49]. It has also been shown that complement-fixation of antigen plays a major role in localizing antigen to the lymphoid follicles via engagement of complement receptors on follicular dendritic cells, which further serve to skew B-cell function [50]. Secondly, complement plays an important role in immune clearance. This function of complement plays a critical role in SLE, where ICs are inappropriately cleared and deposit in tissues where they cause pathologies. Similarly, apoptosis defects likely play a role in both Pathway One and Pathway Two. Faulty negative selection due to defects in apoptosis, as exemplified in the *fas* and *gld*-defective murine models, lead to inappropriate release of autoreactive immune cells from the bone marrow and thymus. This same inability to apoptose perpetuates chronically activated effector cells.

The most critical finding from these studies is that disease alleles from both pathways must be present in the genome to cause fatal disease and that these pathways interact in a non-additive fashion to produce pathogenic autoimmunity. A novel pathway resulting from this interaction, namely the CXCR4/CXCL12 axes, which drives fatal lupus nephritis, will be covered in greater detail in Chapter 5.

PATHOGENESIS OF LUPUS NEPHRITIS

Lupus nephritis is thought to be initiated by deposition of preformed circulating immune complexes (IC) in the glomerular capillary wall. Since ICs vary widely in both

their stereochemical properties and serum concentrations, ICs may preferentially deposit in mesangial, subendothelial, or subepithelial sites. Clearly, not all ICs are pathogenic. The 5 percent of the population bearing ANAs, and specifically anti-chromatin and anti-dsDNA ANAs, never develop nephritis. As described above, *Sle1* congenic mice also do not develop nephritis despite the persistence of high titer IgG ANA. Thus, understanding the pathogenicity of autoantibodies has been an active field of research and remains one of the most controversial topics in the field.

Work in the late 1980s by Weber and colleagues showed that histones, which are highly cationic, had strong affinity for the negatively charged sites in the glomerular capillary wall [51]. Work in the late 1970s by Koffler and colleagues demonstrated that anti-DNA antibodies may also cross-react with intrinsic glomerular basement membrane components such as heparin sulfate proteoglycans [52]. These findings have been supported by recent work by Rekvig and colleagues, which demonstrated that anti-dsDNA and anti-histone H1 antibodies and not a variety of other autoantibodies could cross-react with kidney components [53].

Antibodies formed against complement itself have also been implicated in the pathogenesis of nephritis. Studies have demonstrated the strong correlation between anti-C1q autoantibody positivity and renal involvement [54], the predictive value of anti-C1q autoantibody titers for flares of nephritis [55], and the accumulation of anti-C1q antibodies in the kidneys of both men and mice with lupus [56, 57]. Recent work by Daha and colleagues has provided evidence that anti-C1q antibodies are pathogenic only in concert with other IC deposits [58].

Direct engagement of kidney components has also been shown to play an important role in GN, especially in the membranous form. Nephrophilic antibodies, such as those formed against the glomerular basement membrane and intact glomeruli, have been demonstrated to arise later in the disease course, and may indicate the immune system's response to previously inaccessible antigens released during initial kidney damage. Our recent work has begun to shed light on the identity of nephrophilic antibodies. Using a proteomic array-based approach, they showed that specific clusters of serum nephrophilic antibodies, but not all kidney-recognizing antibodies, correlated with lupus severity [59]. They demonstrated that IgG autoantibodies to glomeruli and laminin, myosin, matrigel, vimentin, and heparin sulphate correlated with disease activity while other antibodies such as vitronectin and entactin did not. These studies pave the way for future work needed to unravel the pathogenic potential of lupus autoantibodies, which may in turn lead to a better understanding of disease mechanism.

After IC deposition, it is thought that the complement cascade plays an important role, although whether this event occurs in the circulation or in the kidney itself is yet unknown. Complement fixation results in the release of chemotactins C3a and C5a, which may promote recruitment of immune cells which then insult the kidney via the release of reactive oxygen species and inflammatory cytokines. Consistent with this hypothesis, Cook and colleagues have recently demonstrated *in vivo* that ablation of the classical pathway component C3 as well as the alternative pathway component Factor D rescued nephritis [60]. These set of studies indicate the important role of complement in the pathogenesis of lupus nephritis.

Recently, with the recognition of the importance of TLRs in SLE pathogenesis, researchers have identified a renal-intrinsic role for TLRs. Tubular epithelial cells have been shown to express TLR4 and can respond to LPS stimulation by releasing chemokines and cytokines [61, 62]. Glomerular mesangial cells have been shown to express TLR3, which recognizes double-stranded RNA, and Anders and colleagues have demonstrated that stimulation of these cells in vitro with synthetic TLR3 ligand induced secretion of IL6 and other chemokines [63]. Importantly, they found that by blocking NFkB—the most distal signaling event following TLR3 ligation—they were able to ablate these responses. Given the large body of work that has focused on the immune consequences of TLR and TLR-pathway dysregulation, it is worth closely examining the effect of inappropriate TLR signaling in the kidney as well. Indeed, genetic lesions in innate components may be so potent in aggravating lupus kinetics precisely because they affect both the immune and kidney compartments simultaneously.

What should be obvious from the present discussion is that it is extremely difficult to dissect renal-intrinsic mechanisms from immunological mechanisms when studying lupus nephritis pathogenesis. In almost every study, the events of the kidney are vitally linked to the events in the immune system. Subsequently, studies aimed at identifying renal-intrinsic factors leading to increased susceptibility are largely obscured by the inability to dissociate inflammatory events mediated by the immune system from those mediated by the kidney.

However, there is good evidence to date that suggests a crucial role for renal endogenous mechanisms. These studies, done primarily in the mouse, exploit bone marrow chimera technology and, more recently, kidney transplantation to assess if the

contributions of certain genes to kidney pathology are intrinsic to the kidney itself. Tipping and colleagues have used bone marrow chimera experiments to show a clear role for kidney-endogenous sources of IL1-beta, IL-12, IFN-gamma, TNF-alpha, and CD40 in mediating GN [64-68]. The role of FcR-gamma was also clarified recently using this approach by Clynes and colleagues, who showed that Fcr-gamma expression was needed only in hematopoetic cells and not renal cells, minimizing the purported role of mesangial cell activation via FcR cross-linking [69]. Given these observations, it follows logically that any alteration in kidney responses to pathogenic insult may have a profound impact on the kinetics and severity of GN. Indeed, this experimental strategy will be needed to establish whether candidate genes identified in murine lupus are *bona fide* nephritis susceptibility genes and to gain insight into how these genes contribute to kidney pathology.

SUSCEPTIBILITY LOCI MAPPED IN MURINE LUPUS MODELS

Table 1a summarizes the statistically significant loci for nephritis that have been uncovered using murine mapping studies [41, 70-96]. The table summarizes the results of mapping studies done in the MRL.*lpr*, BXSB.*yaa*, and the NZB/NZW-derived strains. As can be noted, all mouse strains that develop lupus spontaneously harbor nephritis susceptibility loci. Whereas some of the mapped loci confer susceptibility to ANAs as well as nephritis, others confer susceptibility to nephritis but not ANAs. Chromosomes 1, 4, 7, and 17 appear to be the most commonly implicated chromosomes harboring nephritis susceptibility loci, with these loci originating from several different strain backgrounds. These include repeatedly mapped loci on the distal chromosome 1 (88-

101cM), mid-chromosome 4 (31-48 cM), proximal chromosome 7 (16-31 cM), and centromeric chromosome 17 (around H2 and complement).

Sle1, located on a segment of mouse chromosome one syntenic with human chromosome one, has been further resolved to four sub-loci, termed *Sle1a, Sle1b, Sle1c,* and *Sle1d*, of which *Sle1b* seems to be the strongest loci that predisposes a loss of tolerance to chromatin [43]. Of interest, *Sle1d* has been purported to play a role in the development of GN in the absence of predisposing ANAs.

What is obvious from these studies is that conventional mapping studies are inconclusive in identifying nephritis-mediating genes from other lupus genes. To overcome the limitations, congenic analyses as an alternative strategy has been used to study purported nephritis-loci *in vacuo* [39, 40, 97-99]. The results of these studies are presented in Table 2. However, due to the expression of many of these susceptibility genes in both blood and renal cells, congenic analyses has also failed to confidently distinguish renal-intrinsic factors from hematopoetic factors. As described above, bone marrow chimera and renal transplantation experiments are needed to adequately assess the contributions of nephritis genes on kidney-intrinsic pathology.

SUSCEPTIBILITY LOCI IDENTIFIED IN HUMAN LUPUS

As executed in murine lupus, a limited number of mapping studies have also been executed in human lupus nephritis [100-103]. As detailed in Table 3, these studies point to the existence of nephritis susceptibility loci on human chromosomes 2 (SLEN2), 3, 4, 10 (SLEN1), 11 (SLEN3), and 16. Since most of these loci are not associated with high

serum ANA, a subset of these may harbor genetic elements that promote renal disease in a kidney-intrinsic fashion.

Finally several research groups have identified allelic polymorphisms in specific genes (e.g., *FcRII, FcRIII, PARP, PDCD1*, etc.) that are highly associated with nephritis in SLE patients [104-114]. These findings are summarized in Table 4. One important point on these data is that it still remains likely that the reported genes may not actually be the *bona fide* lupus genes, and that they simply are in linkage disequilibrium with the actual causative genes.

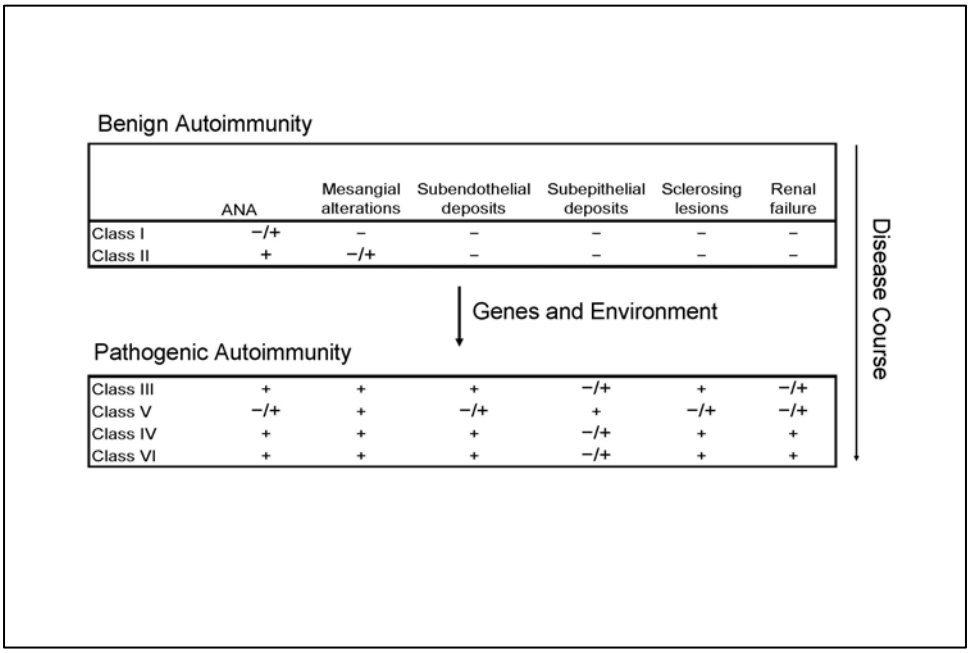

Figure 1. WHO Classes of Lupus Nephritis

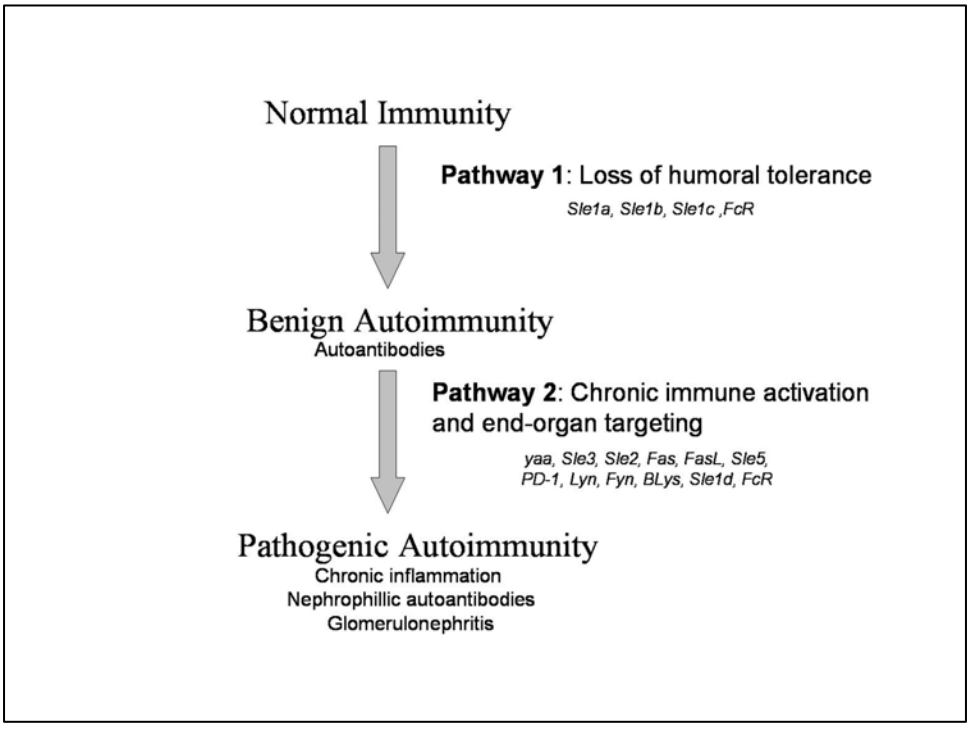

Figure 2. Pathways Model of SLE.

Name of locus	Chr[1]	cM[2]	Disease Strain	Mapped phenotype[3]	Ref
Bxs4/Sle10	1	11	BXSB	nephritis	71
Bxs1/Yaa2	1	32.8	BXSB	nephritis, ANA, etc.	72
Bxs2/Yaa3	1	63.1	BXSB	nephritis, anti-dsDNA,, etc.	71, 72
Bxs3	1	71	BXSB	nephritis, anti-dsDNA,, etc.	71, 72
Sle1	1	88	NZM2410	nephritis	75
Lbw7	1	92	NZB	anti-dsDNA	76
Sbw1	1	92	NZB	splenomegaly	76
Cgnz1	1	92.3	NZM2328	chronic nephritis,proteinuria	86
Nba2	1	94.2	NZB	nephritis, anti-dsDNA, gp70IC	81, 87-89
Agnz1	1	101	NZM2328	acute nephritis	86
Wbw1	2	86	NZW	proteinuria	77
Mrl	2	50	MRL-lpr	anti-dsDNA	78
Sles3	2	16	NZW	Suppressive (nephritis)	41
no name	3	32.8	BXSB	nephritis, ANA	71
Bxs5	3	63	BXSB	nephritis, ANA	71
Lprm2	3	66	MRL-lpr	vasculitis	80
Lprm1	4	35.5	MRL-lpr	vasculitis	80
Nbwa2/Sle15	4	31.2	NZB	nephritis	90
Lbw2	4	42.6	NZB	nephritis, mortality	76
Sle2	4	44.5	NZM2410	nephritis	75
no name	4	48.5	NZB	nephritis	88
Sbw2	4	53	NZB	splenomegaly	76
Lmb1	4	54	C57BL/6	splenomegaly, ANA	80
Sles2	4	57.6	C57BL/6	Suppressive (nephritis, ANA)	41
Nba1	4	70	NZB	nephritis	81
Nba4	5	15	NZB	nephritis	91
Sle6	5	20	NZW	nephritis	41
Lmb2	5	27	MRL-lpr	splenomegaly, ANA	80
Lprm4	5	54	MRL-lpr		79
Lbw3	5	88	NZW	disease accelerator	76
Lxw2	6	25.5	NZW	nephritis	92
no name	6	35	C3H	nephritis	93
Lbw4	6	60	NZB	disease accelerator	76
Sle5	7	4	NZM2410	nephritis,anti-dsDNA	82
Lrdm1	7	6	MRL-lpr	nephritis, anti-DNA, etc.	83
no name	7	16	NZM2410	nephritis,anti-dsDNA	82
Lbw5	7	22	NZW	disease accelerator	76
no name	7	25	NZW	nephritis, anti-DNA, gp70 IC	84
Lmb3	7	26	MRL-lpr	splenomegaly, ANA	81
Sle3	7	28	NZM2410	nephritis,autoantibodies	80
Nba3	7	31	NZB	nephritis	81
Sles4	9	2	NZW	Suppressive (nephritis)	41
Sle12	10	69	NZM2410	nephritis	82
Lmb4	10	50	MRL-lpr	splenomegaly	80
Sle13	11	20	NZM2410	acute nephritis,anti-dsDNA	82
Nba	11	17	NZB	nephritis	95
Lbw8	11	37	NZB	ANA	76
Mrl	11	54	MRL-lpr	ANA, vasculitis	78
Nbwa1/Sle14	12	3.5	NZB	nephritis, ANA	90
Lrdm2	12	61.8	MRL-lpr	nephritis, anti-DNA, etc	83
Bxs6	13	24	BXSB	nephritis	94
Nwa	14	19.5	NZW	ANA	95
Swrl2	14	27.5	SWR	nephritis, IgG ANA	74
Nba	14	40	NZB	nephritis	95
Lprm3	14	44.3	C3H	nephritis	79
Lprm5	16	33.5	MRL-lpr	ANA	79
Nwa1	16	38	NZW	nephritis, anti-dsDNA, etc.	95
H2	17	19	several[4]	nephritis,mortality, ANA, etc.	several[4]
Sles1	17	19	several	fully suppressive	41, 74-75
Lbw6	18	47	NZW	nephritis,mortality	76

1: Indicated is the chromosomal location of the loci, ordered according to the chromosome numbers
2: Indicated is the position of the locus on the chromosome in centimorgans (cM)

3: Where multiple phenotypes were mapped, only "nephritis" and a couple of the other phenotypes have been listed

4: "several" nephritis loci have been mapped to "*H2*", as detailed in references 41, 73-77, 86, 87, 92,

Table 1. Genetic loci associated with lupus nephritis in murine studies

Congenic strain[1]	Disease Strain	Control Strain	Locus	Chromosomal position[2]	Phenotypes noted in congenics[3]: proteinuria	nephritis	deposits	auto-Ab	Ref
Introgression of disease interval onto "normal" strain background									
B6.NZBc1(35-106)	NZB	C57BL/6	*Nba2,others*	1 (35-106)	Yes (low)	Yes	Yes	Yes	87
B6.NZBc1(85-106)	NZB	C57BL/6	*Nba2*	1 (85-106)	no	Yes	Yes	Yes	87
B6.*Sle1*	NZM2410	C57BL/6	*Sle1*	1 (85-122)	no	Mild	no	Yes	40
B6.*Sle3*	NZM2410	C57BL/6	*Sle3*	1 (15-45)	no	Modest	Yes	Yes	40, 43
B6.MRLc7	MRL	C57BL/6	*Lmb3*	7 (1-28)	na[4]	Yes	Yes	Yes	98
Introgression of "normal" interval onto disease-strain background									
NZM2328.*Cgnz1*	NZM2328	C57L/J	*Cgnz1*	1 (88-112)	decreased	decreased	decreased	decreased	99
NZM2328.*Adnz1*	NZM2328	C57L/J	*Adnz1*	4 (16-60)	no change	no change	no change	decreased	99

1: Indicated are congenic mouse strains in which a disease susceptibility interval has been backcrossed onto a control strain background (i.e., the first 5 strains) or in which a disease-resistant interval has been backcrossed onto a disease susceptible strain background (i.e., the last 2 strains).
2: Indicated are the chromosomal locations of the introgressed genetic interval in centimorgans (cM).
3: Listed are the salient phenotypes in the congenic strains compared to the phenotype of the background strain
4: na = not available

Table 2. Monocongenic strains in which lupus-associated nephritis is aggravated or ameliorated

Locus	Ethnic group	LOD score of P-value	Ref
2q34-35 (SLEN2)	African-American	P = 0.000001	101
3q23	African-American	P = 0.00007	101
4q13.1	European-American	P = 0.00003	101
10q22.3 (SLEN1)	European-American	LOD =3.16	101
11p13	African-American	P = 0.00003	101
11p15.6(SLEN3)	African-American	LOD = 3.34	101
16q12	Multiple	P = 0.006	102

Table 3. Nephritis-susceptibility loci mapped in human lupus nephritis

Gene	Chrom Position	Ethnic Group	Nature of association with nephritis in SLE patients	Ref
FcγRIIa	1q23	Dutch Caucasians	R131 allele, P=0.03	112
FcγRIIa	1q23	African-Americans	R131 allele, χ^2 = 11.3	24
FcγRIIa	1q23	Hispanics	R131 allele, P < 0.002	113
FcγRIIa	1q23	Koreans	R131 allelic, χ^2=9.29, P =0.00959	114
FcγRIIa	1q23	Brazilians	R131 allele, P < 0.02	104
FcγRIIIA	1q23	Koreans	F176, P<0.022	105
FcγRIIIA	1q23	Multiple	F158, P = 0.003	106
PARP	1q41-42	Koreans	SNP-1963:A>G, P=0.03,+28077G > A P=0.0008	107
PDCD1	2q37	Swedish	PD-1.3A, χ^2=10.2, P=0.002	108
TNFB	6p21	Koreans	TNFB* 2, P < 0.0001	109
ACE	17q23	Hispanic,Asian	Position 23949 $(CT)_{2/3,}$ P = 0.014	110
Dnase II	19p13.2-q13.4	Koreans	SNP-1066:G>C, P=0.04	111
			SNP+2630:T>C, P=0.04	
			SNP+6235:G>C, P=0.05	

Table 4. Candidate genes associated with nephritis in human SLE

CHAPTER TWO: Materials and Methods

FOR CHAPTER THREE: Regulation of Thymic Selection by the Lupus Susceptibility Gene Ly108

Mice

Male and female B6, B6.OTII, B6.*Sle1b*.OTII, B6.*Sle1b,* B6.*Sle1b*.*SAP*^{ko} and B6.*Sle1b*.388C4 mice were produced in our colony at the University of Texas Southwestern Medical Center, and housed in the University of Texas Southwestern Medical Center Animal Resources Center's specific pathogen-free facility. B6.*Sle1b*.388C4 mice are B6.*Sle1b* mice which are transgenic for the *b* alleles of *Ly108* and *Cd84*, and their construction has been previously described [115]. The care and use of laboratory animals in our facility conforms to the National Institutes of Health guidelines and all experimental procedures conformed to IACUC approved animal protocols.

Flow cytometry and antibodies

Antibodies to the following mouse antigens were used for flow cytometry analyses: CD25-FITC, CD4-APCCy7, CD69-PerCPCy5.5, CD5-APC, CD69-PE, AnnexinV-PE, CD21-FITC, CD23-PE, IgM-PerCPCy5.5, IgM-PeCy7, CD5-APC, B220-APCCy7, B220-FITC, CD138-PE, Gr-1-APCCy7, CD3-FITC, CD4-APCCy7, CD86-PE, AA4.1-FITC, CD43-PE, NK1.1-PECy7, Va2-FITC, Vb5-Bio, CD25-Bio, (BD Biosciences, Franklin Lakes, NJ); Ly108-PE, Ly108-Bio, CD8-PECy7, CD44-APC, CD11b-APC,

F4/80-PECy5, CD11c-PacificBlue, Ie/Ib-FITC, F4/80-PECy5, CD3-PacificBlue (eBioscience, San Diego, CA); CD62L-PE Texas Red, Strepavidin-QDot655, 7-AAD, YO-PRO (Invitrogen, Carlsbad, CA); Ly9-PE, CD84-Bio (BioLegend, SanDiego, CA). For Vβ usage analyses, the BD Biosciences Vβ screening kit was used per manufacturer's instructions (BD Biosciences, Franklin Lakes, NJ). Samples were Fc-blocked with the 2.4G2 antibody (BD Biosciences, Franklin Lakes, NJ). For spleen, bone marrow, and blood, at least 5 x 10^4 cells were acquired in the live gate, as defined by size and granularity. Samples were either acquired on an LSRII flow cytometer or FACSCalibur (BD Biosciences, Franklin Lakes, NJ), and analyzed using Flow Jo software (Tree Star Technologies, San Carlos, CA). MFIs represent median fluorescent intensities.

***In vivo* injection of anti-CD3, anti-Ly108 antibody, and OVA**

Functional grade anti-CD3 (5 ug) and/or anti-Ly108 (5 ug) (eBioscience, San Diego, CA) monoclonal antibodies or their appropriate iosotype controls were injected intravenously (IV) via the retro-orbital route. Animals were allowed to rest for 24 or 48 hours, at which times they were sacrificed and analyzed. For experiments utilizing OTII transgenic mice, OVA (323-339) (AnnaSpec, San Jose, CA), was injected intraperitoneally once a day (0.5 mg) for two consecutive days with or without simultaneous IV anti-Ly108 antibody (5 ug). Mice were harvested 48 hours after the first injection and sacrificed for analyses.

In vitro stimulations and analyses of proliferation and apoptosis

B6 and B6.Sle1b mice were sacrificed and single-cell suspensions of thymocytes were prepared in complete media ((RPMI1640 with L-glutamine, 10 % FCS (HyClone, Logan, UT), HEPES (Sigma-Aldrich, St. Louis, MO), 1X Pen/Strep (Sigma-Aldrich, St. Louis, MO), beta-2 mercaptoethanol (Sigma-Aldrich, St. Louis, MO), L-glutamine (Sigma-Aldrich, St. Louis, MO)) at a final concentration of 1 x 10^6 cells / ml and added in triplicate to 96-well flat bottom tissue culture plates which were pre-coated with functional grade anti-CD3 and/or anti-Ly108 (eBioscience, San Diego, CA) prepared at various concentrations in PBS for 12 hours at 37^o C. At various time points, cells were harvested and stained for cell-surface antigens and the intracellular fluorescent dyes YOPRO and 7-AAD. "Viable" cells were designated as those which were YOPRO- 7-AAD-, "early apoptotic" cells were designated as those which were YOPRO+ 7-AAD-, and "late apoptotic" cells were designated as those which were YOPRO+ 7-AAD+.

CBA Analyses of IL-4 and IFN-γ Production

B6 splenocytes were plated as described above. Cells were stimulated with various doses of anti-CD3 and / or anti-Ly108, for 5 days, after which culture supernatants were harvested for CBA analyses using components of the Th1/Th2 BD CBA Flex Kit (BD Biosciences, Franklin Lakes, NJ) per manufacturer's instructions. Samples were run on a LSRII flow cytometer (BD Biosciences, Franklin Lakes, NJ), and analyzed using Flow Jo software (Tree Star Technologies, San Carlos, CA). Data were analyzed in GraphPad 4 and 5 (GraphPad, San Diego, CA). Briefly, the parameters for the sigmoidal dose-response curve were calculated using the log value of the standard concentrations versus

the MFI of the analyte, and concentrations of test samples were subsequently extrapolated.

Ly108 signal transduction studies

Thymocytes were washed in PBS and then lysed at 4°C in HNTG lysis buffer (50 mM HEPES (pH 7.4), 150 mM NaCl, 1 mM EDTA, 1 mM MgCl2, and 10% glycerol) containing 1% Triton X-100. $1.1x10^8$ cell equivalents were immunoprecipitated overnight at 4°C on 30 µl rProtein G-Agarose beads loaded with anti-Ly108 mAb. Precipitates were washed three times with complete HNTG buffer containing 0.1% Triton X-100. Cleared cell lysates and IPs were mixed with non-reducing sample buffer and run on 4-12% acrylamide gels in MES SDS running buffer and transferred to nitrocellulose membranes. All immunoblots were performed in 5% non-fat dry milk in TBST. Anti-Ly108 mAb (13G3-19D) was obtained from eBioscience. Anti-ZAP70 mAb (1E7.2), anti-p-tyr mAb(PY20), and polyclonal antibodies to Bcl-2(N-19), p-Cdk2/3(T160), p-p27Kip1(Ser10), and ERK2 were obtained from Santa Cruz (Santa Cruz, CA). Polyclonal antibodies specific for Bcl-XL, Bax, Bak, p27Kip1 and Cdk2 were obtained from BD Biosciences (San Diego, CA). Antibodies to SAP were prepared in the laboratory of Cox Terhorst. HRP-conjugated secondary antibodies were purchased from Pierce biosciences. Blots were developed with the SuperSignal chemiluminescence kit from Pierce Biosciences.

Immunokinase Assays

Cdk2 was immunoprecipitated from 50 μg cell extracts as described above. The complexes were assayed for kinase activity towards histone H1 as follows. Immunocomplexes were washed three times with lysis buffer and once with kinase buffer (20 mM Tris, pH 7.4, 10 mM MgCl2, 1 mM DTT). Subsequently, the beads were resuspended in 50 μl kinase buffer containing 2 μg histone H1, 10μCi [γ-32P]ATP and 20 μM ATP. The reaction mixtures were incubated at 30°C for 45 min. Reaction mixtures were boiled in sample buffer and run on SDS-PAGE gels. Gels were stained with Coomassie blue, dried, and autoradiographed. Radioactivity was determined using a scintillation counter.

Illumina BeadChip gene expression analyses and quantitative real-time PCR

RNA was isolated from thymocytes harvested from B6 and B6.*Sle1b* mice before, 24 and 48 hours after treatment with anti-Ly108 antibody and hybridized to the Illumina Sentrix Mouse 6 BeadChip arrays. Analyses were done using BeadArray Studio software (Illumina, San Diego, CA). Differentially expressed genes were first subjected to a Mann-Whitney U-test threshold of $p < 0.05$, and a 1.7-fold difference threshold. Subsequently, genes which were detected at low signal strength were removed. For confirmation of differentially expressed genes, TaqMan gene expression probes for *Calm2* and *Fbxw5* (Applied Biosystems, Foster City, CA) were used in quantitative real-time PCR assays.

Calcium flux

Single-cell suspensions of thymocytes were prepared at 1 x 106 cells/ml in Hank's Balanced Salt Solution (HBSS) (Fisher Scientific, Hampton, NH). 4 x 106 cells were labeled at a final concentration of 6 uM Fluo-3 in HBSS for 30 minutes at 37^{o} C. Cells were immediately quenched with 2 x volume cold HBSS, and subjected to cell-surface staining. Cells were then washed in HBSS and heated to 37o C before stimulation. Cells were acquired on a FACSCalibur (BD Biosciences, Franklin Lakes, NJ). Briefly, cells were allowed to run for 30 seconds to establish baseline levels, then stimulated with various concentrations of biotinylated anti-CD3 antibody and/or biotinylated anti-Ly108 antibody (eBioscience, San Diego, CA) followed by Strepavidin (10 ug / ml) (Sigma, Croydon, Australia) or with thapsigargin (100 nM) (Sigma, Croydon, Australia) and acquired for 400 seconds. Data was analyzed using Flow Jo software (Tree Star Technologies, San Carlos, CA).

***In vivo* proliferation and cell-cycle status studies**

For BrdU studies, the BrdU kit from BD Biosciences was used (BD Biosciences, Franklin Lakes, NJ). Briefly, mice were injected with functional grade anti-Ly108 antibody (5 ug) and allowed to rest for 12, 24, or 36 hours. 4 hours prior to harvesting, BrdU (1 mg) was injected intraperitoneally per manufacturers instructions, after which, mice were sacrificed and thymocyes harvested. Extracellular labeling of CD4 and CD8 was performed first followed by 24 hours of fixation in BD Perm/Fix buffer at 4o C. FITC-conjugated anti-BrdU and 7-AAD (Invitrogen, Carlsbad, CA) were used to

visualize BrdU incorporation as specified by the manufacturer subsequent to 24 hour permeablization and analyzed by flow cytometry as described.

TUNEL visualization

For *in situ* visualization of DNA fragmentation, the Sigma TUNEL kit was used on OCT-embedded thymuses. Briefly, one lobe of the thymus was removed, fixed in 4% paraformaldehyde for one hour followed by a 12 hour incubation in 30% sucrose, and embedded in OCT. Coronal sections were washed and then mounted with Vectashield with DAPI (Vector Laboratories, Burlingame, CA), visualized and photographed with a Zeiss Axioplan 2 and digital camera (Carl Zeiss International, Germany), and analyzed with Axiovision software (Carl Zeiss International, Germany).

Serology

Mice were bled at 8-12 months of age and sera were harvested and stored at -20°C. ELISA detection of serum IgM and IgG autoantibodies directed against chromatin and dsDNA were performed as described previously [116]. OD_{450} was measured using an Elx800 Automated Microplate Reader (BioTek Instruments, Winooski, VT) and the raw optical densities for anti-chromatin ELISAs converted to arbitrary normalized units using a six-point standard curve generated by an anti-nuclear mAb derived from a NZM2410 mouse [116].

In vivo treatment of Ly108 in B6.Sle1yaa

Biweekly intravenous (IV) administration (retro-orbital) of anti-Ly108 antibody or isotype control was begun in B6.Sle1yaa mice at 6-8 weeks of age at a concentration of 0.25 mg/kg for a total duration of 4 weeks. Treatment was terminated, and mice were monitored monthly for serum BUN, 24 hour proteinuria, and ANAs. Mice were allowed to age to 6 months of age and then sacrificed for analyses.

Statistical Analysis

Data were analyzed using InStat3 or GraphPad 4 (GraphPad, San Diego, CA). Where appropriate, one-way ANOVA with Dunnet or Bonferonni post hoc analysis, Welch-corrected t-test, Mann-Whitney U-test, or log-rank Mantel-Cox test were used. Error bars represent SEMs.

FOR CHAPTER FOUR: Identification of the Lupus Susceptibility Locus, *Sle3*

Mice

Female B6, B6.*Sle3*, and all B6.*Sle3* subcongenic lines (previously generated by Dr. Kui Liu) were produced in our colony at the University of Texas Southwestern Medical Center, and housed in the University of Texas Southwestern Medical Center Animal Resources Center's specific pathogen-free facility. The care and use of laboratory animals in our facility conforms to the National Institutes of Health guidelines and all experimental procedures conformed to IACUC approved animal protocols.

Bone Marrow-Derived Macrophages

Bone-marrow was eluted from two femurs and tibias with RPMI1640. 1.5 x 10^6 cells / ml were plated in 12 ml final volume of MCSF growth media ((RPMI1640 with L-glutamine, 10 % FCS (HyClone, Logan, UT), HEPES (Sigma-Aldrich, St. Louis, MO), 1X Pen/Strep (Sigma-Aldrich, St. Louis, MO), 1X Non-essential amino acids (Sigma-Aldrich, St. Louis, MO), beta-2 mercaptoethanol (Sigma-Aldrich, St. Louis, MO), L-glutamine (Sigma-Aldrich, St. Louis, MO), and 20 ng/ml M-CSF (R&D Systems, Minneapolis, MN)) in T75 plastic flasks at 37C and 5%CO_2. Twenty-four hours after, non-adherent cells were removed and placed in new T75 flasks, and then allowed to culture for an additional six days, with media supplementation on day five after initial plating. At the end of seven days, cells were harvested by scraping and re-cultured with various concentrations of LPS (Sigma-Aldrich, St. Louis, MO) in M-CSF-free media at a concentration of 5 x 10^5 cells/ ml in 24-well plates at a final volume of 1 ml. Twenty-

four hours later, cell supernatants were collected for ELISA analyses and cells were harvested by scraping and analyzed for activation marker status by flow cytometry.

Flow cytometry and antibodies

Antibodies to the following mouse antigens were used for flow cytometry analyses: Gr-1-APCCy7, CD40-Biotin, (BD Biosciences, Franklin Lakes, NJ); CD11b-APC, F4/80-PECy5, CD16/32-FITC, CD106-FITC, CD80-PE, CD86-Biotin, Ie/Ib-FITC, F4/80-PECy5, (eBioscience, San Diego, CA). Samples were Fc-blocked with the 2.4G2 antibody (BD Biosciences, Franklin Lakes, NJ). For spleen, bone marrow, and blood, at least 5 x 10^4 cells were acquired in the live gate, as defined by size and granularity. Samples were either acquired on an LSRII flow cytometer or FACSCalibur (BD Biosciences, Franklin Lakes, NJ), and analyzed using Flow Jo software (Tree Star Technologies, San Carlos, CA). MFIs represent median fluorescent intensities.

Cytokine ELISAs

BMDM culture supernatant were collected and used at various dilutions to quantitate IL6, RANTES, and TNF-alpha concentrations by ELISA (R & D Systems, Minneapolis, MN). OD_{450} was measured by an Elx800 Automated Microplate Reader (BioTek Instruments, Winooski, VT) and concentrations were extrapolated from a 4-point standard curve ($R^2 >$ 0.99), where the mean of experimental duplicates was used.

Quantitative real-time PCR

RNA was extracted from BMDM cultures and subjected to RT-PCR analyses for *Klf13* using a commercially available TaqMan probe (Applied Biosystems, Foster City, CA). Since BMDM cultures contain only 70% *bona fide* macrophages, cells were normalized to CD14 mRNA (Applied Biosystems, Foster City, CA). Fold-change of *Klf13* was calculated using the delta-delta C_t method.

RANTES inhibition studies

BMDM were cultured with LPS with either neutralizing antibody to RANTES (0.5 ug / ml) or equivalent concentrations of isotype control (R & D Systems, Minneapolis, MN). Twenty-four hours later, cell supernatants were collected for ELISA analyses and cells were harvested by scraping and analyzed for activation marker status by flow cytometry.

FOR CHAPTER FIVE: CXCR4/CXCL12 dysregulation plays a pivotal role in murine lupus nephritis

Mice

Male B6, B6.*Sle1,* B6.*Yaa,* B6.*Sle1Yaa*, BXSB, MRL.*lpr*, and female, B6.*Sle1Sle2Sle3*, were purchased from The Jackson Laboratories (Bar Harbor ME) or produced in our colony at the University of Texas Southwestern Medical Center, and housed in the University of Texas Southwestern Medical Center Animal Resources Center's specific pathogen-free facility. The care and use of laboratory animals in our facility conforms to the National Institutes of Health guidelines and all experimental procedures conformed to IACUC approved animal protocols.

Patients

From November 2007 to July 2008, patients were enrolled with written consent at Cochin Hospital (Université de Paris Descartes, Paris, France). The design and execution of the study was authorized by the internal review board and conforms to the standards and guidelines of the ethics board. Patients hospitalized in the service of Internal Medicine at Cochin Hospital who were diagnosed with SLE or rheumatoid arthritis based on ACR criteria [117, 118] were included in the study. All demographic and clinical data are currently being prepared for publication (18/07/2008).

Flow cytometry and antibodies in mice

Antibodies to the following mouse antigens were used for flow cytometry analyses: CD21-FITC, CD23-PE, IgM-PerCPCy5.5, IgM-PeCy7, CD5-APC, B220-APCCy7, B220-FITC, CXCR4-PE, CXCR4-Biotin, GL7-FITC, CD138-PE, CD69-PE, CD69-PerCPCy5.5, Gr-1-APCCy7, CD3-FITC, CD4-APCCy7, CD86-PE, AA4.1-FITC, CD43-PE, CD45-FITC, CD45-PECy7, NK1.1-PECy7, AnnexinV-PE (BD Biosciences, Franklin Lakes, NJ); CD11b-APC, CD8-PECy7, CD44-APC, CD11c-PacificBlue, Ie/Ib-FITC, F4/80-PECy5, CD3-PacificBlue (eBioscience, San Diego, CA); CD19-PETexasRed, CD62L-PE Texas Red, PDCA-1-Biotin, Strepavidin-QDot655, Strepavidin-PE Texas Red, 7AAD (Invitrogen, Carlsbad, CA). Samples were Fc-blocked with the 2.4G2 antibody or 10% normal rabbit sera (Invitrogen, Carlsbad, CA). For spleen, bone marrow, and blood, at least 5 x 10^4 cells were acquired in the live gate, as defined by size and granularity. For kidney samples, at least 5 x 10^5 cells were acquired on the leukocyte gate, as defined by size and CD45 positivity. Samples were either acquired on an LSRII flow cytometer or FACSCalibur (BD Biosciences, Franklin Lakes, NJ), and analyzed using Flow Jo software (Tree Star Technologies, San Carlos, CA). MFIs represent median fluorescent intensities.

Flow cytometry and antibodies in humans

Antibodies to the following human antigens were used for flow cytometry analyses: CD14-FITC, CD19-FITC, CXCR4-APC, CD4-PE, CD15-PE, CD8-PECy7 (BD Biosciences, Franklin Lakes, NJ); IgG2a k-APC (eBioscience, San Diego, CA). Whole

blood was labeled and red blood cells lysed after staining using BD Fix and Lyse; MFIs of samples were normalized using BD Spectral Beads (BD Biosciences, Franklin Lakes, NJ). At least 5 x 10^4 cells were acquired in the live gate, as defined by size and granularity. Samples were acquired on a BD Canto flow cytometer (BD Biosciences, Franklin Lakes, NJ), and analyzed using Flow Jo software (Tree Star Technologies, San Carlos, CA). MFIs represent median fluorescent intensities.

Isolation of Renal Leukocytes

ABSTRACT

A detailed delineation of infiltrating renal leukocytes in lupus nephritis has been problematic. Methodologically, classical immunohistochemistry suffers from sample selection bias and lack of absolute quantification of the number and types of infiltrating leukocytes, whereas it is requisite for determination of the geographical distribution of these cells. Published flow cytometric methods for renal leukocyte enumeration suffer from technical issues related to the high auto-fluorescence of endogenous renal cells and difficulty in preparing the bulk kidney for flow cytometric applications. Thus, we developed a novel cell isolation technique which we use to track and enumerate all infiltrating leukocyte subpopulations in the kidneys of mice at various time points over the course of anti-GBM sera challenge, as a proof of principle. Using this method, we observed that whereas there was early infiltration of neutrophils and monocytes, it was the influx of CD4+ T-cells that coincided with peak proteinuria and serum BUN. Using this technique, coupled with classical immunohistochemistry, it is possible to

quantitatively and qualitatively assess the renal leukocyte load in inflammatory nephropathies such as lupus nephritis.

INTRODUCTION

Since nephritis, by definition, is partly the consequence of infiltrating leukocytes, a detailed understanding of the types and numbers of infiltrating leukocytes could shed valuable insight into the pathogenesis and clinical management of nephritis. Moreover, a reliable manner of isolating renal leukocyte subsets for meaningful subsequent analyses (i.e., gene profiling, stimulation assays, cytokine profiles, spectratyping) could prove to be an incredibly useful tool in understanding dysregulated pathways contributing to pathogenesis.

To date, most studies focused on the role of various subsets in mediating nephritis utilize a combination of knockout mice, antibody therapies, immunohistochemistry, and only limited flow cytometric techniques [119]. From a methodological standpoint, each technique possesses caveats which limit their explanatory power.

Since the intra-communication between all immune cells subsets and inter-communication between immune and relevant non-immune cells (i.e., mesangial cells, endothelial cells) is pleitropic, systems using knockout mice lacking various immune cell subsets are difficult to interpret. That is, it is difficult to interpret the effects on the development of nephritis by the lack of a cell type since the observed phenotype maybe far distal to the experimentally-induced lesion, especially when the lesion is of such breadth and non-specificity as i.e. the totality of CD4 T-cell subsets.

Immunohistochemistry (IHC) provides powerful geographic detailing of immune cells. IHC, however, does not provide absolute quantitation of infiltrates and lacks sufficient resolution for dissecting the various subsets within major immune populations. Indeed, a combination of difficulties in antigen retrieval, a limited palette of antibody specificities, a limited degree of multi-fluorochrome localization, and the experimental bias inherent in 5 μm sections makes IHC more a qualitative technique than a quantitative technique with statistical power.

To date, there have been limited reports using flow cytometry to quantitatively enumerate the infiltrating renal leukocyte populations [120-122]. The reasons for this are mostly technical in nature. Simple analysis of crude single-cell preparations of total kidney shows that renal cells are roughly the same size and granularity as leukocytes, and, most importantly, by far outnumber renal leukocytes. Subsequently, acquisition of bulk renal single-cell preparations on the flow cytometer oftentimes does not yield enough leukocyte events. The fact that renal cells are far in excess of leukocytes also renders detailed delineation of leukocyte subsets difficult, since it essentially requires multi-plex flow cytometry exceeding most 4-plex applications. Furthermore, renal cells are highly auto-fluorescent and endogenously express biotin, which make them difficult for most antibody and fluorescence-based applications, including IHC and flow cytometry. Consequently, studies which attempt to utilize flow cytometry on bulk renal single-cell preparations are faced with a series of technical impediments which limits interpretative power.

We used a novel isolation protocol combined with 10-plex flow cytometric methods to provide the first detailed cataloguing of renal leukocyte subsets. As a proof

of principle, we have chosen to use the anti-GBM sera challenge model of nephritis and a time-course experimental design to detail the number and type of infiltrating cells in this model. Our results demonstrate a specific order of leukocyte influx consistent with the current understanding of inflammatory processes—granulocyte influx, followed by monocyte influx, followed by T-cell influx, which coincided with peak proteinuria and serum BUN levels.

MATERIALS AND METHODS

Mice and anti-GBM sera challenge

Male 129/SvJ mice, 6-8 weeks of age were purchased from Jackson Laboratories (Bar Harbor ME) or derived at the University of Texas Southwestern Medical Center, and housed in the University of Texas Southwestern Medical Center Animal Resources Center's specific pathogen-free facility. The preparation of nephrotoxic rabbit sera (NTS) and nephrotoxic serum nephritis has been detailed in a previous communications [123-125]. Briefly, mice were immunized with rabbit IgG (day 0) and on day 5 intravenously injected with NTS. Mice were harvested on day 6, day 11, and day 14 for evaluation. The care and use of laboratory animals conformed to the National Institutes of Health guidelines and all experimental procedures conformed to an IACUC approved animal protocol.

Isolation of Renal Leukocytes

Mice were perfused with 20 ml cold PBS until kidneys were blanched. Kidneys were de-capsulated, and one-half of one kidney was harvested for histological analyses. The remainder were mechanically disrupted by vigorous mincing with razor blade and incubated with Digestion Buffer (1 mg/ml collagenase IV (Sigma-Aldrich) and 100 U/ml DNase (Roche) in RPMI1640 with 10% FCS) in a volume of 10 mL for 5 min in a 37°C water-bath, and then at 37°C for 30 min while shaking. Cells were further mechanically disrupted by passage through syringe and then subjected to hypotonic shock with Ack (potassium acetate) lysis buffer. Cells were washed with Wash Buffer (10% FCS in RPMI1640). Cells were further disrupted by passage through syringe, filtered, and then centrifuged at 3000 rpm at 25°C through a 40% Percoll gradient (40% Percoll in RPMI1640). Leukocytes were recovered in the pellet and then enumerated by trypan blue exclusion and subjected to FACS analysis.

Flow cytometry and antibodies

Antibodies to the following mouse antigens were used for flow cytometry analyses: CD138-PE, CD69-PE, CD69-PerCPCy5.5, Gr-1-APCCy7, CD45-FITC, NK1.1-PECy7, (BD Biosciences, Franklin Lakes, NJ); CD11b-APC, CD8-PECy7, CD44-APC, CD11c-PacificBlue, F4/80-PECy5, CD3-PacificBlue, CD4-AlexaFluor700 (eBioscience, San Diego, CA); CD19-PETexasRed, CD62L-PETexasRed, PDCA-1-Biotin, Strepavidin-QDot655 (Invitrogen, Carlsbad, CA). Samples were Fc-blocked with 2.4G2 (Invitrogen, Carlsbad, CA). For kidney samples, at least 5 x 10^5 cells were

acquired on the leukocyte gate, defined first by size and granularity of cells, then by pulse width properties for multiplet exclusion, and then by granularity and CD45 positivity. Samples were acquired on an LSRII flow cytometer (BD Biosciences, Franklin Lakes, NJ), and analyzed using Flow Jo software (Tree Star Technologies, San Carlos, CA). For analyses, a leukocyte gate was drawn as defined by granularity and CD45 positivity. Multiplets were then excluded on this population by drawing a singlet gate as determined by FSc-A and FSc-H.

Assessment of Renal Disease

24 hour urine samples were collected using metabolic cages for proteinuria analyses, which was assessed using the Coomassie Plus Protein Assay kit (Pierce, Rockford, IL) with BSA as a standard. OD630 was measured using an Elx800 Automated Microplate Reader (BioTek Instruments, Winooski, VT). Blood urea nitrogen (BUN) was assessed using the QuantiChrom Urea Assay kit (BioAssay Systems, Hayward, CA).

Statistical Analyses

A least squares linear regression model (Gauss-Markov) of the form, $Y = \beta 1 + \beta_2 X_2 + \ldots + \beta p X p + \varepsilon$, was used to assess the strength of correlation between renal cell subsets and proteinuria or serum BUN. The statistical package Intercooled STATA (StataCorp LP, College Station, TX) was used to analyze the data set. Pearson's co-efficients are reported. F-statistics and minimal prediction confidence intervals were

calculated to quality control the appropriateness of the linear regression model used. Comparisons of differences in mean were done using InStat3 or GraphPad 4 (GraphPad, San Diego, CA) as described in figure legends.

RESULTS

Preparation of renal cells for FACS analyses is detailed in Figure 3A. Unsurprisingly, we found that serial syringe filtration of bulk renal single-cell preparations greatly improved the dissociation of cell-conglomerates remaining from collagenase digestion, and provided disruption which did not interfere with cell-surface antigens which are sensitive to certain enzymatic digestions. To enrich for leukocytes from this preparation, a variety of Percoll density gradients were prepared and tested. 40% Percoll was selected as a gradient which would retain all leukocytes (as measured by CD45 positivity) in one fraction whilst excluding a large number of renal cells. Using this gradient, all of the leukocytes were recovered in the pellet (data not shown). By enriching for leukocytes and simultaneously assessing ten surface lineage markers, a highly detailed phenotyping of renal leukocytes was possible (Figure 3B). The gating strategy and cell-subset nomenclature found in Figure 3B are employed in all studies of renal leukocytes.

Using this isolation protocol, we subjected a series of 129/SvJ mice to anti-GBM sera challenge in order to get a detailed understanding of the kinetics of leukocyte influx and efflux. On the indicated days, mice were sacrificed and their renal leukocytes enumerated. We noticed a distinct pattern of cell influx and efflux (Figure 4). We found a large influx of neutrophils one day after anti-GBM sera administration, in the absence

of other appreciable changes in cellularity versus baseline. Neutrophils could be found in the kidney until three days post-challenge, and then decreased back to baseline numbers. A notable increase in activated monocytes was detected three days post-challenge and remained above baseline until the study was terminated. Six days following challenge, an impressive accumulation of T-cells, both naïve and antigen-experienced, was detected. This accumulation of T-cells coincided with peak proteinuria and serum BUN. Regression analyses found highly significant correlation between T-cells—and no other cell types—and proteinuria and BUN ($p<0.001$).

DISCUSSION

We demonstrate the applicability of a novel technique in characterizing and enumerating total renal leukocytes by flow cytometry by cataloging the kinetics of leukocyte trafficking into and out of the kidneys of anti-GBM serum challenged mice. This study illustrates the potential usefulness of this isolation protocol for studying diseases of the kidney where infiltrating leukocytes play an indispensable role, such as lupus nephritis, Goodpasteur's syndrome, ischemia reperfusion, among others.

This isolation protocol helps overcome the largest impediment in meaningfully analyzing total renal leukocytes, which is that they are by far outnumbered by renal cells. This fact has made interpretation of many assays, not just quantitation by IHC or conventional flow cytometry, performed on bulk renal single cell preparations problematic. For example, it is difficult to interpret real time PCR results performed on RNA prepared from bulk renal single cell preparations using standard housekeeping genes (i.e., β2m, actin, etc.), especially if one wants to get an idea of the transcriptional

regulation of the gene in the leukocyte population. Moreover, since a wild-type kidney contains much less infiltrates than a diseased kidney, the ratio of leukocyte to kidney RNA also differs greatly, and is not captured by standard house-keeping genes used for normalization. By first enriching the bulk kidney for leukocytes using the described protocol, and then cell-sorting for the population of interest, more controlled experiments can be performed. This isolation protocol simplifies the technical limitations of working with a tissue where the cell-type of interest is not well well-represented in the total sample. And most powerfully, this technique allows for absolute quantification of all cell subsets that can be resolved by flow cytometry.

In our kinetic analyses of anti-GBM sera challenge, we found a trafficking pattern of leukocytes consistent with current immunological dogma. We found early infilitration by granulocytes and cells of the myeloid lineage, followed by an influx of CD4 and CD8 T-cells. Interestingly, the presence of CD4 cells was found to be correlative with the onset of detectable loss in renal function as assessed by proteinuria and serum BUN levels. This observation is consistent with a wealth of early and recent studies describing the indispensability of CD4 T-cells in the development and severity of nephritis [126-129].

***In Vitro* Splenocyte Stimulation.**

Sterile splenocyte suspensions were plated in triplicate at 0.5 X 10^6 cells/ml in complete medium (RPMI1640 with L-glutamine, 10 % FCS (HyClone, Logan, UT), HEPES (Sigma-Aldrich, St. Louis, MO), 1X Pen/Strep (Sigma-Aldrich, St. Louis, MO), beta-2 mercaptoethanol (Sigma-Aldrich, St. Louis, MO), L-glutamine (Sigma-Aldrich, St.

Louis, MO)), with varying concentrations of the following stimuli: recombinant CXCL12 (R & D Systems, Minneapolis, MN), with or without anti-IgM F(ab)'$_2$, anti-CD40 (Jackson ImmunoResearch, West Grove, PA). Cells were cultured at 37°C for 72 h and analyzed by flow cytometry.

Transwell Migration.

6.5 mm Transwell plates with 5.0 μm pore polycarbonate membranes (Corning Inc., Corning, NY) were used. Briefly, 600 μl of 50 ng/ml CXCL12 in complete RPMI 1640 medium were placed in the lower chamber and pre-incubated at 37°C for 2 hours to equilibrate the membrane. Sterile splenocyte suspensions were prepared, and 1.5 X 10^6 cells in 100 μl volume were loaded into the upper well of the transwell plate. In some experiments, cells were resuspended in complete RPMI medium containing various doses of the CXCR4 inhibitor CTCE-9908 (Chemokine Therapeutics, Vancouer, Canada). Cells were allowed to migrate for 2 hours at 37°C. Cells in the lower chamber were counted using trypan blue exclusion and analyzed by flow cytometry.

Renal Cell Supernatant and ELISA.

Mice were perfused with 20 ml PBS, and renal single cell suspensions of the kidney were prepared (500 μl PBS per 2 kidneys). Cell suspensions were centrifuged at 1500 rpm for 7 min, supernatant collected and further centrifuged at 14000 rpm for 10 min. Supernatant was collected and used at various dilutions to quantitate CXCL12 concentration by ELISA (R & D Systems, Minneapolis, MN). OD_{450} was measured by an

Elx800 Automated Microplate Reader (BioTek Instruments, Winooski, VT) and concentrations were extrapolated from a 4-point standard curve ($R^2 > 0.99$), where the mean of experimental duplicates was used.

Immunohistochemistry.

Paraffin sections of kidney (5-μm) were boiled in 10 mM citrate, quenched with 0.01% NaBH4, blocked with murine IgG (Jackson ImmunoResearch, West Grove, PA), and stained with mouse monoclonal anti-SDF-1/CXCL12 antibody (R & D Systems, Minneapolis, MN) at 4°C overnight. Sections were then washed and incubated with goat anti-mouse conjugated to Cy3 (Jackson ImmunoResearch, West Grove, PA) for 1 h at room temperature. Sections were washed and then mounted with Vectashield (Vector Laboratories, Burlingame, CA), visualized and photographed with a Zeiss Axioplan 2 and digital camera (Carl Zeiss International, Germany), and analyzed with Axiovision software (Carl Zeiss International, Germany).

***In vivo* inhibition of CXCR4.**

The peptide antagonist CTCE-9908 (Chemokine Therapeutics, Vancouer, Canada) was resuspended in 5% dextrose water. Two cohorts of B6.*Sle1Yaa* male mice were assembled for the *in vivo* "prevention" or "treatment" studies. In "Cohort I", comprising of 2-mo-old mice, 5 were injected with vehicle and 11 received CTCE-9908. In "Cohort II", comprising of ANA-seropositive 4-mo-old mice, 5 were injected with vehicle and 8 were injected with CTCE-9908. In both study groups, 100 μl of CTCE-9908 at 50 mg/kg

or vehicle placebo were injected intraperitoneally three times a week for the course of study. All mice were monitored for serum autoantibodies, proteinuria, azotemia, and evidence of renal pathology, as detailed below.

Serology.

Mice were bled before and at 1, 2, 3, and 4 mo after treatment with CTCE-9908 or placebo and the sera were stored at -20°C. ELISA detection of serum IgM and IgG autoantibodies directed against chromatin and dsDNA were performed as described previously [116]. OD_{450} was measured using an Elx800 Automated Microplate Reader (BioTek Instruments, Winooski, VT) and the raw optical densities for anti-chromatin ELISAs converted to arbitrary normalized units using a six-point standard curve generated by an anti-nuclear mAb derived from a NZM2410 mouse [116].

Assessment of Renal Disease.

24 hour urine samples were collected using metabolic cages for proteinuria analyses, which was assessed using the Coomassie Plus Protein Assay kit (Pierce, Rockford, IL) with BSA as a standard. OD_{630} was measured using an Elx800 Automated Microplate Reader (BioTek Instruments, Winooski, VT). Blood urea nitrogen (BUN) was assessed using the QuantiChrom Urea Assay kit (BioAssay Systems, Hayward, CA). Glomerular and tubulo-interstitial disease was assessed as detailed previously [130].

Statistical Analysis.

Data were analyzed using InStat3 or GraphPad 4 (GraphPad, San Diego, CA). Where appropriate, one-way ANOVA with Dunnet or Bonferonni post hoc analysis, Welch t-test, Mann-Whitney U-test, or log-rank Mantel-Cox test were used. In the *in vivo* inhibition studies using CTCE-9908, due to early mortality of placebo control mice, 5 month old B6.*Sle1Yaa* mice, which were not statistically different than placebo controls in their phenotypes were pooled with the remaining placebo controls for the statistical analyses. Error bars represent SEMs.

TABLES AND FIGURES

A

- Perfuse mouse with 20 mL cold PBS
- Harvest kidney and decapsulated
- Finely chop kidney with flat razor blade
- Collect kidney in 10 mL Digestion Buffer
- Incubation 5 minutes at 37C
- Incubation 30 minutes at 37C, with agitation
- Passage through 22-gauge needle in 5 ml syringe
- Centrifuge 1100 rpm, 4C, 5 min
- Decant and resuspend pellet in 5 ml Ack Lysis Buffer
- Adjust volume to 10 ml with Wash Buffer
- Centrifuge 1100 rpm, 4C, 5 min
- Decant and resuspend pellet in 5 ml Wash Buffer
- Passage through 22-gauge needle in 5 ml syringe
- Filter through nylon mesh
- Wash mesh and syringe with an additional 5 ml
- Apply 10 mL 40% Percoll Solution and mix gently
- Centrifuge 3000 rpm, 25C, 20 min
- All leukoyctes are recovered in the pellet

B

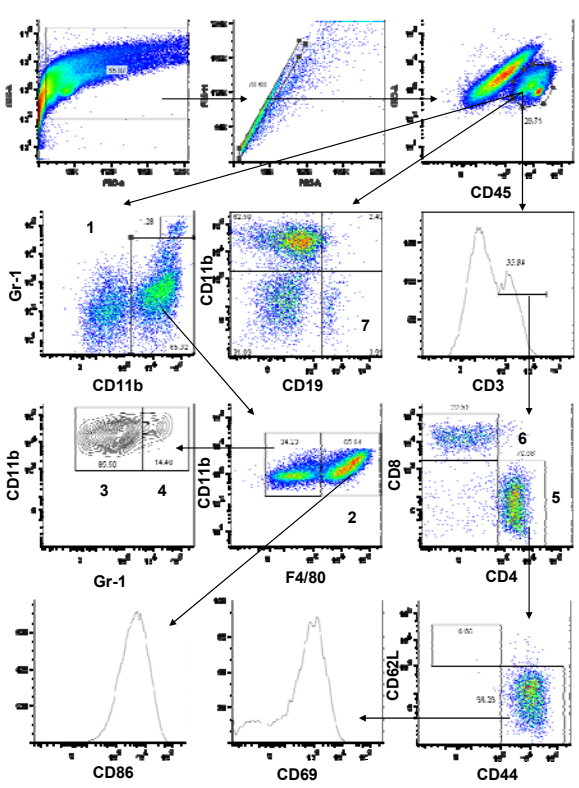

Figure 3. Isolation protocol and renal leukocyte designation and analyses.
In A) is listed the isolation protocol for renal leukocyte FACS. Buffer compositions can be found in the Materials and Methods of this section. In B), FACS analyses of renal leukocytes is schematized. Numbered populations are defined as follows: 1) Neutrophils, 2) Macrophages, 3) Resident monocytes, 4) Inflammatory monocytes, 5) CD4 T-cell, 6) CD8 T-cell, 7) B-cell

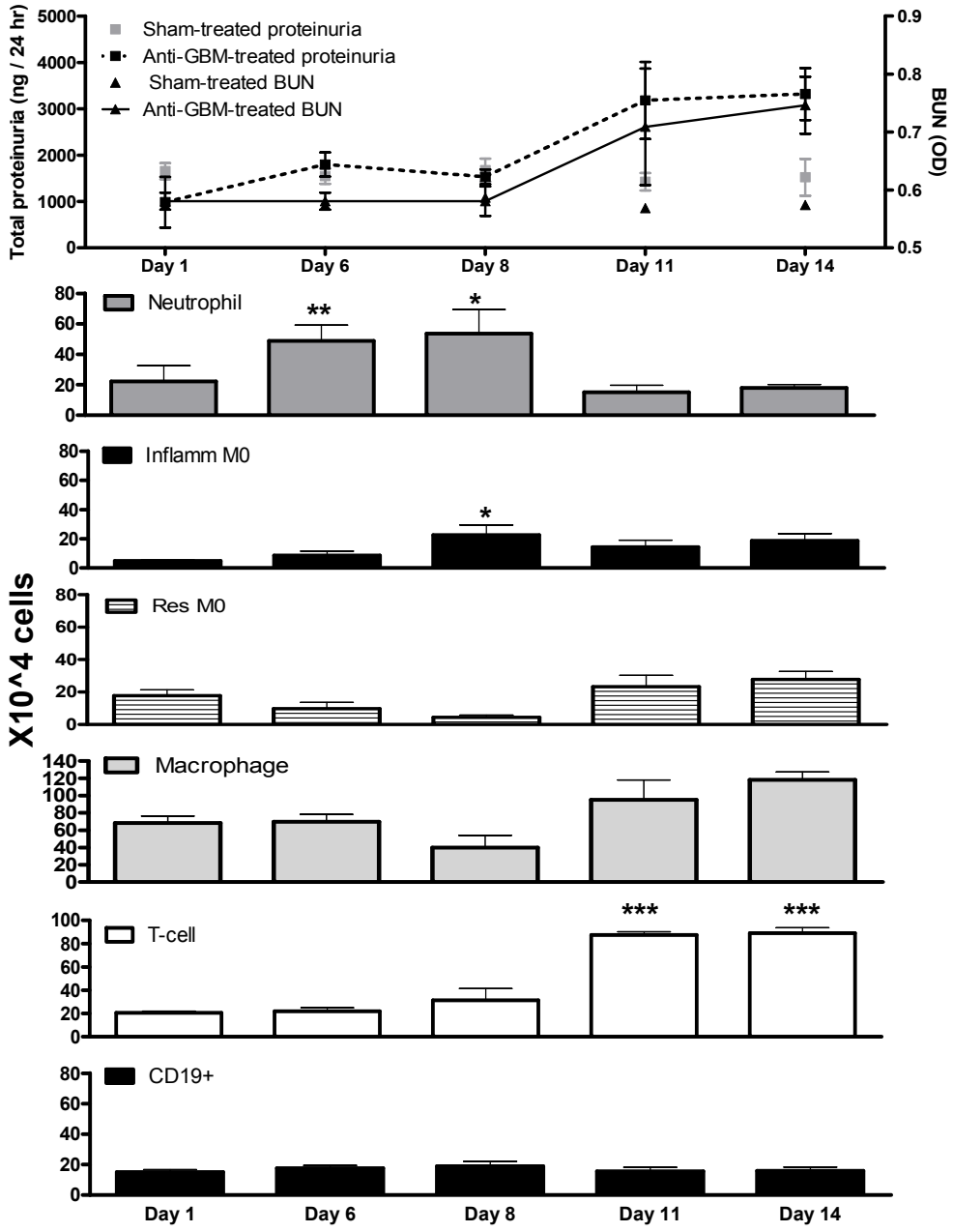

Figure 4. Evolution of proteinuria, serum BUN, and renal leukocyte content over the course of anti-GBM-induced nephritis.
Shown in the top panel is the evolution of proteinuria (left axis, boxes) and BUN (right axis, triangles) as it corresponds to the renal content of various leukocyte subsets. Shown P values pertain to comparisons of differences in cell numbers for a given subset between days post anti-GBM administration by ANOVA (Bonferroni post-hoc test, *, $P < 0.05$; **, $P < 0.01$; ***, $P < 0.001$).

CHAPTER THREE: Regulation of Thymic Selection by the Lupus Susceptibility Gene *Ly108*

INTRODUCTION

One of the hallmarks of systemic lupus erythematosus (SLE), both in humans and mice, is the loss of tolerance towards nuclear antigens, resulting in the production of antinuclear autoantibodies (ANA). It is clear that genetic predisposition is a central element in susceptibility to systemic lupus erythematosus (SLE) [14, 26]. To identify the susceptibility loci in SLE, our group has performed congenic dissection in the lupus-prone NZM2410 mouse model, and work to date has revealed three major disease-linked loci, *Sle1, Sle2,* and *Sle3* [70]. *Sle1*, located on a region of chromosome 1 syntenic between mouse and man, was found to be causal for the breach in immune tolerance that culminates in antinuclear autoantibody (ANA) production on the B6 background [37, 42, 70]. Fine mapping of *Sle1* revealed a cluster of four loci, designated *Sle1a–Sle1d* [131], of which *Sle1b* was found to be the most potent member, indispensably mediating a gender-biased and highly penetrant ANA production [115, 132].

The B6.*Sle1b* congenic develops high-titer IgG anti-nuclear autoantibody (ANA) directed towards H2A/H2B/dsDNA subnucleosomes at 90% penetrance at 9 months of age [43, 132]. The strongest candidate genes in the *Sle1b* locus to date remain the SLAM/CD2 gene cluster, and in particular, the family member *Ly108*, based on its highly polymorphic nature, diverse roles in immune biology [31, 133] and recently demonstrated associations between the SLAM family and SLE in humans [115]. Moreover, using a BAC-transgenic rescue approach, we recently showed that, of the

SLAM/CD2 family members, only *Ly108* and *Cd84* on B6.*Sle1b* were required to mediate the breach of tolerance to chromatin [115]. In addition, recent work in our lab has implicated a clear role for the NZM2410-derived autoimmune *z* allele of *Ly108* in the induction of B-cell anergy [35]. The production of high-affinity IgG ANA by B-cells from B6.*Sle1b* mice prompted us to investigate if $Ly108^{z}$ could also play a role in the T-cell compartment, and, specifically--given the role of $Ly108^{z}$ in early B cell development--in the thymus.

T cells play a central role in driving the development of lupus, both in mouse and man [134]. In addition to rendering help to B cells for autoantibody production, immunoglobulin class-switching and affinity maturation, T cells promote disease pathology in a other ways, including facilitating tissue damage in the end organs [135-137]. Indeed, previous studies demonstrated that ablation of CD4 T cells using genetic or experimental approaches had the potential to ameliorate disease [138-140]. It was further shown that lupus-prone mice defective in class switch and somatic hypermutation do not develop IgG ANA and subsequent lupus pathologies, illustrating the indispensable role of T-cells in mediating the disease [141]. Although it is evident that T cells are essential for disease, the degree to which genetically dictated, intrinsic T cell anomalies contribute to lupus is not clear.

Here we investigate the role of a spontaneously occurring polymorphism in the SLAM/CD2 family receptor member, Ly108, in mediating T-cell tolerance and disease pathogenesis in murine lupus.

RESULTS

Sle1b mediates a defect in thymic tolerance

In 8 to 12 month old B6.*Sle1b*.OTII mice, where greater than 40% of the thymocytes are specific for OVA (data not shown), there was no difference observed in the IgM ANA titer (Figure 5A), whereas there was a marked reduction in IgG ANA titers (Figure 5A) compared to B6.*Sle1b* controls ($P<0.02$), indicating a direct role for *Sle1b* in dictating an autoimmune T-cell repertoire. Moreover, in 8 week old B6.*Sle1b* mice, thymic cellularity was significantly increased compared to B6 controls ($P<0.02$) (Figure 5B). This increase was observed for all thymic subsets: double negative ($P<0.02$), double positive ($P<0.02$), single-positive CD4 ($P<0.01$) and CD8 ($P<0.02$) thymocytes. Specifically, we noted no differences between B6 and B6.*Sle1b* in the final developmental stages of both double-negative and double-positive thymocytes, DN4 and the positively selected CD69+ CD5+ double-positive thymocytes, respectively. By contrast, the number of late single-positive CD4+ CD69- CD62L+ cells were significantly increased in B6.*Sle1b* versus B6 mice suggesting a preferential alteration in negative selection in B6.*Sle1b* mice ($P<0.02$). Moreover, differential Vβ usage (Figure 5 C, Figure 6A) was observed in single-positive CD4 and CD8 cells in B6.*Sle1b* animals compared to B6 mice. Together, these data clearly demonstrate that *Sle1b*^{z} is responsible for a significant qualitative and quantitative perturbation in thymocyte subsets, highlighting its role in thymic selection.

Ly108 is the causative lesion in *Sle1b*

To investigate the causative genetic lesion within *Sle1b* mediating this loss of thymic tolerance, we surveyed the expression of Ly108, CD84, and Ly9, which were shown to be the key genes in the SLAM/CD2 family mediating humoral autoimmunity [115]. We found that B6.*Sle1b* thymic and splenic T-cell subsets expressed 1.5-fold less total cell-surface Ly108 compared to B6 controls and that, moreover, Ly108 expression was tightly regulated as cells progressed though T-cell development (Figure 5D). Except for the early double negative stage DN1, we were unable to detect any significant differences in CD84 or Ly9 expression (Figure 6B).

We further observed that cell-surface expression levels of Ly108 correlated tightly with anti-chromatin IgG ANA titers. We recently reported that a B6.*Sle1b* mouse transgenic for the non-autoimmune $Ly108^b$ and $Cd84^b$ alleles (B6.*Sle1b*.388C4) was able to reduce the penetrance of ANA positivity to less than 30% [115]. We found that, in fact, all seropositive B6.*Sle1b*.388C4 mice displayed inappropriately reduced cell-surface levels of Ly108 (Figure 5E) despite successfully incorporating the BAC transgene, suggesting that either or both the $Ly108^z$ and $Cd84^z$ alleles are directly mediating the breach in tolerance to chromatin. Moreover, we show that the altered cell-surface expression of Ly108 is gene-intrinsic and is directly caused by the $Sle1b^z$ haplotype [31] and not background modifiers, as shown by the significant decrease in the expression of Ly108 on thymocytes derived from BALB/c ($P<0.001$ vs B6 mice) and 129/SvJ ($P<0.001$ vs B6 mice) mice, which share the $Ly108^z$ allele with B6.*Sle1b* (Figure 6C). Despite containing the autoimmune $Sle1b^z$ haplotype, however, neither BALB/c nor 129/SvJ spontaneously develop autoimmunity, indicating a clear role for epistatic modifiers of

Sle1b^{z}-mediated autoimmunity [41]. We also observed cell-surface Ly108 expression differences in primary and secondary B-cells in B6.*Sle1b* mice compared to B6 controls, which was not surprising given our recent work delineating the role of Ly108 in the control of B-cell tolerance [35] (data not shown).

B6.Sle1b thymocytes are protected from apoptosis in vitro via Ly108 signaling

To directly test the effect of Ly108 on thymocyte function, we used the commercially available monoclonal functional-grade anti-Ly108 antibody, which we determined to be an activating antibody via the assessment of B and T-cell activation status (Figure 7A) and the production of IL4 and IFN γ secretion of splenic T-cells following ligation (Figure 7B).

B6.*Sle1b* double-positive thymocytes were found to be more resistant to CD3-induced apoptosis ($P<0.01$) (Figure 6A). Moreover, whereas Ly108 stimulation had little effect on CD3-induced cell-death of thymic single-positive CD4 cells in B6 controls, it seemed to eliminate CD3-induced cell-death in B6.*Sle1b* thymocytes (Figure 6B). B6.*Sle1b* double positive thymocytes were also found to be less sensitive to serum starvation-induced apoptosis ($P<0.02$) (Figure 7D), and dexamethasone-induced apoptosis ($P<0.01$) (Figure 7C), demonstrating a clear role for *Sle1b*^{z} on thymocyte apoptosis *in vitro*.

Ly108^{z} signaling rescues CD3-mediated and antigen-specific-mediated deletion

These data were corroborated *in vivo* by testing the effect of Ly108 signaling on CD3-induced apoptosis (Figure 8, Table 6. Thymus cell subsets after Ly108 Ab

treatment). Similar to the data obtained *in vitro*, co-administration of anti-Ly108 antibody and anti-CD3 intravenously into B6.*Sle1b* led to protection of apoptosis in single-positive CD4 but not in double-positive thymocytes ($P<0.02$) (Figure 8D). Surprisingly, whereas engagement of Ly108 *in vivo* was protective of naturally occurring antigen-induced deletion in B6.*Sle1b*, ligation of Ly108 in B6 mice led to added deletion in both single-positive CD4 and double-positive thymocytes (Figure 8E). Indeed, signaling through $Ly108^z$ led to a 1.3-fold increase in cellularity in B6.*Sle1b* ($P<0.02$) but not in B6 controls, where signaling through $Ly108^b$ significantly decreased thymic cellularity ($P<0.01$). Since B6.*Sle1b* expressed less cell-surface Ly108, we confirmed, by *in vivo* titration of the antibody, that these results were not a function of the concentration of antibody used *in vivo*, as saturation was achieved in both strains at the concentration employed (Figure 7B).

To directly test the effect of Ly108 on thymic selection *in vivo*, we generated B6.*Sle1b*.OTII mice. B6.*Sle1b*.OTII leukocytes expressed Ly108 at identical levels to B6.*Sle1b* and displayed no obvious differences in the number of transgenic T-cells or all other leukocyte subsets compared to B6.OTII mice (data not shown). When we simultaneously administrated OVA and anti-Ly108 antibody, we observed a complete protection of OVA-induced deletion in B6.*Sle1b*.OTII mice but not in B6 controls (Figure 8F).

These data demonstrate that $Ly108^z$ but not $Ly108^b$ protect deletion of autoreactive T-cells in the thymus.

Ly108^{b} and *Ly108*^{z} alleles exhibit distinct proximal signaling characteristics

To understand the mechanism by which Ly108 was impacting thymic deletion, signal transduction via Ly108, as well as analyses of differential gene expression subsequent to Ly108 signaling were assayed in B6.*Sle1b* and B6 mice 24 hours after injection of anti-Ly108 antibody. We did not detect a complete elimination of autoimmunity observed in B6.*Sle1b*.*SAP*^{ko} mice (Figure 9), suggesting a yet unidentified adaptor molecule operating in the thymus. We also did not detect any differences in proximal TCR signaling (Figure 10).

Thymocytes were harvested from B6 and B6.Sle1b mice prior to and 48 hours following anti-Ly108 mAb administration. Whole cell lysates and immunoprecipitates with anti-Ly108 were subjected to Western blot analysis. Figure 11A confirms that Ly108 expression was lower in B6.Sle1b versus B6 thymocytes, which is consistent with the flow cytometry data. Treatment with anti-Ly108 mAb did not change the overall expression levels of Ly108 or the adaptor, SAP, in either strain. Interestingly, in spite of lower levels of expression in B6.Sle1b thymocytes, Ly108 showed higher phosphorylation and SAP association either prior to or following antibody treatment compared to B6 thymocytes, indicating that Ly108z expressing thymocytes exhibit enhanced signaling through Ly108. The increased association of SAP with Ly108 in B6.Sle1b compared to B6 indicates that B6.Sle1b thymocytes have increased levels of phosphorylated Ly108 prior and subsequent to ligation with Ly108. These results imply that the anti-Ly108 mAb is indeed an agonist since it results in enhanced phosphorylation of Ly108z following treatment both in vivo (Figure 11B) and in vitro on transfected cells (data not shown). We have also observed increased expression of CD69 and cytokine

production in mature T cells following anti-Ly108 mAb engagement (data not shown). The results presented in Figure 3 also imply that the predominant expression of the Ly108-1 isoform by B6.Sle1b thymocytes results in stronger signaling potential than is exhibited by the Ly108-2 expressing B6 thymocytes, clearly delineating significant functional variations between these two isoforms. These data are consistent with recently published reports of Ly108 isoform signaling [142].

Ly108^{z} signaling leads to differential gene expression in B6.Sle1b thymocytes

Microarray analyses of thymocytes harvested 24 hours after *in vivo* administration of anti-Ly108 antibody revealed significant dysregulation of 25 genes. Amongst the dysregulated genes, *Calm2* (1.7-fold reduced versus B6) and *Fbxw5* (1000-fold increased versus B6) were the strongest candidates given their purported roles [143, 144] in modulating intracellular calcium and cell-cycle progression, respectively. *Calm2* hypoexpression was confirmed by RT-PCR analyses (Figure 12B). Further work is being done on *Fbxw5* to confirm its overexpression by RT-PCR.

Ly108^{z} signaling decreases thymocyte apoptosis by modulating calcium metabolism

Calm2 encodes calmodulin 2, a member of calcium-binding proteins critical in calcium-mediated signal transduction [144]. Calcium flux subsequent to TCR-ligation is critical in determining thymocyte apoptosis and selection [145, 146]. Since we observed a 1.7-fold decrease in *Calm2* in B6.*Sle1b* following Ly108-crosslinking, we tested the ability of primary B6.*Sle1b*.OTII and B6.OTII thymocytes to flux calcium.

We found that B6.*Sle1b*.OTII thymocytes fluxed significantly less calcium upon CD3-crosslinking compared to B6.OTII controls over a range of CD3 concentrations (Figure 13A, Figure 14). When we crosslinked both CD3 and Ly108, we found that, while B6.OTII thymocytes did not respond differently, a substantial difference in kinetics was observed in B6.*Sle1b*.OTII thymocytes. Indeed, B6*Sle1b*.OTII thymocytes exhibited a 12 second lag in peak calcium flux when engaged with Ly108 in concert with CD3. Moreover, we found the defect in calcium flux to be primarily a dysregulation in the intracellular stocks of calcium in B6.*Sle1b*. Indeed, we observed marked differences in calcium flux following thapsigargen stimulation in B6.*Sle1b* compared to B6 controls (Figure 13B).

This difference in calcium metabolism translated to differences in apoptosis subsequent to Ly108 ligation. Analyses of the expression of apoptotic molecules revealed a significant difference in the expression of the pro-apoptotic molecule Bak, which was decreased in treated B6.*Sle1b* thymocytes when compared to B6 controls. We detected no differences in proximal CD3 signaling, CD3 expression, Ly108 localization with the CD3 complex, or a variety of other apoptotic molecules (Figure 10). We confirmed this decrease in thymocyte apoptosis observed in *B6.Sle1b* but not in B6 subsequent to anti-Ly108 injection *in situ* using TUNEL staining. We observed significantly less DNA fragmentation in treated B6.*Sle1b* mice compared to B6 controls ($P<0.02$) (Figure 13D).

Taken together, these data show that $Ly108^z$ acts to decrease thymocyte apoptosis by down-modulating calcium metabolism.

Ly108^z signaling decreases thymocyte apoptosis by modulating thymocyte cell cycle

Fbxw5 encodes a member of the F-box protein family which has recently been shown to impact thymic selection by controlling cell-cycle exit [147]. Thus, we wanted to investigate whether Ly108 signaling played any role in thymocyte cell-cycle regulation. Using BrdU incorporation assays, we detected an impressive arrest of cells in G0/G1 phase at 36 hours following anti-Ly108 injection in B6.*Sle1b* but not B6 mice (Figure 15A, Figure 17). As thymocyte deletion occurs typically in S phase [148], such an arrest in G0/G1 phase, coupled with decreased calcium mobilization, would enhance protection of potentially autoreactive thymocytes from deletion.

To determine the molecular mechanisms by which engagement of Ly108 affects thymocyte cell cycle regulation, we examined the expression of key cell cycle regulatory proteins in thymocytes from B6 and B6.Sle1b mice prior to and after anti-Ly108 mAb injection. Progression through each stage of the cell cycle is driven by a group of cyclin-dependent kinases (cdks) and their regulatory cyclin subunits. Active cdk2/cyclin E complexes, for example, phosphorylate key nuclear factors, which are required for the G1/S transition, and commit the cell to DNA replication [149]. Similarly, the kinase activity of cdk1/cyclin B is necessary for the initiation of mitosis. In actively dividing, non-malignant cells, cdk protein levels remain stable throughout the cell cycle, so the kinase activity of these complexes is generally regulated by other methods, including cyclin expression, activating and inhibitory phosphorylation events, and Cdk inhibitors (CDKs) [150].

Figure 16 shows Western blot analysis of whole cell lysates from B6 and B6.Sle1b thymocytes at 0, 12, and 24 hours following anti-Ly108 mAb injection. Lysates

were subjected to SDS-PAGE electrophoresis and immunoblotted with antibodies against various proteins, including ERK2 to control for loading. In Fig. 7A, the active form of Cdk2, represented by the faster migrating band at 33kDa, was expressed at similar levels in both strains and remained unchanged following anti-Ly108 mAb injection. However, phosphorylation of Cdk2 on threonine 160, which is required for full kinase activity [151], decreased in both B6 and B6.Sle1b mice after antibody administration with a more pronounced effect observed in B6.Sle1b thymocytes.

During G0 and G1 phase, Cdk2 kinase activity is also negatively regulated by association with a cdk inhibitor known as p27Kip1 [152-154]. In Fig. 7B, examination of p27 levels in thymocytes revealed a dramatic increase in p27 expression in thymocytes from both B6 and B6.Sle1b following anti-Ly108 injection. However, the kinetics and magnitude of this increase differed between the two strains. Compared to B6, p27 increased at an accelerated rate in B6.Sle1b thymocytes, resulting in higher p27 levels after 24 hours.

The inhibitory activity of p27 can also be regulated through a series of phosphorylation events, which influence subcellular localization, as well as protein turnover [155]. Phosphorylation on serine 10 affects p27 differently, in a cell cycle-dependent manner [156]. However, Figure 16B shows that phospho-p27(S10) levels were similar in both strains, and remained unchanged in response to antibody injection. Therefore, it appears that anti-Ly108 injection may affect cell cycle progression by increasing p27 levels that could result in a decrease in Cdk2 activity, and this seems to be more pronounced in B6.Sle1b thymocytes showing an accumulation of cells in G0/G1 and G2+M.

To examine Cdk2 kinase activity directly, we immunoprecipitated Cdk2 from thymocyte lysates and used this for an in vitro kinase activity with Histone H-1 as a substrate. Figure 16C shows that Cdk2 kinase activity was decreased in B6.Sle1b thymocytes 24 hours post Ly108 mAb injection. This outcome correlates with the peak accumulation of p27 and suggests that the observed cell cycle arrest is due to diminished Cdk2 kinase activity.

These data demonstrate that Ly108^{z} ligation leads to modifications in the regulation of key cell-cycle molecule.

Together these data demonstrate that Ly108 plays a key role in thymic selection and that the autoimmune allele of *Ly108* mediates a breakdown in thymic selection via modifications of cell-cycle control and calcium mobilization leading to the development of autoimmunity (Figure 18).

DISCUSSION

We demonstrate that the *Ly108*^{z} allele, derived from the *Sle1b* locus, plays a pivotal role in thymic selection by modulating cell-cycle progression and sensitivity to apoptosis. The critical role for T cells in the development of autoimmunity was evidenced by the significant decrease in the observed titer and incidence of ANAs in B6.*Sle1b* mice carrying the OTII transgene compared to B6.*Sle1b* controls. This marked reduction in IgG ANA titers, but not IgM titers, indicated that control of the T cell repertoire by *Sle1b* plays a key role in mediating humoral autoimmunity. This hypothesis

was further supported by the thymic hypercellularity and differential Vβ usage in single-positive CD4 and CD8 thymocytes observed in B6.*Sle1b* mice.

We show that the defect in central tolerance mediated by *Sle1b* is mediated by *Ly108*. Analyses of thymic expression patterns of the SLAM/CD2 family members Ly108, CD84, and Ly9 [157], along with our analyses of autoimmunity in B6.*Sle1b* mice transgenic for the non-autoimmune alleles of Ly108 and CD84, and the manipulations utilizing a monoclonal anti-Ly108 antibody, favor the hypothesis that Ly108 is the key molecule that impairs thymic selection and thus responsible for autoimmunity towards chromatin antigens. This observation is well-supported by the recently uncovered role of Ly108 in maintaining B-cell tolerance, where it was demonstrated that the preferential expression of the autoimmune *Ly108*^{z} allele on B cells of B6.*Sle1b* mice decreased the sensitivity of immature B cells to deletion via induction of RAG re-expression [35]. Moreover, the role of the SLAM family members and, in particular, of Ly108, in NK T cell differentiation in the thymus, was recently described [158]. Li et al showed that Ly108, through homotypic self-interactions on thymocytes, provided costimulatory signals which, in synergy with TCR signaling, were required to drive NK T-cell differentiation [159]. Our report is the first demonstration that the same homotypic signals play a role during conventional T cell development in the thymus. Our results show that a decrease in Ly108 expression in the thymus, in this case mediated by a naturally occurring polymorphism, is associated with alterations in thymic selection. The molecular explanation for this decrease in surface Ly108 expression observed likely represents a defect in protein translation or transcript stability mediated by the *z* haplotype and warrants further study.

To understand the mechanism by which Ly108 affects thymic selection, we assayed the sensitivity of thymocytes from B6 and B6.*Sle1b* mice to apoptosis. Under basal conditions *in vitro*, double-positive B6.*Sle1b* thymocytes were found to be more resistant to apoptosis induced by CD3-crosslinking, dexamethasone exposure, and serum starvation compared to B6 thymocytes. We interpreted these results as an effect of homotypic Ly108 interaction in culture, although the interpretability of these results was ultimately limited by the known difficulties in handling thymocytes in tissue culture. Subsequently, we moved into an *in vivo* system, with the use of an anti-Ly108 antibody with stimulatory properties. By injecting saturating doses of Ly108, we were able to test the effects of Ly108 signaling on CD3-induced apoptosis. In this system, we demonstrated that single-positive CD4 thymocytes were protected from CD3-mediated cell-death, indicating a role for Ly108 in mediating negative selection. This hypothesis was formally demonstrated by the complete protection of OVA-induced deletion in B6.*Sle1b*.OTII mice but not in B6.OTII controls when OVA was simultaneously administrated with anti-Ly108 antibody. The demonstration that $Ly108^{z}$ but not $Ly108^{b}$ protects autoreactive cells from deletion by inhibiting apoptosis was also observed for B cell development [35], where Ly108 seemed to act as a molecular thermostat with which self-reactive B cells are censored during early development. Our results extend these observations to T cells and place Ly108 as a key component for deletion of autoreactive cells within central lymphoid organs in general.

Our results, which link a reduction in surface Ly108 expression with impaired thymic tolerance, are in contradiction with studies performed in the "pseudo Ly108 knockout" mice [133], which display no abnormalities in thymic tolerance. Several

explanations could account for the discrepancy in these results. First, the "pseudo Ly108 knockout" mice are "pseudo" knockouts for Ly108 because, although they lack two exons in the extracellular domains, they still possess the entire intracellular domain replete with all signaling moieties required for tonic signaling, independent of receptor ligatiion. Second, these pseudo knockout mice have been studied on a mixed 129/B6 background, which contain both the autoimmune $Ly108^z$ and the non autoimmune $Ly108^b$ alleles of Ly108 as well as, more importantly, background modifiers which are capable of fully suppressing autoimmunity. Indeed, in this report, we show that the altered cell-surface expression of Ly108 is gene-intrinsic and is directly caused by the *Sle1b*^{z} haplotype [31] and not background modifiers, and that, despite containing the autoimmune *Sle1b*^{z} haplotype, neither BALB/c nor 129/SvJ spontaneously develop autoimmunity, indicating a clear role for epistatic modifiers of *Sle1b*^{z}-mediated autoimmunity [41]. These experiments highlight the highly complex epistatic nature of lupus susceptibility and provide direct evidence that it is the alteration in surface Ly108 expression in conjunction with an appropriate genetic background that together mediate autoimmunity.

To understand the mechanism by which Ly108 impacted thymic deletion, signal transduction via Ly108 was assayed in B6.*Sle1b* and B6 mice 24 hours after injection with anti-Ly108 antibody. We first asked whether proximal signal transduction was different between B6.*Sle1b* and B6 thymocytes following Ly108 ligation, since, in addition to differences in cell-surface expression described in this communication, there are known differences in the Ly108 signaling domains between B6.*Sle1b* and B6 [31]. Notably, there is increased representation of the isoform of Ly108 which contains one

less intracellular tyrosine stimulating motif (ITSM) domain, resulting in an overall decrease in net surface-Ly108 ITSMs in B6.*Sle1b* mice vis a vis B6 mice. Since we injected anti-Ly108 antibody at saturating doses for both B6.*Sle1b* and B6 controls, we interpreted the observed differences in thymic tolerance as intrinsic to both the quantity of signal transduction, as well as the quality of signal transduction, which is realized through the differential signaling modalities present between the two strains. In thymocytes, SLAM-receptor-initiated signaling is mediated at least in part by SLAM associated protein (SAP), an adaptator which recruits the Src kinase Fyn, which in turn phosphorylates the SLAM receptor and further recruits another set of signaling molecules [160]. SAP deficient humans and mice exhibit a marked impairment of antibody production with severe defects in B cell isotype switching, affinity maturation and memory B cell generation [161]. Our results clearly indicate that Ly108z represents a gain of function polymorphism in comparison to Ly108b. In spite of the increased expression of Ly108 in B6 thymocytes, Ly108 engagement appeared to more effectively initiate proximal signaling events in B6.Sle1b thymocytes, as evidenced by enhanced receptor phosphorylation and SAP adaptor recruitment. This is in accordance with recently published studies examining Ly108-1 and Ly108-2 signaling in transfected cell lines wherein Ly108-1 exhibited higher baseline phosphorylation and association with SAP. All of these characteristics indicate that Ly108z is intrinsically more activated in thymocytes and signals more strongly in response to ligation.

Analyses of differential gene expression were performed in B6.*Sle1b* and B6 mice 24 hours after injection of anti-Ly108 antibody. Microarray analyses of thymocytes subsequent to Ly108 signaling revealed significant dysregulation of several genes

amongst which *Calm2* and *Fbxw5* were the strongest candidates, given their roles in modulating intracellular calcium concentration [144, 162] and cell-cycle progression, respectively [147].

Analysis of calcium metabolism demonstrated a significant decrease and delay in maximal calcium flux upon CD3 crosslinking in B6.*Sle1b* thymocytes compared to B6 controls. Previous work has demonstrated that apoptosis, especially in thymocytes, can be positively or negatively influenced by subtle changes in Ca^{2+} concentration within intracellular compartments. Indeed, Orrenius et al showed that cellular calcium overload or perturbations of intracellular calcium stores led to cytotoxic stress and ultimately cell death [163]. Furthermore, uptake of calcium release from the endoplasmic reticulum (ER) by the mitochondria has been shown to lead to apoptosis [164]. Moreover, the pro-apoptotic molecules Bak and Bax localise to both the ER and mitochondria, and overexpression of those proteins has been shown to promotes calcium mobilisation from the ER to the mitochondria during apoptosis [165]. Cells deficient in Bak or Bax have dramatically reduced ER concentrations of calcium, display a secondary decrease in mitochondrial Ca^{2+} uptake and are highly resistant to calcium-dependant death stimuli [166]. Our results fit perfectly with these observations since we observed both a reduction of Ca^{2+} mobilisation through the ER in B6.*Sle1b* mice, as exemplified by the marked reduction in thapsigargin-induced calcium flux in B6.*Sle1b* compared to B6 thymocytes, along with a decrease in levels of Bak protein in B6.*Sle1b* thymocytes, an effect strengthened by Ly108 crosslinking. This effect is also associated in our model with a decrease in thymocyte apoptosis as shown by TUNEL staining. Interestingly, deficiency in Bak and Bax has been shown to perturb thymic selection through the

resistance to both death by neglect and antigen receptor apoptosis [167]. These observations help explain the significant expansion of non-positively selected DP thymocytes in B6.*Sle1b* mice since cells that failed positive selection die by neglect. Moreover, the perturbation of antigen-induced cell death in Bak-deficient mice also support the resistance to negative selection we observed in B6.*Sle1b* single-positive CD4 thymocytes

Along with an impact on the apoptotic pathway, Ly108 also seems to control thymocyte proliferation. Indeed, thymocyte proliferation was reduced in B6.*Sle1b* mice compared to B6--activation of Ly108 *in vivo* resulted in a rapid arrest in the G0/G1 phase of the cell cycle in treated B6.*Sleb* mice but not B6 controls. This phenomenon was associated with a decrease in the kinase activity of cyclin-dependant kinase (Cdk2), a molecule that play a crucial role in the progression from G1 to S phase in the cell cycle [168]. In the thymus, Cdk2 is required for antigen-mediated negative selection [169]. Inhibition of Cdk2 was found to completely protect thymocytes from mitochondrial pertuerbations, from caspase cleavage and, finally, from apoptosis, which is what was observed in B6.*Sle1b* mice [170].

In this communication, we report a novel mechanism for thymic tolerance induction mediated by the SLAM/CD2 family member Ly108. We identify for the first time the teleologic signalling pathways subsequent to Ly108 receptor engagement, and demonstrate that Ly108 plays an important role in thymocyte development in general, and particularly in the control of negative selection. We define the mechanism by which a defect in Ly108, in this case mediated by a spontaneously occurring polymorphism found in the lupus-prone NZM2410 genome, can lead to a breach in humoral

autoimmunity through loss of T-cell tolerance. Finally, this study provides the first mechanistic explanation for the role of Ly108 in mediating thymic self-tolerance, and demonstrates the indispensability of T-cells in mediating pathogenic autoimmunity in SLE.

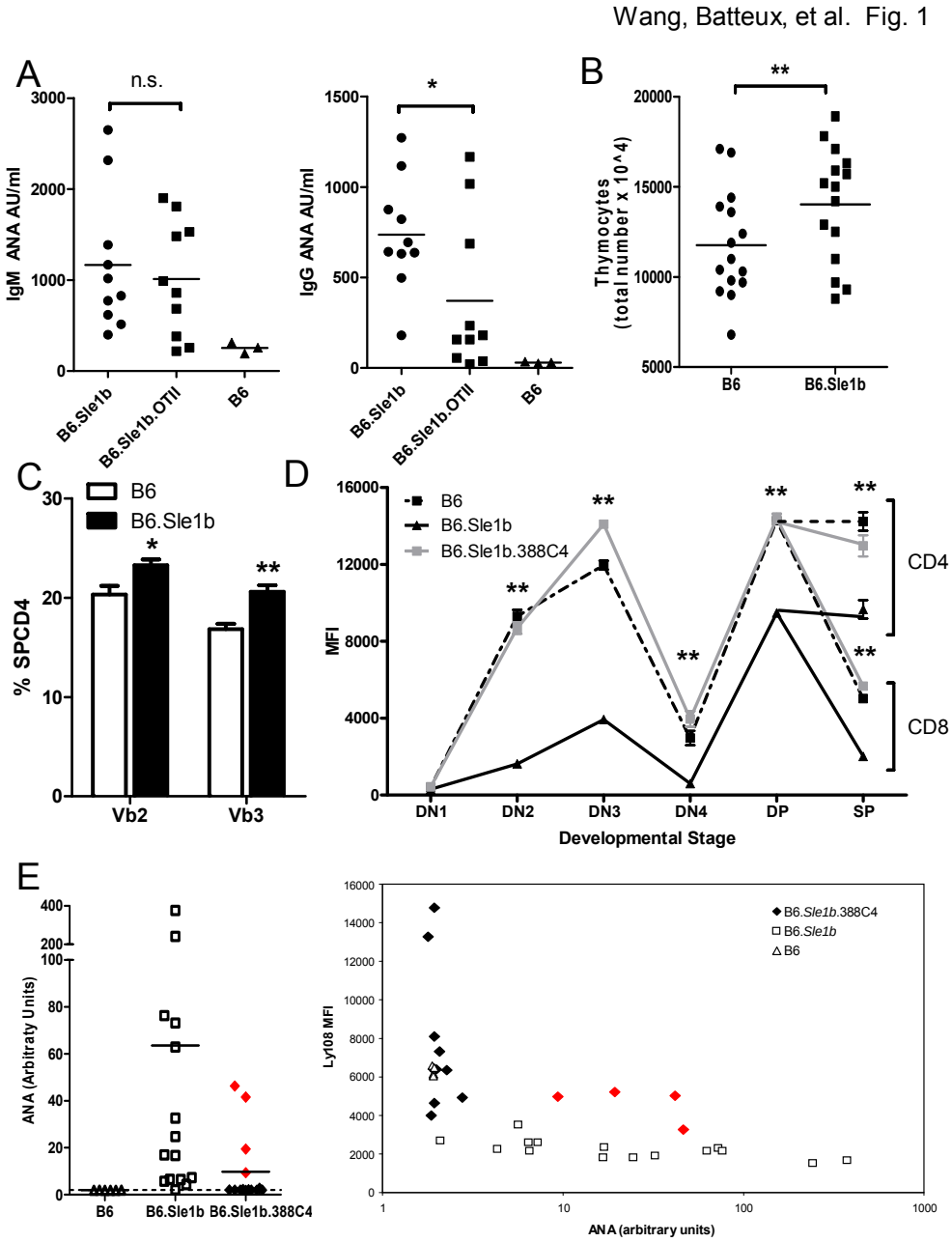

Figure 5. Reduction of total cell-surface Ly108 density resulting from Sle1bz correlates with ANA.

Shown in A) are the IgM (left) and IgG (right) ANA titers for 9-12 month old B6.*Sle1b* (n=10), B6.*Sle1b*.OTII (n=10), and B6 (n=3) mice. In B) are the thymic cell numbers for 8-week old B6 (n=15) and B6.*Sle1b* (n=15) mice. Displayed in C) are the percentage of single positive CD4 thymocytes expressing the designated Vβ (B6 (n=4), B6.*Sle1b* (n=4), 8 weeks of age). Shown in D) are the median MFI values of Ly108 for various thymocyte developmental stages of 8-week old B6 (n=5), B6.*Sle1b* (n=5), and B6.*Sle1b*.388C4 (n=5) mice, representative of at least three independent experiments. Displayed in E) are the IgG ANA titers for 9-12 month B6 (n=6), B6.*Sle1b* (n=15), and B6.*Sle1b*.388C4 (n=14) mice (left), and the median MFI values of Ly108 plotted against the IgG ANA titers (right). The dotted line represents three standard deviations above the mean B6 ANA titer, and the red points correspond to B6.*Sle1b*.388C4 mice with positive ANA titers. For statistics, ANOVA with Dunnet post-hoc test or parametric Welch-corrected t-test was used for statistical analyses (*, $P < 0.05$; **, $P < 0.01$; ***, $P < 0.001$).

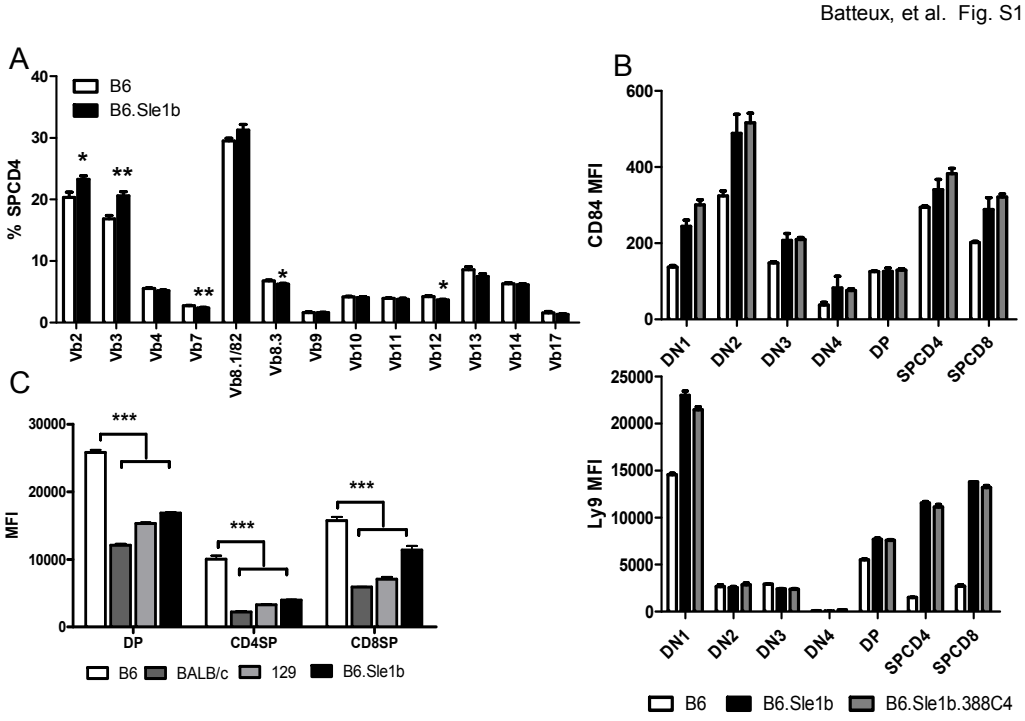

Figure 6. Vβ usage in B6 and B6.*Sle1b*; CD84 and Ly9 expression; Ly108 expression is haplotype-mediated.

In A) is shown the percentage of single positive CD4 thymocytes expressing the indicated Vβs (n=4 mice per group). Shown in B) are the median MFI values for CD84 (top) and Ly9 (bottom) for the indicated thymic subsets (n=4 mice per group, representative of two independent experiments). And displayed C) is the median MFI values of Ly108 on the indicated thymic subsets of B6, BALB/c, 129/SvJ, and B6.Sle1b

(n=3 per group, representative of three independent experiments). For statistics, either ANOVA with Dunnet post-hoc analyses or parametric Welch-corrected t-test was used for statistical analyses (*, $P < 0.05$; **, $P < 0.01$; ***, $P < 0.001$).

	B6 (n=15)	*B6.Sle1 (n=15)*
Total Thymocytes (x10^3)	**117 600 ± 29 486**	**140 200 ± 31 893****
Total Double Negative	**5 228 ± 2 505**	**7 204 ± 2 330****
DN1 ($CD44^+$ $CD25^-$)	329 ± 80	553 ± 238****
DN2 ($CD44^+$ $CD25^+$)	59 ± 21	68 ± 31
DN3 ($CD44^-$ $CD25^+$)	1 471 ± 432	2 034 ± 510****
DN4 ($CD44^-$ $CD25^-$)	3 369 ± 2 500	4 548 ± 2 121
Total Double Positive	**97 903 ± 22 726**	**117 112 ± 21 591****
$CD3^{int}$ $CD69^-$ $CD5^-$	78 226 ± 18 977	95 204 ± 28 997**
$CD3^{high}$ $CD69^+$ $CD5^+$	5 426 ± 1 369	5 803 ± 1 654
Total Single positive CD4	**8 093 ± 1 620**	**10 169 ± 1 552*****
$CD69^+$ $CD62L^-$	4 675 ± 993	6 040 ± 945****
$CD69^-$ $CD62L^+$	1 357 ± 302	1 757 ± 518*
Total Single positive CD8	**3 162 ± 894**	**4 693 ± 1 559*****

Table 5. Thymus cell subsets

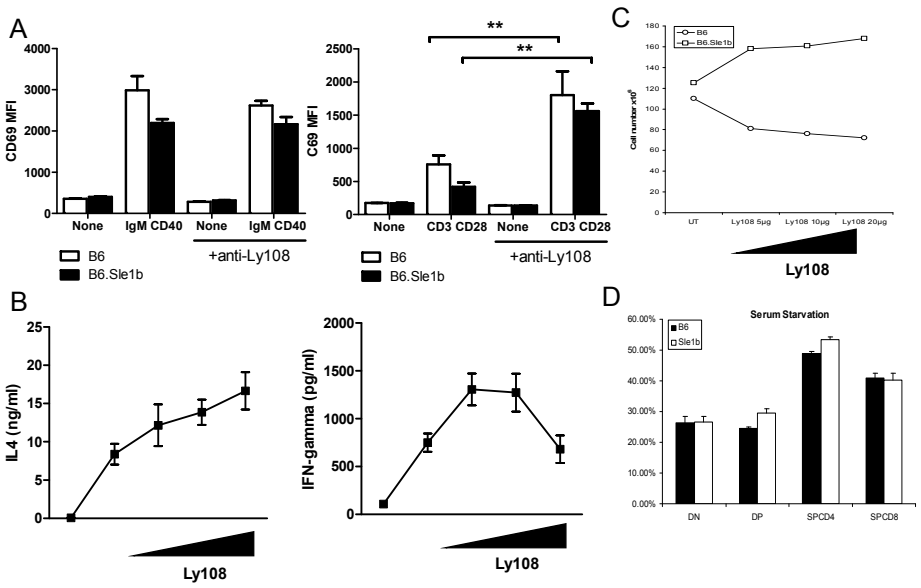

Figure 7. The anti-Ly108 antibody is an activating antibody; *in vivo* titration of anti-Ly108 antibody; and serum starvation.

Shown in A) are the mean MFI values for CD69 on B-cells (left) and T-cells (right) on splenocytes 72 hours after culture with either Fab' anti-IgM (10 µg/ml) and anti-CD40 (10 µg/ml) or plate-bound anti-CD3 (2 µg/ml) and anti-CD28 (1 µg/ml) with or without Ly108 (5 µg/ml) (n=4 mice per group, average of experimental duplicates). Shown in B) are the levels of IL4 (left) and IFN-γ (right) present in cell-culture supernatant after 72 hours of stimulation in vitro with anti-CD3 (2 µg/ml) and anti-CD28 (1 µg/ml) with increasing amounts of anti-Ly108 (n=4 mice per group, average of experimental duplicates). In C) is displayed the absolute thymocyte cell numbers 48 hours after anti-Ly108 injection of at the indicated dosages (n=3 mice per group). Shown in D) are the percentage of viable cells of the indicated thymic subsets following serum starvation (n=4 mice per group, average of experimental duplicates, representative of two independent experiments). For statistics, parametric Welch-corrected t-test was used for statistical analyses (*, $P < 0.05$; **, $P < 0.01$; ***, $P < 0.001$).

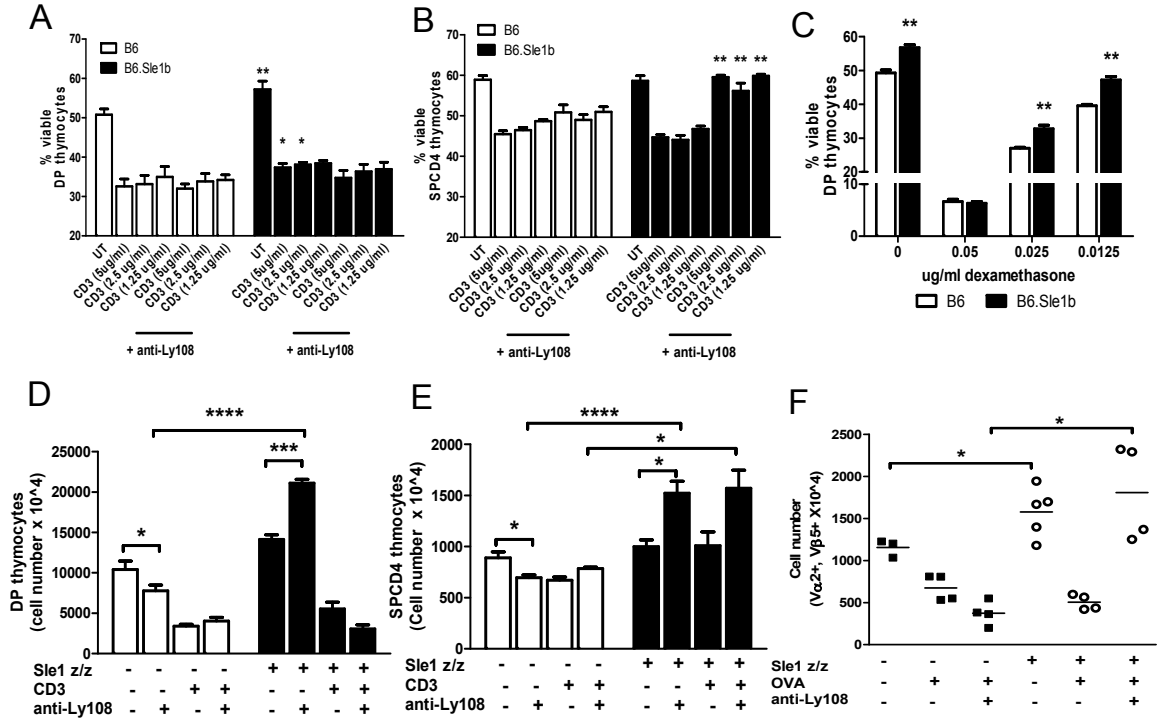

Figure 8. Ly108z but not Ly108b crosslinking mediates an impairment of thymocyte apoptosis in vitro and in vivo.

Shown in A) are the percentages of live double positive thymocytes and in B) the percentages of live single positive CD4 thymocytes from 8 week old B6 (n=7) and B6.*Sle1b* (n=7) after 24 hours *in vitro* with the indicated concentrations of CD3 and Ly108 (representative of at least 3 independent experiments; designation of live and apoptotic is described in Materials and Methods). Displayed in C) are the percentages of live double positive thymocytes after 24 hours *in vitro* with the indicated doses of dexamethasone (n=4 per group, representative of two independent experiments). In D) and E) are shown the absolute cell numbers of double positive thymocytes and single positive CD4 thymocytes, respectively, 48 hours following IV injection of anti-Ly108 (5 μg) and anti-CD3 (5 μg) antibody (n=6 per group, representative experiment of at least five). In F) is displayed the absolute number of Vα2+ Vβ5+ OTII transgenic single positive CD4 T-cells following OVA challenge (1 mg) with or without simultaneous anti-Ly108 (5 μg) injection (n>3 per group, 8-week old mice). For statistics, ANOVA with

Dunnet post-hoc test or parametric Welch-corrected t-test was used for statistical analyses (*, $P < 0.05$; **, $P < 0.01$; ***, $P < 0.001$).

	B6 (*n=13 per group*)				*B6.*Sle1 (*n=13 per group*)			
Cell number (x10^3)	**PBS**	**αLy108**	**αCD3**	**αLy108+αCD3**	**PBS**	**αLy108**	**αCD3**	**αLy108+αCD3**
Total Thymocytes	**108 923 ± 15 929**	**82 307 ± 22 655**	**40 154 ± 9 218**	**41 615 ± 16 419**	**131 333 ± 33 947**	**181 000 ± 57 098**	**49 615 ± 23 820**	**41 846 ± 13 855**
Total Double Negative	**4 662 ± 1 533**	**4 567 ± 1 746**	**3 716 ± 2 480**	**3 471 ± 910**	**5 503 ± 1 691**	**7 475 ± 2 387**	**3 664 ± 1 297**	**3 919 ± 2 692**
DN1 (CD44$^+$ CD25$^-$)	429 ± 160	377 ± 147	307 ± 156	349 ± 122	427 ± 126	683 ± 183	470 ± 117	463 ± 141
DN2 (CD44$^+$ CD25$^+$)	79 ± 40	52 ± 26	31 ± 19	32 ± 18	57 ± 26	102 ± 35	47 ± 29	27 ± 19
DN3 (CD44$^-$ CD25$^+$)	1 650 ± 431	1 287 ± 484	690 ± 307	795 ± 212	2 035 ± 556	2522 ± 694	981 ± 460	853 ± 382
DN4 (CD44$^-$ CD25$^-$)	2 503 ± 1 163	2 849 ± 1 446	2 687 ± 2 460	2 294 ± 869	2 984 ± 1 211	4 161 ± 1 735	2 165 ± 1 265	2 576 ± 2 725
Total Double Positive	**92 813 ± 13 638**	**67 507 ± 21 327**	**27 708 ± 8 944**	**26 993 ± 15 859**	**112 465 ± 33 405**	**153 411 ± 53 563**	**32 417 ± 23 111**	**20 365 ± 12 200**
CD3^{int} CD69$^-$ CD5$^-$	79 009 ± 11 060	62 612 ± 19 258	25 676 ± 7 003	25 640 ± 14 581	105 476 ± 31 808	144 633 ± 53 923	30 996 ± 25 312	17 149 ± 12 437
CD3^{high} CD69$^+$ CD5$^+$	4 022 ± 1 611	3 078 ± 1 271	2 131 ± 604	2 140 ± 996	4 122 ± 1 680	5 642 ± 2 498	2 302 ± 1 317	1 965 ± 803
Total Single positive CD4	**8 187 ± 1 270**	**7 391 ± 2 013**	**6 298 ± 1 751**	**7 749 ± 1 751**	**9 273 ± 1 566**	**14 014 ± 3 397**	**9 570 ± 2 411**	**11 892 ± 4 553**
CD69$^+$ CD62L$^-$	4 788 ± 835	4 346 ± 1 233	3 248 ± 1 062	3 775 ± 761	5 560 ± 1 027	8 016 ± 1 838	4 731 ± 1 312	4 854 ± 2 069
CD69$^-$ CD62L$^+$	1 464 ± 287	1 545 ± 597	1 738 ± 543	2 385 ± 614	1 738 ± 470	2 832 ± 1 009	2 826 ± 990	3 747 ± 1 362
Total Single positive CD8	**3 258 ± 860**	**2 841 ± 810**	**2 431 ± 969**	**3 401 ± 956**	**4 092 ± 1 183**	**6 100 ± 1 326**	**3 964 ± 1 157**	**5 669 ± 2 527**

Table 6. Thymus cell subsets after Ly108 Ab treatment

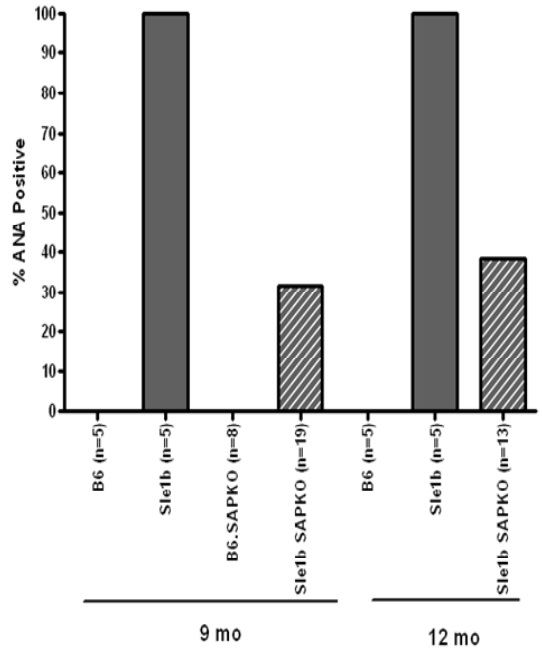

Figure 9. *Sle1b* effects are SAP independent.
Shown in A) are the IgG ANA titers in B6 (n=5), B6.*Sle1b* (n=5), B6.*Sle1b*.SAP^{ko} (n=13). In B) are shown the Western blots for the immunoprecipitation of Ly108 and immunblots for SAP (representative of n=6 mice per group).

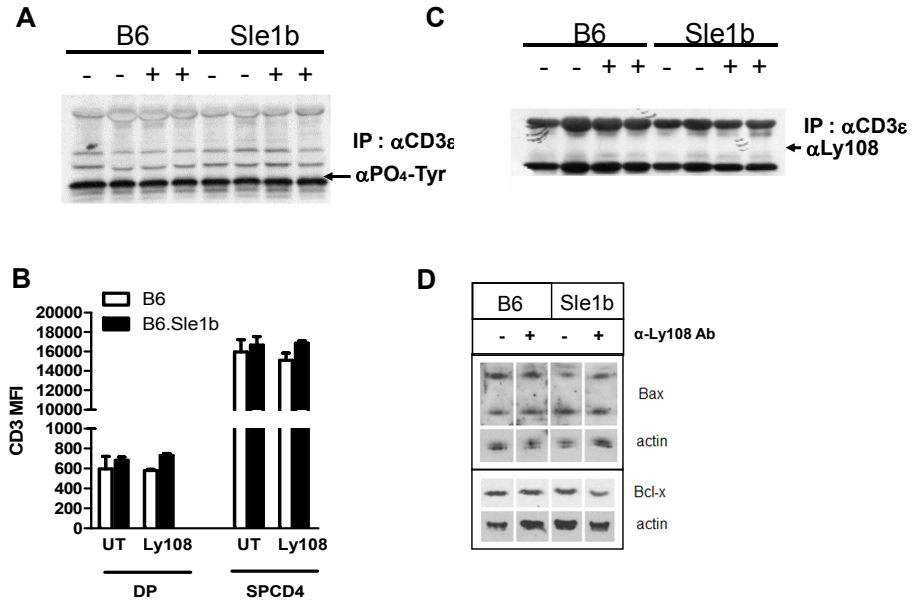

Figure 10. Negative results for TCR signaling and apoptosis.
Shown in A) is the Western blot for phosphor-tyrosine after anti-CD3ε immunoprecipitation (representative of n=4 per group). Displayed in B) are the CD3 median MFIs for the indicated thymic subsets 48 hours after anti-Ly108 injection (n=6 mice per group, representative of at least five experiments). In C) is displayed the immunoblot for Ly108 after anti-CD3ε immunoprecipitation (representative of n=4 per group). Shown in D) are the Western blot results for Bax and Bcl-x. (n=4 per group, representative of two independent experiments).

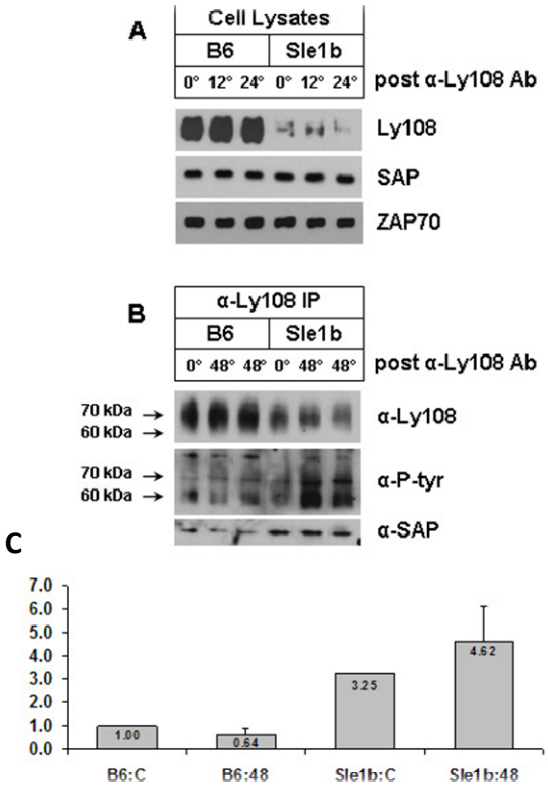

Figure 11. Engagement of Ly108z leads to increased phosphorylation and SAP binding.
A.) Western blots of whole cell lysates from B6 and B6.Sle1b thymocytes at 0, 12 and 24 hours following anti-Ly108 mAb injection. Membranes were immunoblotted with anti-Ly108 mAb, polyclonal anti-SAP Abs, or polyclonal anti-ZAP70 Abs. B.) Western blots of anti-Ly108 immunoprecipitations from cell lysates of B6 or B6.Sle1b thymocytes at 0 or 48 hours following Ly108 injection are shown. Lysates were immunoprecipitated with anti-Ly108 mAbs, then blotted with polyclonal anti-SAP Abs and anti-Ly108 mAbs, or with anti-phospho-tyrosine Abs. For immunoprecipitation results, all results for each specific blot are from the same gel and exposure but the order of some lanes is changed on the figure compared to the original gel for clarity (indicated by a line). Results are representative of at least three independent experiments. The bottom portion of the figure represents normalized association of SAP with Ly108 for each co-immunoprecipitation as determined by densitometric analysis (the value for SAP association with Ly108 in B6 thymocytes was set as 1.00 and results from the other co-immunoprecipitations were compared to that value).

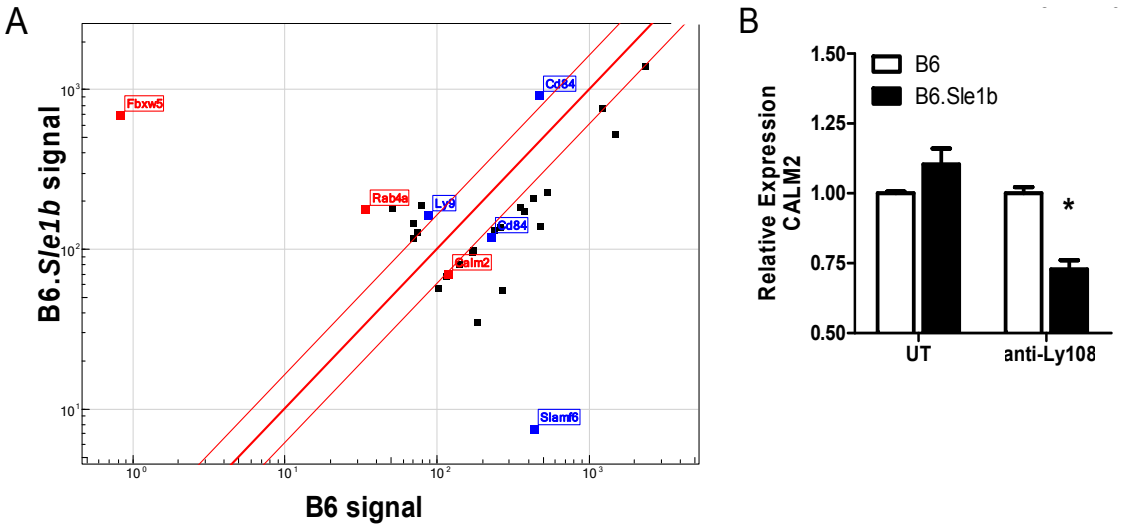

Figure 12. Ly108^{z} ligation results in differential gene expression.
Shown in A) is a plot of relative signal intensities of statistically different genes 24 hours after anti-Ly08 injection in 8-week old B6 (n=3) and B6.*Sle1b* (n=3). Shown in B) and C) are confirmatory RT-PCR results for *Calm2*. For statistics, parametric Welch-corrected t-test was used for statistical analyses (*, $P < 0.05$).

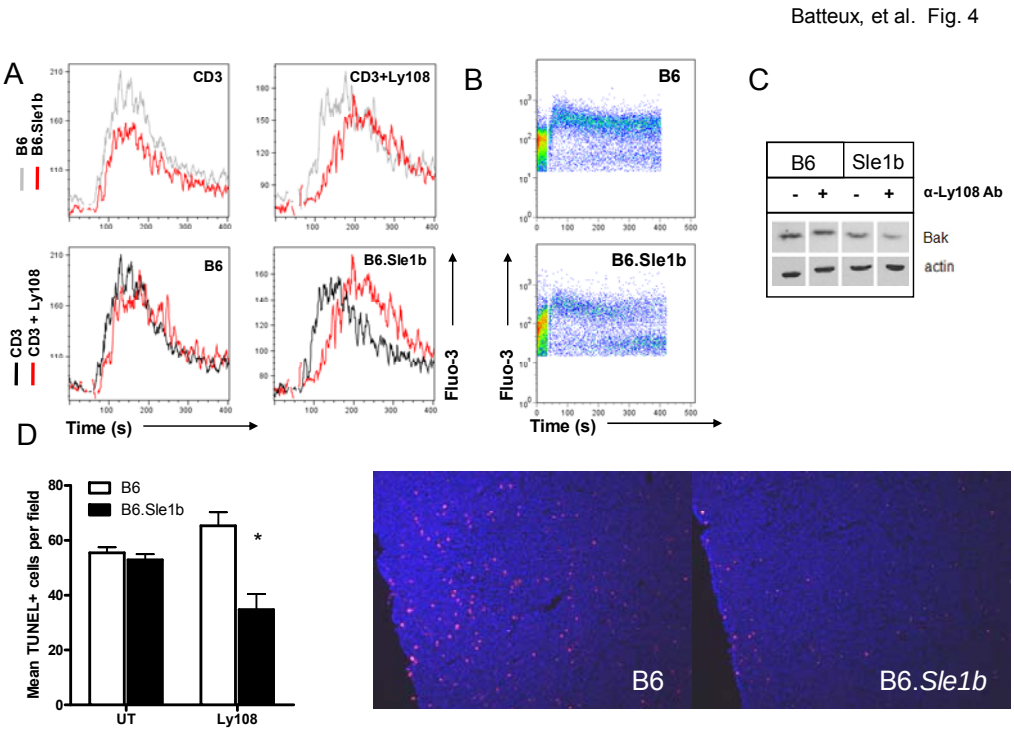

Figure 13. Engagement of Ly108z leads to differential signal transduction which results in decreased transcription of Calm2 and increased transcription of Fbxw5. Shown in A) are representative traces of calcium mobilization (Fluo-3 detection) following the indicated stimuli. In the top row are displayed overlays of B6 (grey) and B6.*Sle1b* (red) thymocyte fluxes following anti-CD3 stimulation (10 µg/ml) (left) and anti-CD3 (10 µg/ml) plus anti-Ly108 (10 µg/ml) stimulation (right); in the bottom row are displayed overlays of calcium mobilization following anti-CD3 (black) and anti-CD3 plus anti-Ly108 (red) stimulation (representative of at least six independent experiments). Refer to Material and Methods for a complete description of stimulation and acquisition parameters. Shown in B) are representative primary plots of calcium mobilization following thapsigargin (100 nM) stimulation (representative of two experiments). Displayed in C) are representative Western blots for Bak (representative of two experiments, n=4 mice per group per experiment). In D) are the average number of TUNEL positive cells per field in thymic sections prepared 36 hours after anti-Ly108 injection (n=6 mice per group, 3 sections per mouse, 10 fields per section). For statistics, parametric Welch-corrected t-test was used for statistical analyses (*, $P < 0.05$).

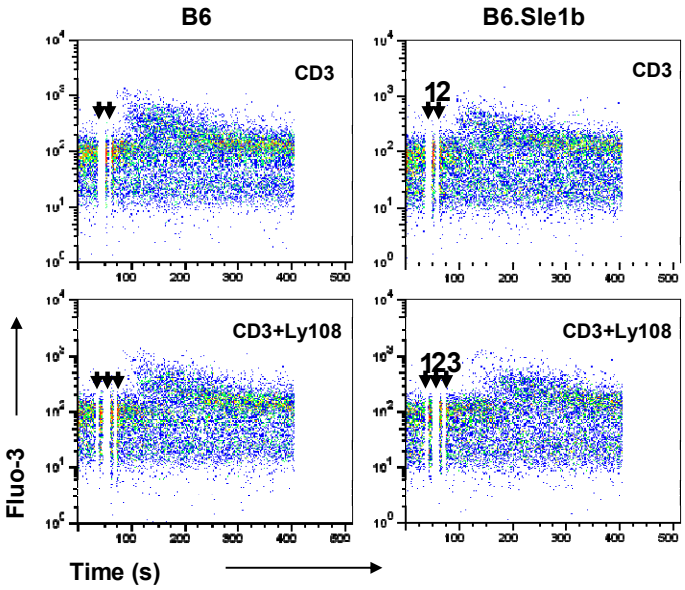

Figure 14. Schema of calcium flux assays.
Shown are representative contour plots of calcium mobilization (Fluo-3 detection) of B6 (top) and B6.*Sle1b* (bottom) thymocytes at the indicated CD3 concentrations (representative of n=3 per condition).

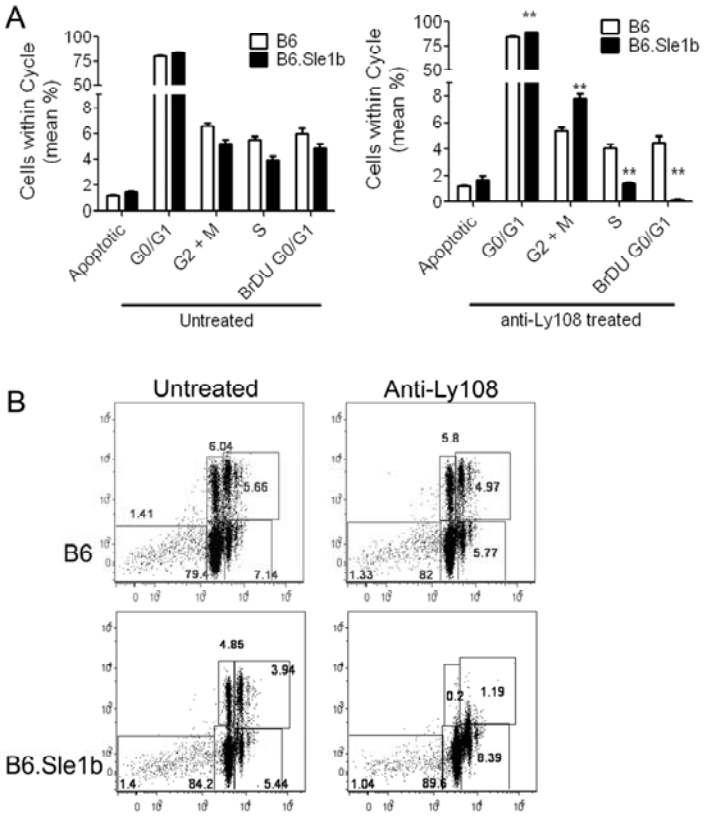

Figure 15. Ly108^z signaling leads to a defect in cell-cycle checkpoint.
Shown in panel A are the mean percentages of B6 (n=3) and B6.Sle1b (n=3) thymocytes (representative of at least two independent experiments) in the indicated stages of cell cycle before (left) and 36 hours after (right) anti-Ly108 injection as assessed by BrDU versus 7-AAD staining, with representative FACS plots displayed in panel B. For statistics, parametric Welch-corrected t-test was used for analysis (*P<0.05, **P<0.01, ***P<0.001).

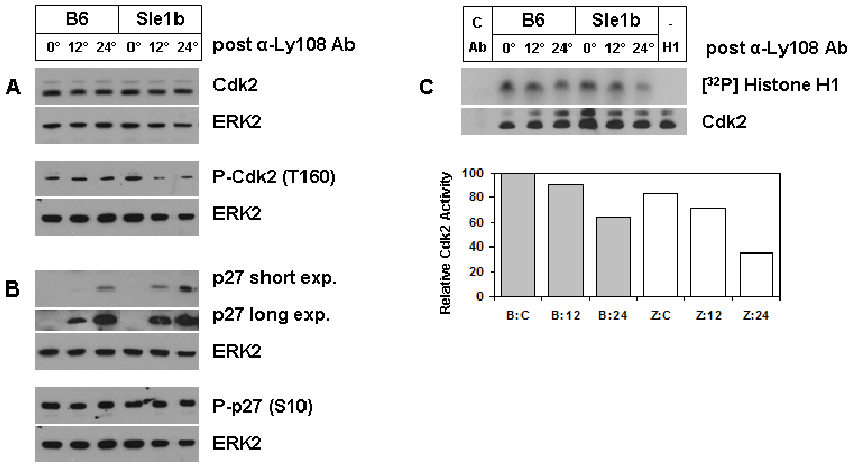

Figure 16. Expression of cell cycle regulatory proteins
Western blots of whole cell lysates from B6 and B6.Sle1b thymocytes at 0, 12 and 24 hours following anti-Ly108 mAb injection are shown. Membranes were immunoblotted with antibodies specific for A.) the G1 • S transition regulator, Cdk2 and its active form (polyclonal anti-Cdk2 Abs or anti-P-Cdk2(Thr160) mAbs) and B.) the Cdk2 inhibitor, p27 (anti-p27 Abs or anti-P-p27(Ser10) Abs). Long and short exposure times are shown for p27 profiles. Each membrane was subsequently stripped and reblotted with anti-ERK2 Abs to ensure equal loading and transfer of samples. C.) Cdk2 was immunoprecipitated from B6 and B6.Sle1b thymocyte whole cell lysates at 0, 12, and 24 hours following anti-Ly108 mAb injection. The immunocomplexes were analyzed for kinase activity towards histone H1 in an in vitro kinase assay, and for the amount of Cdk2 immunoprecipitated by Western blotting. Relative kinase activity was determined by setting a value of 100 percent for B6 controls.

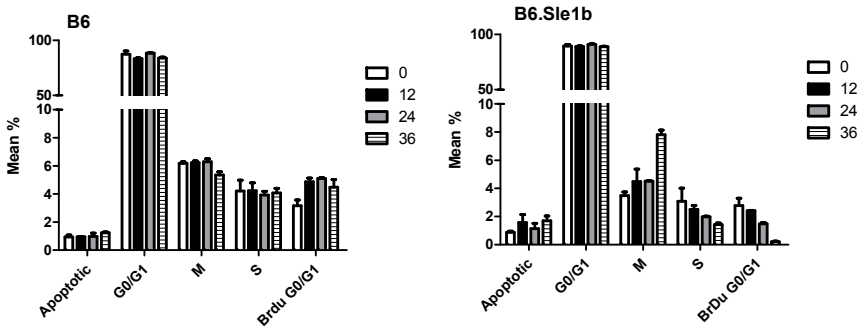

Figure 17. Time course of cell cycle studies.
Displayed are the percentage of cells in the indicated cell cycle stages at the indicated times post anti-Ly108 injection in B6 (left) and B6.*Sle1b* (right) (n=3 per group, representative of two independent experiments).

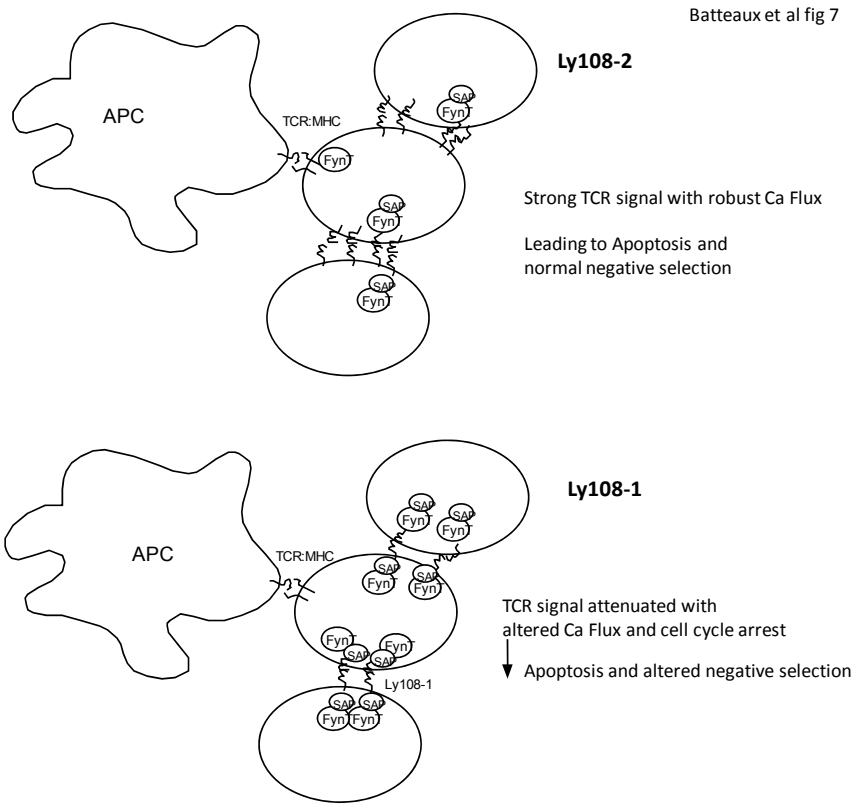

Figure 18. Model of Ly108 signaling consequences on T-cell signaling.

CHAPTER FOUR: Identification of Lupus Susceptibility Locus, *Sle3*

INTRODUCTION

Congenic dissection of the NZM2410 murine lupus model uncovered three main lupus susceptibility loci, termed *Sle1, Sle2,* and *Sle3*, located on chromosomes 1, 4, and 7, respectively [9]. Of the three loci, *Sle1* and *Sle3* are, by far, the most potent, and, in concert, capable of driving fatal lupus on the B6 background to a penetrance very nearly resembling the parental NZM2410 strain. *Sle1* mediates a breach in humoral tolerance in the absence of visceral pathologies and is required for the initial breach in the pathogenesis of lupus [37]. The B6.*Sle3* congenic, on the other hand, displays no overt autoimmune phenotypes. Indeed, the B6.*Sle3* congenic produces only mild levels of IgM ANA, exhibit a slight skew in CD4 to CD8 T-cell ratios, and, in low frequencies, develop low-grade glomerulonephritis (GN). However, whereas *Sle3* alone, as a B6 congenic, displays no overt autoimmune phenotypes, it can interact, in a non-additive fashion, with *Sle1* to drive fatal autoimmunity [42, 171], demonstrating that a secondary lesion is required to drive fatal autoimmunity.

Sle3, located on murine chromosome 7, was initially mapped to an interval bounded by microsatellite markers D7MIT157 and D7MIT40, a 73.2 Mb region [40, 70], but has since be refined to the intervals bounded by D7MIT157 and D7MIT233. *Sle3* has been recently demonstrated to play a role in mediating antigen-presenting cell (APC) activation thresholds to Toll-like receptor (TLR) ligands [47]. Zhu et al demonstrate clearly that B6.*Sle3*-derived APCs are hyperactivated by TLR4 agonist lipopolysacharide (LPS) and subsequently produce higher levels of inflammatory cytokines such as IL6 and TNF-alpha and are more competent in stimulating antigen-presentation to T-cells.

Moreover, the dysregulation in APC sensitivity to TLR4 ligand observed in *Sle3* was found to be an APC-intrinsic gene. In this regard, the action of *Sle3*, is not unlike the BXSB-derived *yaa* lesion, which has recently been shown to be gene translocation event leading to 2-fold expression of TLR7, and is consistent with the growing body of literature on the epistatic role of TLR-dysregulation in APCs in accelerating otherwise non-pathogenic autoimmunity [32-34, 172].

To identify *Sle3*, we used the APC-intrinsic defect in activation threshold observed in B6.*Sle3*-derived APCs to perform positional mapping.

RESULTS

Identification of *Sle3a* and *Sle3b* sub-loci

A panel of truncated subcongenics were derived (Figure 12A). Using the degree of cell-surface activation marker upregulation and cytokine secretion profiles as functional readouts of APC activation, primary bone marrow-derived macrophages derived from these subcongenics were screened for the parental B6.*Sle3* APC-hyperactivation phenotype. We found that the *Sle3* phenotype was mediated by two sub-loci, termed *Sle3*a and *Sle3b* (Figure 12B), bounded by microsatellite markers D7MIT157 to D7MIT158 and D7MIT158 to D7MIT233, respectively. The support area of *Sle3a* spans roughly 2.8 Mb and is a highly gene-dense region containing the Siglech and Kallikrein gene clusters. This region was subsequently granted to other personnel in the Wakeland lab for study, and is thus not the focus of this section of my dissertation.

Identification of the critical interval of *Sle3b*

The support area of *Sle3b* spans roughly 22 Mb, and is comparatively gene sparse. *Sle3b* was subsequently fine-mapped using the subcongenics tiling this region. Positional mapping of *Sle3b* placed *Sle3b* in the critical interval bounded by microsattelite markers D7MIT176 and D7MIT231. The data are summarized in Figure 13.

***Klf13* as the primary candidate gene in *Sle3b*, a mechanistic role for RANTES in macrophage hyperactivation**

The critical interval is roughly 3.4 Mb and contains 25 genes, displayed in Table 7. Contained in the critical interval of *Sle3b* is the transcription factor Klf13, which has been shown to regulate RANTES (CCL5) secretion in activated T-cell subsets [173]. In preliminary data, we noted a 200-fold upregulation of *Klf13* mRNA in stimulated B6.*Sle3* macrophages compared to B6 controls (Figure 14A). Since macrophages are also known to secrete C-C chemokines, including RANTES [174], we investigated the possibility that increased RANTES secretion following TLR4 stimulation could explain the hyperactivation of B6.*Sle3* macrophages. In preliminary data, we noted a two-fold increase in RANTES secretion compared to controls (Figure 14B). Co-culture of B6.*Sle3* BMDMs with LPS in the presence of RANTES was capable of suppressing activation of B6.*Sle3* BMDMs seen in B6 levels (Figure 14C).

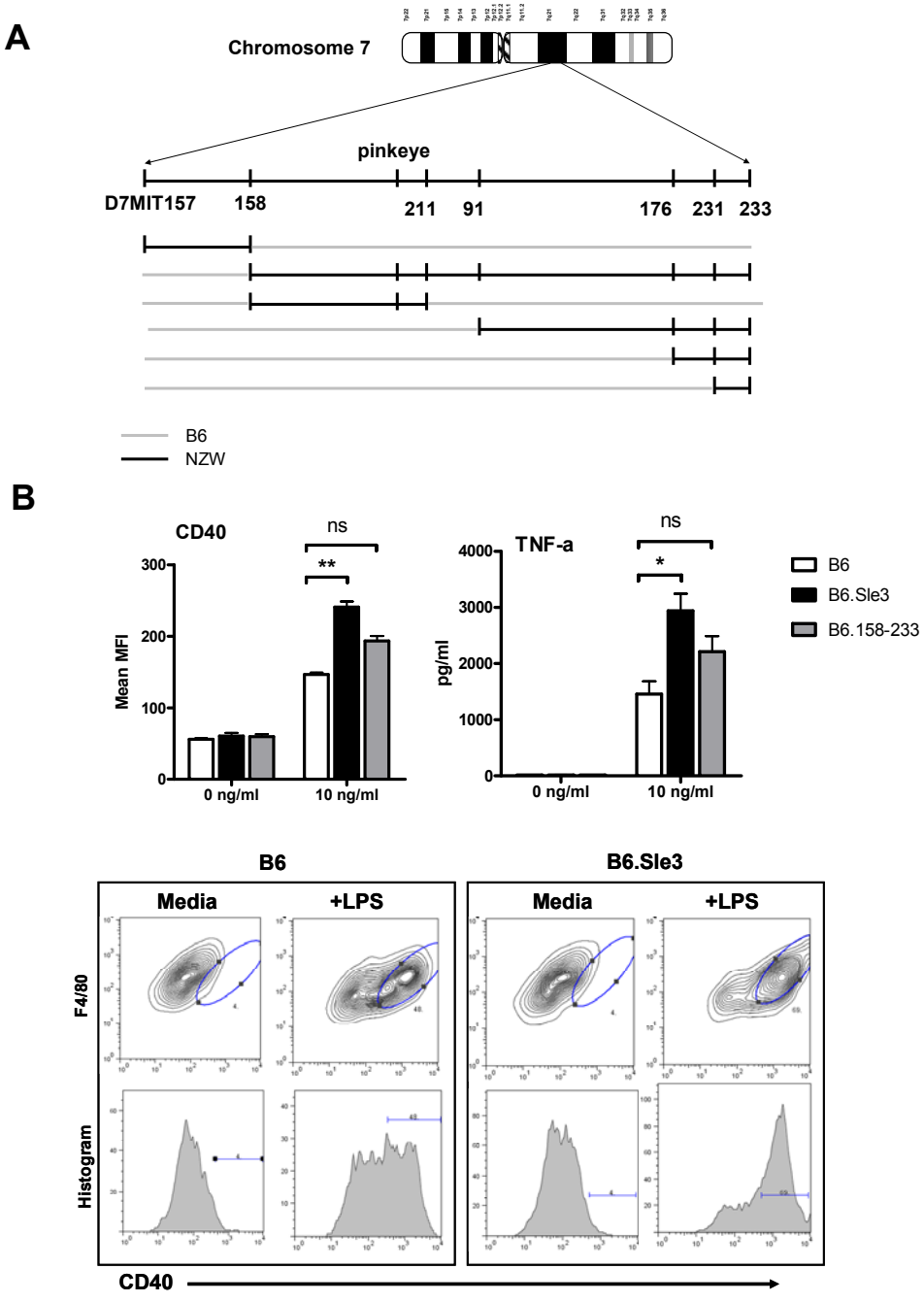

Figure 19. *Sle3* is composed of two sub-loci, *Sle3a* and *Sle3b*.

A

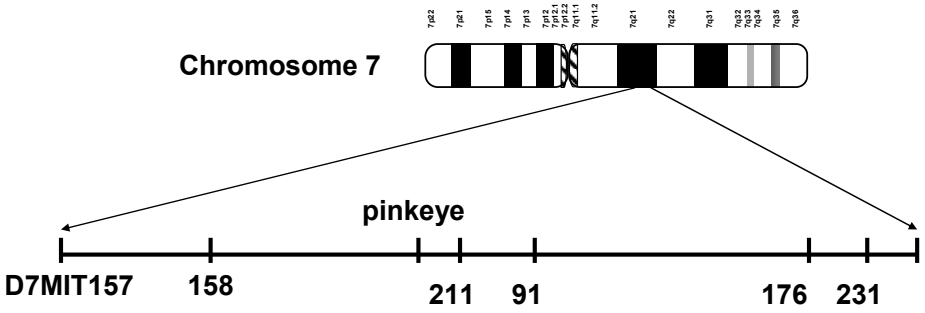

Congenic	n=	Size (MB)	Activation Markers (MFI CD40, CD80, CD86, FcR, CD106)	Cytokine (TNF, IL6)
157-233	27	25	+++	+++
158-233	18	22	++	++
158-211	9	11	Negative	Negative
91-233	9	11	++	++
176-233	12	5	++	++
231-233	6	2	Negative	Negative

B

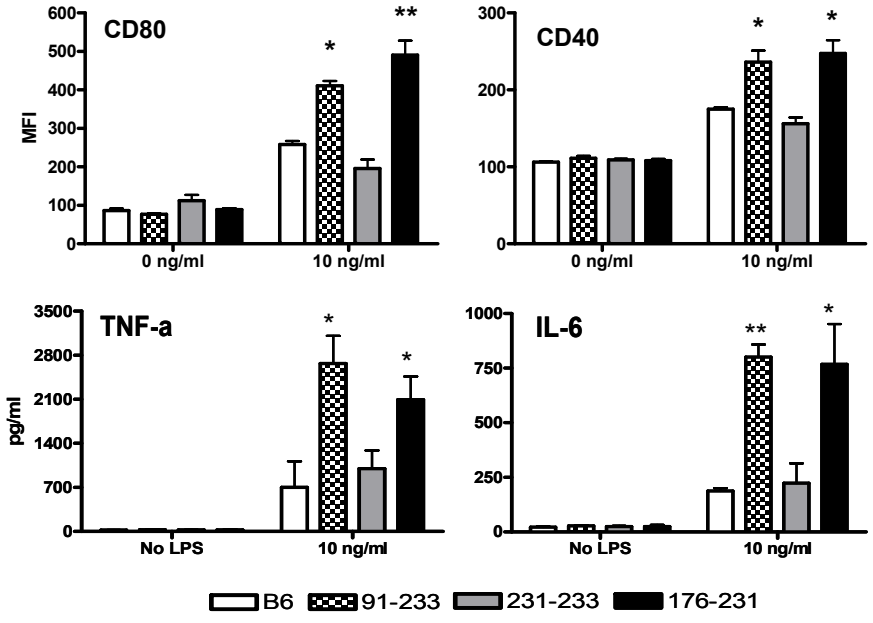

Figure 20. Summary of positional mapping of *Sle3b*.

In (A) is the shown the summary of positional mapping data. In (B) are shown representative experiments used for fine mapping. In the top row are displayed MFIs of CD80 and CD40 on BMDMs. Below are the culture supernatant concentrations of TNF- and IL-6. (*, $P < 0.05$; **, $P < 0.01$; ***, $P < 0.001$, by ANOVA with Bonferroni ad-hoc test)

Start Position (bp)	End Position (bp)	Gene Name	Function
59292677	59293717		
59294184	59294369	UNKNOWN	
59355836	59356381	UNKNOWN	
59400632	59508548	Otud7	de-ubiquitination
59641217	59688732	Klf13	regulation of RANTES
59641217	59688732	Q9DCC0_MOUSE	
59824199	59828588	UNKNOWN	
59938182	60020933	Trpm1	ion transport
59958398	59958503	mmu-mir-211	
60040245	60091890	UNKNOWN	
60040245	60091890	BB128963	
60122745	60126676	6030441H18Rik	
60129133	60144828	Mphosph10	ribonuclueoprotein component
60145363	60164708	Mcee	amino acid metabolism
60552996	60611836	Apba2	neuronal synaptic vesicle
60614080	60714195	5730507A09Rik	
60730046	60730885	Ndnl2	arrests cell cycle
61154135	61212882	Tjp1	tight junction integrity
61502881	61559874	Tarsl2	tRNA synthetase-like
61502881	61559874	Tm2d3	beta-amyloid-binding
61642825	61643686	XP_620508.2	
61720180	61908301	Pcsk6	neuroendecrine
61918511	61932548	Snrpa1	ribonuclueoprotein component
61937626	61947369	H47	non-classical MHC
61967482	62031755	Chsy1	chondroitin synthase
61977270	61977374	U6	ribonuclueoprotein component
62116716	62246308	Lrrk1	serine/threonine kinase
62248862	62285444	Aldh1a3	alcohol metabolism
62248862	62285444		

Table 7. Genes contained in the critical interval of *Sle3b*.

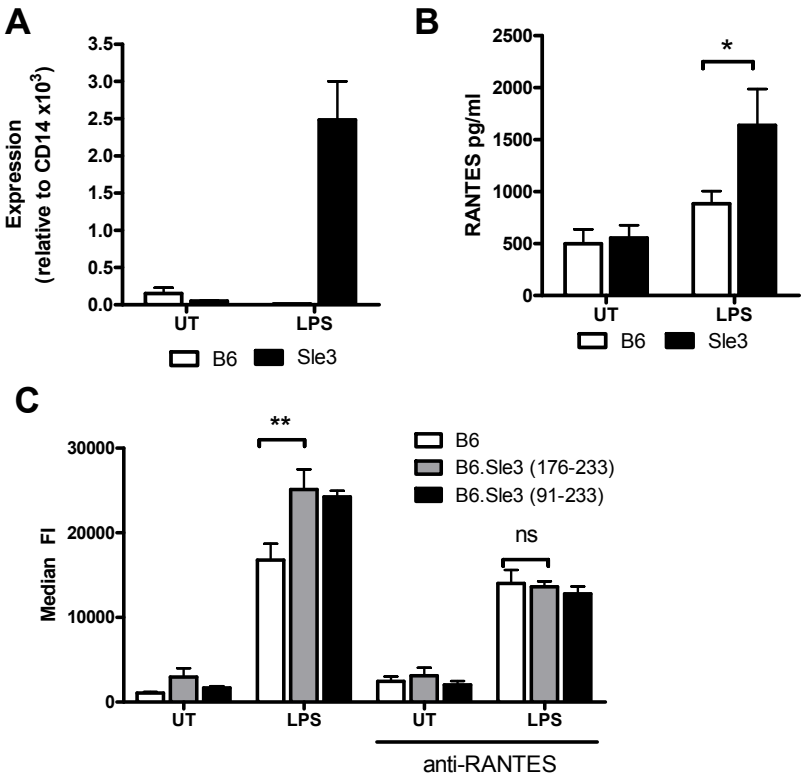

Figure 21. Increased Klf13 expression leads to increased RANTES production which partially mediates *Sle3* macrophage hyperactivation in response to TLR4 signaling.

Shown in (A) are the normalized RT-PCR results of KLF-13 expression before and after LPS stimulation. In (B) is shown the culture supernatant concentrations of RANTES before and after LPS stimulation in B6 and B6.Sle3 (176-233) BMDMs. In (C) is displayed MFIs of CD80, and the results on CD80 expression after using co-culture with anti-RANTES antibody. (*, $P < 0.05$; **, $P < 0.01$; ***, $P < 0.001$, by ANOVA with Bonferroni ad-hoc test)

CHAPTER FIVE: CXCR4/CXCL12 dysregulation plays a pivotal role in murine lupus nephritis

INTRODUCTION

CXCR4 (CD186) is a G-protein coupled receptor which subserves many functions in the immune system. Studies of mice carrying targeted gene disruption of CXCR4 have revealed its critical role in hematopoesis, B-cell lymphopoesis, myelopoesis, germinal center organization, and maintenance of stem cell pools in the bone marrow [175-179]. In addition, CXCR4 is a well-studied molecule in both HIV and cancer. Of note, CXCR4-tropism was found to be correlative with chronic immune activation and AIDS pathogenesis [180, 181], and studies in a variety of human cancers have shown the chemotactic potential of CXCR4 to be exploited during tumor cell metastasis [182]. CXCR4 defects in humans lead to a syndrome characterized by warts, hypogammaglobulinemia, immunodeficiency, and myelokathexis, collectively termed the WHIM syndrome [183].

CXCR4 monogamously recognizes the CXC chemokine ligand 12 (CXCL12), also known as stromal cell-derived factor 1 (SDF-1), or pre-B-cell-growth-stimulating factor (PBSF). CXCL12 is known to be basally expressed by a variety of tissues including skin, heart, and kidney [184], and has been shown to be selectively upregulated in a wide range of tissues in response to damage, particularly the kidney [185]. The upregulation of CXCL12 has been postulated to promote mobilization and recruitment of CD34+ progenitor cells to sites of damage as a mechanism of repair and repopulation. In the immune system, CXCL12 plays a major role in determining differential leukocyte

output from the bone marrow. Low bone marrow levels of CXCL12 induced by inflammation promote granulocyte production and suppress B-cell generation [186].

We initially became interested in CXCR4 because we observed that it was dysregulated in expression in the BXSB model of spontaneous lupus. Microarray screens of LPS-stimulated bone-marrow-derived macrophages revealed that CXCR4 was highly upregulated when compared to C57BL/6 (B6) controls (data not shown). Given the known roles of CXCR4 in chemotaxis and B-cell lymphopoiesis [178, 179] and the reported roles of CXCL12 in other forms of renal damage, we postulated that increased CXCR4 expression may play a role in mediating autoreactivity and nephritis in lupus. In this work, we examine the expression of CXCR4 and its ligand in different murine models of lupus, and the therapeutic potential of blocking this axis in murine lupus.

RESULTS

Increased CXCR4 expression on leukocytes of multiple lupus models is a consequence of disease

Examination of several murine lupus models, including BXSB, MRL.*lpr*, and B6.*Sle1Yaa*, revealed that CXCR4 was significantly upregulated on multiple cell types in 8-10 month old mice, regardless of their genetic composition, when compared to B6 controls (Table 8 and Figure 22). Similar differences were noted in a fourth lupus-prone strain, B6.*Sle1Sle2Sle3* (data not shown). Cell types that exhibited the largest upregulation of CXCR4 compared to B6 in all murine models included cell subsets of both the myeloid and B-cell lineages. In particular, inflammatory monocytes, neutrophils, plasma cells and pre-plasma cells expressed the highest absolute levels of CXCR4,

particularly in the lupus-prone strains (Table 8, Figure 22). Both in terms of the mean fluorescence intensities, as well as the percentage of cells expressing CXCR4, myeloid and B-cells from lupus mice exhibited about a two-fold increase in surface expression of CXCR4. Though these differences were most marked on splenic leukocytes, a similar pattern of expression difference was also noted on leukocytes isolated from lymph nodes, peripheral blood, and the bone marrow (Table 8. and data not shown). Although we detected an increase in CXCR4 expression on memory CD4+ T-cells, these results did not reach statistical significance.

The hyperexpression of CXCR4 on leukocytes from lupus-prone mice could result from polymorphisms of the *CXCR4* gene (which may directly regulate CXCR4 expression), or arise as a consequence of the disease process. To distinguish between these possibilities, we adopted two approaches using the B6.*Sle1Yaa* mouse as a disease model. First, evaluation of young (2-mo-old) pre-disease B6.*Sle1Yaa* mice did not reveal hyper-expression of CXCR4 (Figure 23A). Second, we examined monocongenic mice bearing the two main genetic elements that dictate lupus development in B6.*Sle1Yaa* mice—*Sle1*^{z}, and *Yaa*. Congenic dissection of 9-month old B6.*Sle1Yaa* mice revealed that the upregulation of CXCR4 was present only in mice with active lupus disease, in the bicongenic strain (Figure 23B and C). Indeed, the upregulation of CXCR4 was neither observed in B6.*Sle1* mice—indicating that the upregulation was not downstream of the loss of humoral tolerance, which is the hallmark feature of this strain [35, 132], nor in B6.*Yaa* mice—indicating that CXCR4 upregulation was not downstream of TLR7 dysregulation [32, 33] (Figure 23). Furthermore, direct sequencing of the *CXCR4* gene revealed no sequence polymorphisms between B6 and B6.*Sle1Yaa* (data not shown).

Taken together, these data indicate that the upregulation of CXCR4 on B6.*Sle1Yaa* leukocytes is unlikely to be the direct consequence of any single genetic contribution responsible for disease, nor the genetic background, but instead is a common downstream consequence of the disease process.

Increased CXCR4 expression leads to increased migration to positive CXCL12 gradients and increased B-cell survival

We next examined the functional consequences of upregulation of CXCR4 in diseased mice. B6.*Sle1Yaa* splenocytes, which express more CXCR4, were found to migrate 3-fold better to positive CXCL12 gradients when compared to B6 controls (Figure 24A). Among the cell-types that expressed CXCR4, the migratory potential of neutrophils, monocytes, and B-cells differed most significantly between the strains, although all cell types from diseased mice which express higher CXCR4 levels migrated better to CXCL12, compared to the B6 controls (Figure 24, and data not shown). Also, when CXCL12 was added to both the top and bottom chambers, no significant migration was observed (data not plotted), excluding chemokinesis as a possible explanation for these data.

In addition to its role in chemotaxis, CXCL12 has also been shown to impact B-cell lymphopoesis [187]. Therefore, we assessed whether increased CXCR4 expression affected the responses of B cells to stimulation with CXCL12. We found that BCR-ligated B-cells from B6.*Sle1Yaa* spleens were less apoptotic when exposed to CXCL12 (Figure 24B). We detected no differential B-cell responses to CXCL12 in terms of proliferation or the expression of activation markers (data not shown). We also detected no difference in the proliferation or activation of B6.*Sle1Yaa* T-cells when they were

exposed to CXCL12 (data not shown). These data indicate that the increased expression of CXCR4 on lupus leukocytes is associated with multiple functional consequences, the most profound of which include enhanced BCR-triggered B-cell survival and chemotaxis to positive CXCL12 gradients.

Increased renal expression of CXCL12 in lupus

Nephritis is a leading cause of morbidity and mortality in lupus, both in mice and in patients. Since end organ disease in lupus is partly the consequence of infiltrating leukocytes, we next asked if the increased renal disease in lupus might be in part driven by heightened CXCR4/SDF1 activity. In support of this, we observed a robust increase in CXCL12 expression in the kidneys of B6.*Sle1Yaa,* but not B6 mice, both by immunohistochemistry (Figure 25A) and by ELISA (Figure 25B). We observed increased CXCL12 in both the glomeruli and the medulla, with additional expression in the interstitium, Bowman's capsules, and glomerular tufts of B6.*Sle1Yaa* kidneys, but not in B6 controls (Figure 25A). Similar increases were also observed in BXSB and MRL.*lpr* kidneys (data not shown). These data suggest that increased CXCL12 expression in the kidney may be a common downstream event in the progression of lupus nephritis, perhaps reflecting the kidney's natural repair response to damage. Consistent with the robust CXCL12-tropic migratory capacity of B6.*Sle1Yaa* leukocytes seen *in vitro*, we detected an impressive accumulation of CXCR4+ cells within B6.*Sle1Yaa* kidneys *ex vivo* (Figure 26). Collectively, these data suggest that the CXCR4/CXCL12 axis may be instrumental for leukocyte trafficking into the kidneys, and thus may play an important role in mediating renal pathology in lupus nephritis.

Pharmacological inhibition of CXCR4 significantly ameliorates disease

The association of increased expression of CXCR4 and CXCL12 with disease in multiple models of spontaneous lupus nephritis suggested that this axis may play an important role in mediating the disease. If so, pharmacological blockade of this axis may be an effective strategy for therapeutic intervention in lupus nephritis. To directly test this, we used the CXCR4 peptide antagonist CTCE-9908, obtained from Chemokine Therapeutics. Initial characterizations indicated that CTCE-9908 was effective in blocking chemotaxis by B6.*Sle1Yaa* splenocytes *in vitro*, with the migration of all cell types being inhibited equally (Figure 27). To test the therapeutic efficacy *in vivo*, B6.*Sle1Yaa* mice were subjected to two sets of placebo-control studies. The preventive efficacy of CXCR4 blockade treatment was tested on a cohort of 2-month old B6.*Sle1Yaa* mice, which typically do not have anti-nuclear antibodies in their sera, or kidney disease. The potential therapeutic efficacy of CXCR4 blockade was tested on 4-month old B6.*Sle1Yaa* mice, which by this age have already developed detectable impairment of renal function, high titers of ANAs and a large spectrum of immunological changes [32].

Blocking the CXCR4 axis from the age of 2 months, significantly prolonged survival (by roughly two months), reduced splenomegaly (by roughly half), subdued T-cell and B-cell activation, blocked autoantibody production (almost completely), and ameliorated nephritis (Figure 28, and data not shown). The observed change in splenomegaly was accompanied by significant reductions in peripheral T and B-cells, as well as various myeloid cells (Cohort I in Table 9). Surprisingly, similar disease amelioration and lifespan prolongation was also seen when treatment was started after disease onset (Figure 29, and data not shown). Although splenomegaly was not reversed

in the latter study (Cohort II in Table 9 and data not shown), renal disease was significantly dampened by the "treatment" regime. In both the preventative and treatment studies, the absolute numbers of leukocytes, particularly various myeloid cell subsets, recruited into the kidneys were profoundly reduced by CXCR4 blockade (Table 9, Figure 30). Both the preventative and therapeutic treatments were not associated with any changes in body weight, hemoglobin levels, red blood cell counts or liver function tests (data not shown), alluding to the safety of the administered drug.

Increased renal expression of CXCL12 in human lupus

Given the heightened expression of CXCR4/CXCL12 in murine lupus and its demonstrated role in disease pathogenesis, we were interested in determining if this axis was similarly upregulated in human lupus nephritis. To this end, we explored if heightened CXCL12 may also be an underlying feature of end-organ disease in human SLE. Analyses of renal biopsies obtained from lupus nephritis patients also revealed that CXCL12 expression correlated with renal pathology (Figure 31). CXCL12 expression was limited to the glomeruli with minimal tubular expression in patients with WHO Type I nephritis. As renal pathology worsened, CXCL12 expression increased in terms of intensity and expressing renal segments. Indeed, in patients with Type IV GN, CXCL12 was detected at high levels in virtually all renal segments, and resembled the staining patterns seen in the kidneys from 8-10 month old lupus mice (Figure 25). As a non-inflammatory control, biopsies from minimal change disease patients were also analyzed. CXCL12 expression in these kidneys was minimal, and was localized to substructures in the glomerular tufts (Figure 31). Further studies are underway to determine if the cell-

types expressing CXCL12 in these patients are podocytes, the cell-types damaged in this disease. These findings are consistent with reports citing CXCL12 as a chemokine released upon renal damage [185]. The present report constitutes the first demonstration of increased CXCL12 expression after renal damage in humans. Taken together, these data indicate that a similar mechanism of CXCR4/CXCL12-mediated leukocyte trafficking to the kidney may be occurring in human lupus as well.

Increased CXCR4 expression in human lupus PBLs

From November 2007 to July 2008, peripheral blood leukocytes were collected from hospitalized patients at the Université de Paris Descartes at Paris, France. The descriptive clinical and demographic data is in preparation.

Figure 32 summarizes the profile of CXCR4 expression on patients with SLE, control patients, and disease-control rheumatoid arthritis patients. We found specific upregulation of CXCR4 on B and T-cells of SLE patients compared to both control and rheumatoid arthritis patients. These data suggest that CXCR4 upregulation is a disease-specific process, and that, combined with the increased CXCL12 observed in nephritic kidneys, anti-CXCR4 therapy may be a suitable targeted therapy for SLE patients at risk for renal sequella.

DISCUSSION

The data presented in this communication suggest an important role for CXCR4/CXCL12 in mediating lupus and lupus nephritis. It is clear that CXCR4 is hyper-expressed in all mouse models of lupus examined in this study. These are genetically

diverse models, including strains harboring lupus susceptibility loci from the NZB/NZW and BXSB mouse models, as well as MRL.*lpr*. This observation suggests that CXCR4 hyper-expression might be a generalized feature of lupus, independent of the underlying genetic basis. In all of the strains examined, the highest levels of CXCR were noted on myeloid cells (particularly on neutrophils and inflammatory macrophages) as well as terminally differentiated B-cells (notably on plasma cells and pre-plasmablasts), an observation that is consistent with the expression patterns reported in the literature [176-178, 187]. Although we detected an increase in CXCR4 expression on memory CD4+ T-cells isolated from mice with lupus, these result did not reach statistical significance; this trend, however, is consistent with our previous studies using microarray analysis of splenic CD4+ T-cells which revealed significantly increased CXCR4 mRNA in B6.*Sle1Yaa* mice when compared to B6 [32].

Given the increased expression of CXCR4 on myeloid cells and terminally differentiated B-cells, it appears most likely that altered trafficking patterns of these two cell types may be contributing to disease in lupus. With respect to the myeloid cells, the enhanced trafficking of these cells to the kidneys may be a key contributor to the heightened nephritis seen in these mice. This notion is supported by the observation that kidneys from lupus-afflicted mice exhibit profound increases in the absolute numbers of $CXCR4^{+}$ myeloid cell infiltrates, as well as the ligand for CXCR4, CXCL12. This was bolstered by the finding that blocking CXCR4 reverses the infiltration of myeloid cells into the kidneys and the accompanying disease. Among the myeloid cell subtypes that are most likely responsible for the renal pathology in these disease models are neutrophils and inflammatory monocytes, based on their highest CXCR4 expression levels, and

previous literature reports. Indeed, the role of intra-renal CXCL12 in recruiting inflammatory cells into the kidneys has been elegantly demonstrated in other experimental models of nephritis [185, 188]. We have also demonstrated a similar increase in CXCL12 expression in renal biopsies from patients with lupus nephritis, with increases in the intensity and promiscuity of expression correlating well with worsened pathology and specific, and increased CXCR4 expression on PBLs of SLE patients. These findings suggest that the CXCR4/CXCL12 axis may be playing a similar role in human lupus nephritis.

The potential mechanisms through which $CXCR4^+$ B-cells may be contributing to lupus are less obvious. Besides the enhanced chemotaxis towards CXCL12, the heightened CXCR4 levels on B-cells is also likely to confer prolonged survival. One can envision a scenario in which this could contribute to a breach in peripheral B-cell tolerance. The prolonged survival of autoreactive germinal center B-cells and plasma cells, as a consequence of increased CXCL12-triggered signaling [189-191] could potentially lead to increased autoantibody levels. This model is consistent with the observation that blocking CXCR4/CXCL12 reduces autoantibody levels, particularly in the preventative study. Potentially, the increased CXCR4 levels on plasmablasts may facilitate increased trafficking of these cells to the kidneys and promote their survival within intrarenal niches; however, we did not find any increase in $CXCR4^+$ plasma cells (or B-cells) within B6.*Sle1Yaa* kidneys (data not shown). Whether the $CXCR4^+$ plasma cells in lupus might have homed to yet other (i.e., non-renal) niches is a question that warrants further study. Finally, since CXCR4 levels are tightly regulated in different subsets of germinal center B-cells [177, 179], a further possibility is that the heightened

CXCR4 levels observed on lupus B-cells may lead to altered trafficking and affinity maturation patterns within the germinal centers—a possibility that needs to be formally evaluated.

Given the observation that the heightened expression of CXCR4 on myeloid and B-cells may have biological consequences that facilitate lupus pathogenesis, a key question that arises is the potential therapeutic utility of CXCR4 blockade in lupus. Indeed, there has been an isolated report on the therapeutic benefit of targeting its ligand, CXCL12: Balabanian *et al* showed that treatment of New Zealand Black / New Zealand White (NZB/W) mice with anti-CXCL12 antibody ameliorated several lupus phenotypes, although in their study, the analyses focused on the role of peritoneal B1a cells [192]. Given that CXCR4 also plays an important role in AIDS and tumor metastases, there has been a flurry of research reports based on novel CXCR4 blocking agents [193-196]. This includes CTCE-9908 from Chemokine Therapeutics, which has proven effective in Phase I/II trials in osteosarcoma and prostate cancer [197, 198]. Given the demonstrated safety and efficacy of this agent in the completed and ongoing human clinical trials, this appeared to be a suitable drug choice for testing in murine lupus. Indeed, the early use of a peptide antagonist of CXCR4 prevented all serological, cellular and clinical manifestations of lupus, indicating that all component lupus phenotypes (and the associated pathogenic events) are absolutely dependent upon CXCR4 expression, early in the disease process. As discussed above, this might relate to the absolute requirement of CXCR4 on B-cells and myeloid cells, for the initiation of autoantibody production and renal disease.

In contrast, when CXCR4 blockade is instituted late in disease, well after the onset of proteinuria and elevated serum autoantibodies, most of the cellular changes associated with lupus in the B6.*Sle1Yaa* model were recalcitrant to treatment. However, late-phase therapy was still able to curtail the progression of renal disease, with attendant prolongation of lifespan in these mice. These observations have important ramifications. First, they suggest that the dominant cause of death in these mice is nephritis, rather than splenomegaly (or associated hematological abnormalities). Second, they indicate that renal disease in lupus can be divorced from systemic cellular and serological changes—in other words, mice with severe splenomegaly and high autoantibody levels can live a "normal" lifespan if the renal disease is therapeutically controlled, a scenario which is reminiscent of FcR-deficient lupus mice. Finally, these studies raise hope that instituting CXCR4 blockade in patients with active lupus nephritis might also be therapeutically effective.

		B6 (n=10)	B6.*Sle1Yaa* (n=6)	BXSB (n=6)	MRL.*lpr* (n=6)
SPLEEN	Mean B6 mfi				
CD11b$^+$ B220$^-$ mfi of CXCR4 and fold Δ	20.2 ± 2.1	1.0 ± 0.1	1.9 ± 0.1**	1.5 ± 0.1**	1.3 ± 0.1*
% of CXCR4+ cells		16.7 ± 10.9	31.3 ± 9.5*	39.6 ± 9.4**	22.0 ± 4.2
Resident Monocyte (CD11b$^+$ Gr-1^{lo})	18.3 ± 3.3	1.0 ± 0.1	1.2 ± 0.4	1.2 ± 0.7	1.2 ± 0.2
		16.0 ± 9.0	18.5 ± 2.8	29.9 ± 4.9*	25.6 ± 8.2
Inflamm. Monocyte (CD11b$^+$ Gr-1^{int})	18.8 ± 2.8	1.0 ± 0.0	1.7 ± 0.2**	1.7 ± 0.3***	1.6 ± 0.2**
		16.8 ± 9.9	34.2 ± 14.5*	51.4 ± 16.2***	39.6 ± 7.5*
Neutrophil (CD11b$^+$ Gr-1^{hi} SSc^{hi})	16.2 ± 2.2	1.0 ± 0.0	1.5 ± 0.2*	1.7 ± 0.2**	1.5 ± 0.2**
		15.2 ± 8.4	44.9 ± 15.0**	35.4 ± 8.3**	30.4 ± 9.0*
Myeloid DC (CD11b$^+$ B220$^-$ CD11c$^+$)	1.0	UD	UD	UD	UD
		UD	UD	UD	UD
Plasma DC (CD11b$^+$ B220$^+$ CD11c$^+$)	18.4 ± 4.4	1.0 ± 0.0	0.5 ± 0.1	1.3 ± 0.1	0.4 ± 0.1
		4.3 ± 1.7	3.1 ± 1.9	5.2 ± 2.1	2.8 ± 1.1
B220$^+$ CD11b$^-$ mfi of CXCR4 and fold Δ	20.3 ± 2.4	1.0 ± 0.0	1.8 ± 0.2**	1.7 ± 0.1**	0.6 ± 0.1
% of CXCR4+ cells		12.3 ± 9.0	17.9 ± 5.2**	20.8 ± 5.0**	17.5 ± 6.4
T1 (CD23$^-$ CD21^{lo} IgM$^+$)	6.9 ± 1.4	1.0 ± 0.1	1.6 ± 0.3*	1.5 ± 0.1*	0.7 ± 0.1
		15.8 ± 6.4	23.3 ± 4.4*	36.8 ± 5.1*	6.4 ± 3.0
T2 (CD23$^+$ CD21^{hi} IgM^{hi})	19.9 ± 5.1	1.0 ± 0.1	1.4 ± 0.1*	1.6 ± 0.1**	0.5 ± 0.1**
		21.0± 9.3	32.4 ± 9.3*	38.9 ± 5.3*	15.1 ± 6.1
MZ (CD23$^-$ CD21^{hi} IgM$^+$)	21.1 ± 3.8	1.0 ± 0.1	1.1 ± 0.3	1.2 ± 0.2*	0.9 ± 0.3
		20.4 ± 1.6	22.7 ± 9.7	27.3 ± 4.7*	12.5 ± 4.4
Follicular (CD23$^+$ CD21$^+$ IgM^{lo})	7.5 ± 1.7	1.0 ± 0.1	0.9 ± 0.1	1.5 ± 0.1**	1.0 ± 0.0
		9.3 ± 2.5	17.0 ± 6.4*	25.9 ± 4.7**	7.0 ± 2.7*
Plasma (B220$^-$ CD138$^+$)	60.0 ± 0.9	1.0 ± 0.0	2.5 ± 0.2**	1.8 ± 0.0	1.6 ± 0.1**
		23.2 ± 11.1	49.0 ± 10.5**	41.4 ± 7.6**	33.0 ± 9.4*
Pre-Plasma (B220$^+$ CD138$^+$)	75.7 ± 9.2	1.0 ± 0.1	1.8 ± 0.2**	1.5 ± 0.2*	0.6 ± 0.1*
		39.8 ± 9.8	50.1 ± 9.0*	62.7 ± 6.7**	15.6 ± 6.4*
CD4$^+$ CD8$^-$ mfi of CXCR4 and fold Δ	5.4 ± 0.9	1.0 ± 0.1	1.4 ± 0.7	1.7 ± 0.2	1.3 ± 0.1
% of CXCR4+ cells		6.1 ± 1.5	8.9 ± 0.8	9.4 ± 2.7*	4.5 ± 0.9
Memory (CD62L$^-$ CD44^{hi})	8.0 ± 0.9	0.9 ± 0.1	0.9 ± 0.4	1.3 ± 0.1	0.9 ± 0.0
		8.8 ± 2.2	9.1 ± 0.9	9.8 ± 0.7	4.5 ± 1.0
Naïve (CD62L$^+$ CD44^{lo})	1.0	UD	UD	UD	UD
		UD	UD	UD	UD
PERIPHERAL BLOOD					
CD11b$^+$ B220$^-$ mfi of CXCR4 and fold Δ	13.1 ± 2.1	1.0 ± 0.1	1.3 ± 0.1**	1.1 ± 0.1*	1.3 ± 0.2
% of CXCR4+ cells		11.6 ± 5.0	18.1 ± 5.1*	22.6 ± 7.1**	11.9 ± 5.7
Resident Monocyte (CD11b$^+$ Gr-1^{lo})	12.2 ± 2.0	1.0 ± 0.1	1.6 ± 0.8	1.3 ± 0.2	1.2 ± 0.2
		4.9 ± 1.6	12.5 ± 7.0	7.4 ± 2.8	7.5 ± 4.6
Inflamm. Monocyte (CD11b$^+$ Gr-1^{int})	16.0 ± 2.1	1.0 ± 0.1	1.5 ± 0.2*	1.6 ± 0.2*	1.4 ± 0.1**
		9.5 ± 4.5	21.7 ± 9.4*	30.4 ± 3.8**	18.6 ± 9.9*
Neutrophil (CD11b$^+$ Gr-1^{hi} SSc^{hi})	14.1 ± 2.2	1.0 ± 0.2	1.2 ± 0.2**	1.2 ± 0.1*	1.2 ± 0.2
		8.4 ± 4.5	18.0 ± 4.5*	31.3 ± 5.7**	18.9± 9.9*

Table 8. CXCR4 Expression Levels.
ANOVA with Dunnet post-hoc test was used for statistical analyses (*, $P < 0.05$; **, $P < 0.01$; ***, $P < 0.001$).

	B6 (n=4)	CTCE I (n=7)	CTCE II (n=5)	B6.Sle1Yaa (n=4)
SPLEEN	**Cells x 10^4**			
Resident Monocyte ($CD11b^+$ $Gr\text{-}1^{lo}$)	323.0 ± 26.8	1164.4 ± 223.4	4708.0 ± 1195.7	2435.0 ± 491.1
Inflamm. Monocyte ($CD11b^+$ $Gr\text{-}1^{int}$)	81.2 ± 18.9	1026.4 ± 209.8	2148.0 ± 419.0	1535.3 ± 415.1
Neutrophil ($CD11b^+$ $Gr\text{-}1^{hi}$ SSc^{hi})	100.8 ± 42.1	516.9 ± 119.1	896.8 ± 132.8	462.0 ± 79.2
T1 ($CD23^-$ $CD21^{lo}$ IgM^+)	194.0 ± 30.5	116.8 ± 29.6	29.7 ± 14.9	338.5 ± 75.9
T2 ($CD23^+$ $CD21^{hi}$ IgM^{hi})	322.0 ± 32.7	221.1 ± 48.9	871.0 ± 291.2	668.6 ± 247.2
MZ ($CD23^-$ $CD21^{hi}$ IgM^+)	430.3 ± 29.7	26.5 ± 6.7	4.0 ± 1.8	104.3 ± 37.5
Follicular ($CD23^+$ $CD21^+$ IgM^{lo})	3805.0 ± 406.0	2870.0 ± 410.5	12322.0 ± 4464.3	15460.0 ± 2447.3
Germinal Center ($B220^+$ $GL7^+$)	129.3 ± 31.0	316.7 ± 62.4	511.4 ± 146.1	689.8 ± 105.6
Plasma ($B220^-$ $CD138^+$)	35.0 ± 5.4	627.4 ± 124.7	1217.2 ± 389.7	1214.5 ± 187.2
$CD4^+$ $CD8^-$				
Memory ($CD62L^-$ $CD44^{hi}$)	1687.5 ± 535.4	6267.1 ± 878.0	41460.0 ± 10.942.0	21700.0 ± 3774.3
Naïve ($CD62L^+$ $CD44^{lo}$)	5340.0 ± 607.0	760.7 ± 127.0	1639.0 ± 380.2	1061.0 ± 301.4
$CD8^+$ $CD4^-$				
Memory ($CD62L^-$ $CD44^{hi}$)	405.5 ± 102.0	5811.4 ± 973.4	27680.0 ± 8369.0	11920.0 ± 996.2
Naïve ($CD62L^+$ $CD44^{lo}$)	5615.0 ± 931.6	1510.9 ± 263.2	2592.0 ± 431.8	3999.0 ± 1414.0
KIDNEY				
CD45+	21.6 ± 2.7	38.9 ± 6.1**	57.9 ± 15.6***	98.5 ± 11.4
Resident Monocyte ($CD11b^+$ $Gr\text{-}1^{lo}$)	7.1 ± 1.1	18.6 ± 3.4**	20.3 ± 6.8**	42.5 ± 7.1
Inflamm. Monocyte ($CD11b^+$ $Gr\text{-}1^{int}$)	0.2 ± 0.0	1.5 ± 0.4*	2.0 ± 0.6*	3.0 ± 0.6
Neutrophil ($CD11b^+$ $Gr\text{-}1^{hi}$ SSc^{hi})	0.4 ± 0.0	0.6 ± 0.2	2.0 ± 0.8*	2.6 ± 0.5
$CD4^+$ $CD8^-$	0.9 ± 0.1	4.7 ± 1.1*	4.2 ± 0.9*	7.9 ± 1.4
$CD8^-$ $CD4^+$	0.6± 0.1	2.6 ± 0.4	2.6 ± 0.8	4.1 ± 1.3

Table 9. Immune cell subsets in CXCR4-anatagonist-treated mice.
For kidney subsets, ANOVA with Dunnet post-hoc test was used for statistical analyses (*, $P < 0.05$; **, $P < 0.01$; ***, $P < 0.001$).

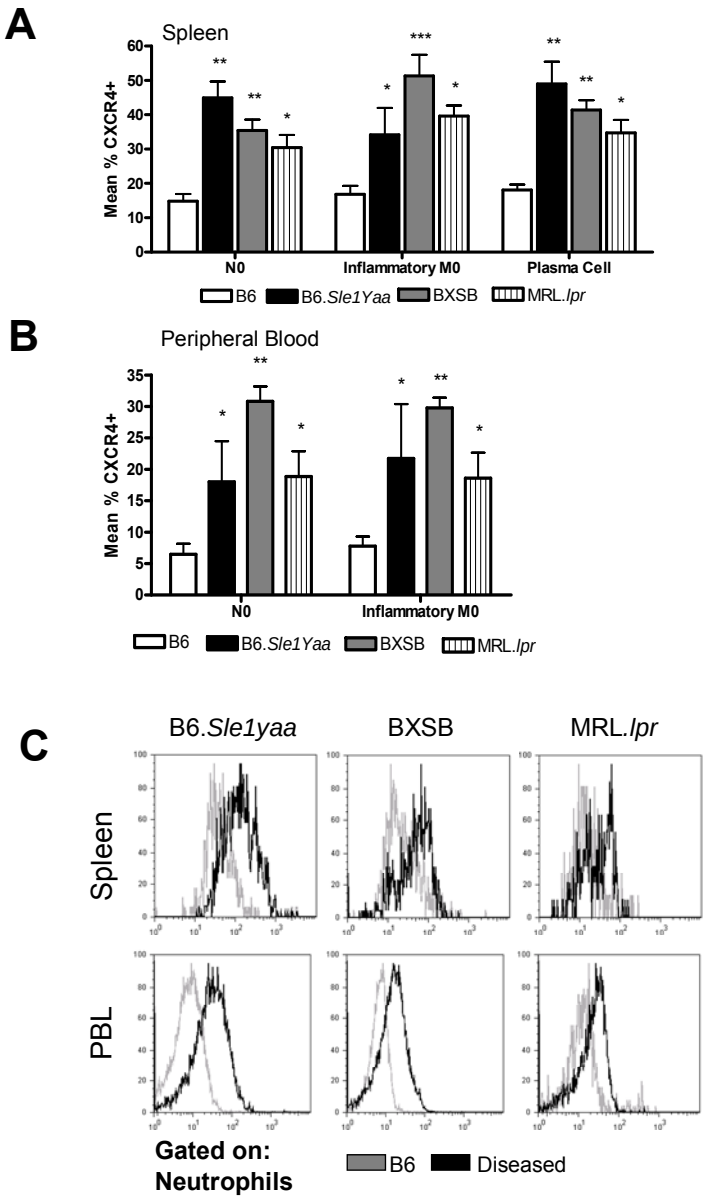

Figure 22. Increased CXCR4 in murine models of lupus.
N = 6, male, 9 - 12 mo. old B6.*Sle1Yaa*, BXSB, MRL.*lpr* and B6 mice (N = 10) subjected to flow cytometric analyses. Increased expression of CXCR4 was detected on neutrophils (N0, $CD11b^{+}$, $r\text{-}1^{hi}$), inflammatory monocytes (inflammatory M0, $CD11b^{+}$, $Gr\text{-}1^{int}$), and plasma cells ($B220^{lo}$, $CD138^{+}$) in the spleen and peripheral blood, compared to B6 (*, $P < 0.05$; **, $P < 0.01$; ***, $P < 0.001$, by Welch-corrected t-test). The mean fluorescence intensities and the percentage of each cell type that expressed CXCR4 are detailed in Table *INSERT*. Shown in (C) are representative histogram overlays.

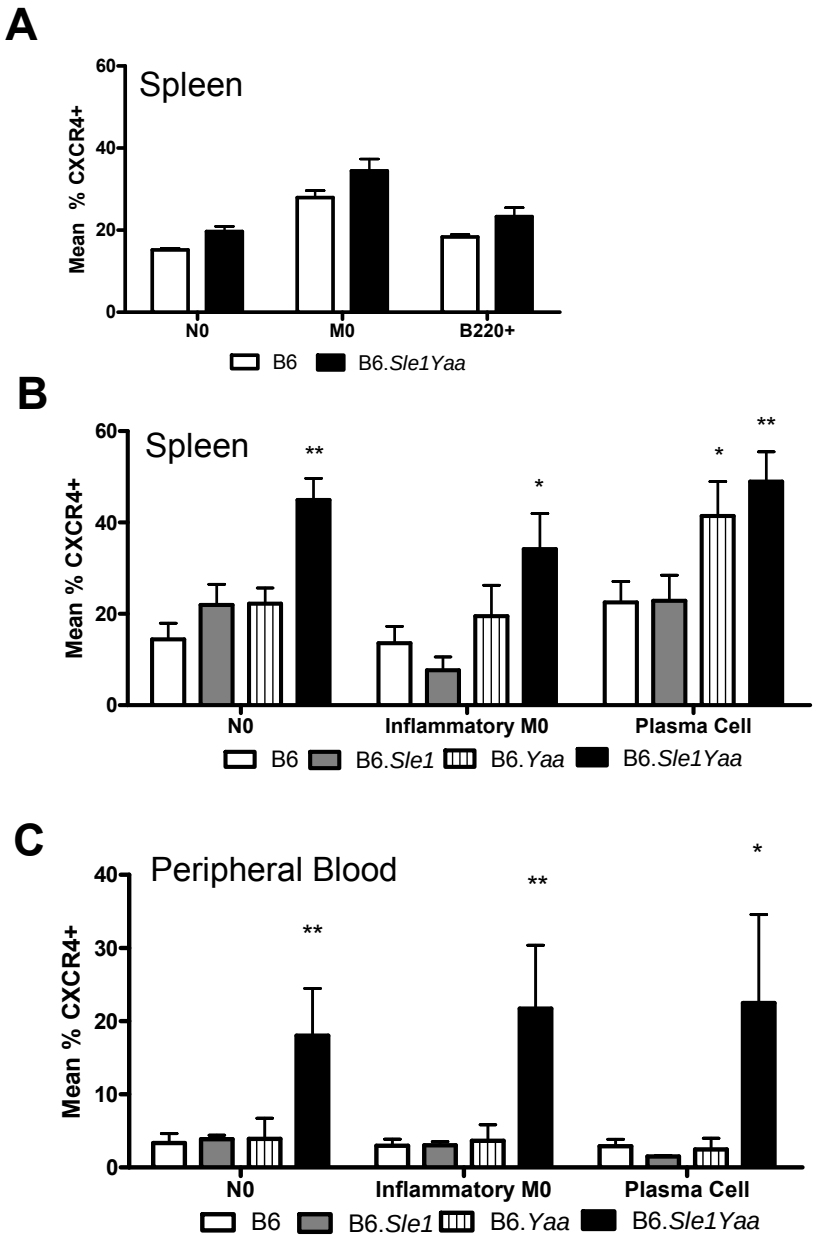

Figure 23. CXCR4 hyperexpression in B6.*Sle1Yaa* mice is not the direct consequence of either locus, but arises as a result of the disease.
Shown in (A) is a comparison of mean CXCR4 levels on young (age ≤ 2 mo.) B6.*Sle1Yaa* compared to old (9 - 12 mo.) B6.*Sle1Yaa* mice (N = 15). Shown in (B) are the mean percentages of myeloid cells or plasma cells that express CXCR4 in B6.*Sle1Yaa* mice, or the related monocongenic strains (N = 6 each). ANOVA with Dunnet post-hoc test was used for statistical analyses (*, $P < 0.05$; **, $P < 0.01$; ***, $P < 0.001$).

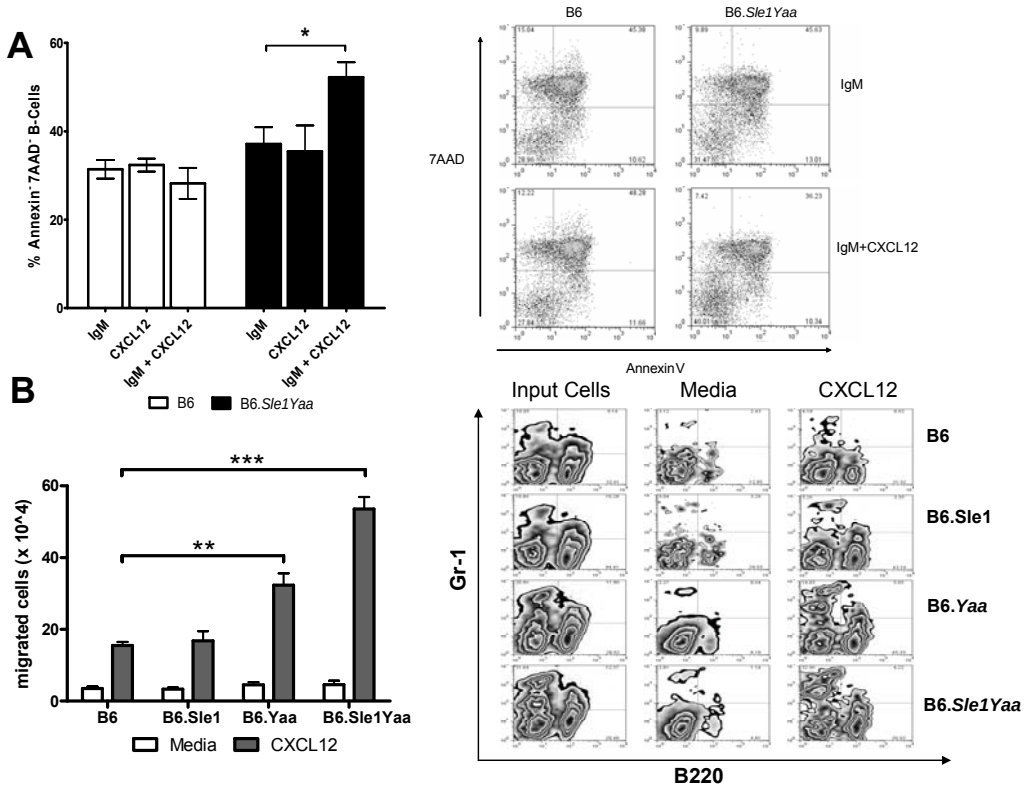

Figure 24. Functional consequences of CXCR4 upregulation on B6.*Sle1yaa* leukocytes.

(A). Splenocytes from 9 - 12 mo. old B6, B6.Sle1, B6.Yaa and B6.Sle1Yaa mice were subjected to transwell migration assays towards 50 ng/ml CXCL12 placed in the bottom chamber. Cells that had extravasated into the bottom chamber were enumerated and phenotyped by flow cytometric analyses. *, $P < 0.05$; **, $P < 0.01$; ***, $P < 0.001$, by ANOVA with Dunnet post-hoc analyses.

(B). B6 and B6.Sle1Yaa splenic B-cells were stimulated with anti-IgM F(ab)'2 antibodies and recombinant CXCL12, and assayed by flow cytometry for apoptosis, using Annexin V and 7-AAD.

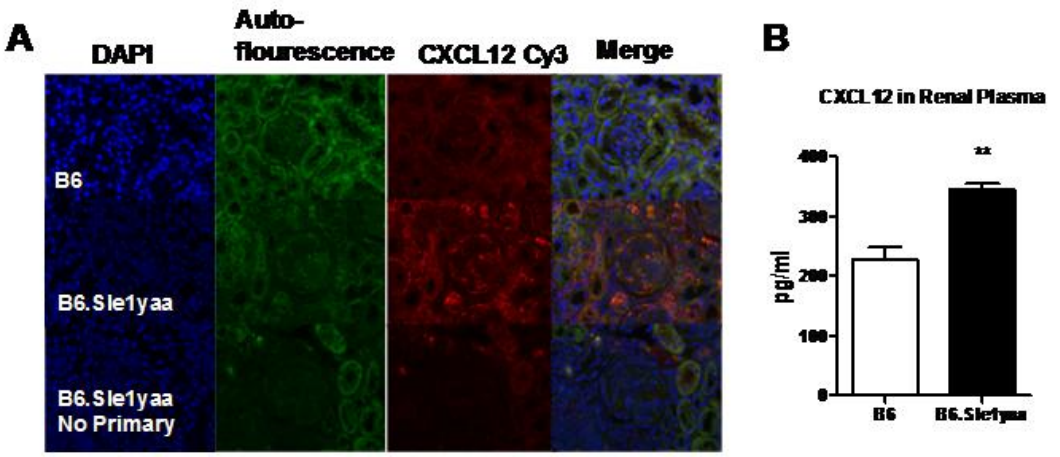

Figure 25. Increased CXCL12 expression in lupus kidneys.
CXCL12 was detected on paraffin-fixed sections of B6.Sle1Yaa mice (and B6 controls) using colometric immnohistochemistry (A). Displayed below are the zoom-in magnifications of the same pictures. Shown pictures are representative of 5 independent samples for each strain. Renal plasmaharvested from 9 - 12 mo. B6 and B6.Sle1Yaa mice (N = 6) were examined for CXCL12, by ELISA (B). **, $P < 0.01$ by Welch-corrected t-test.

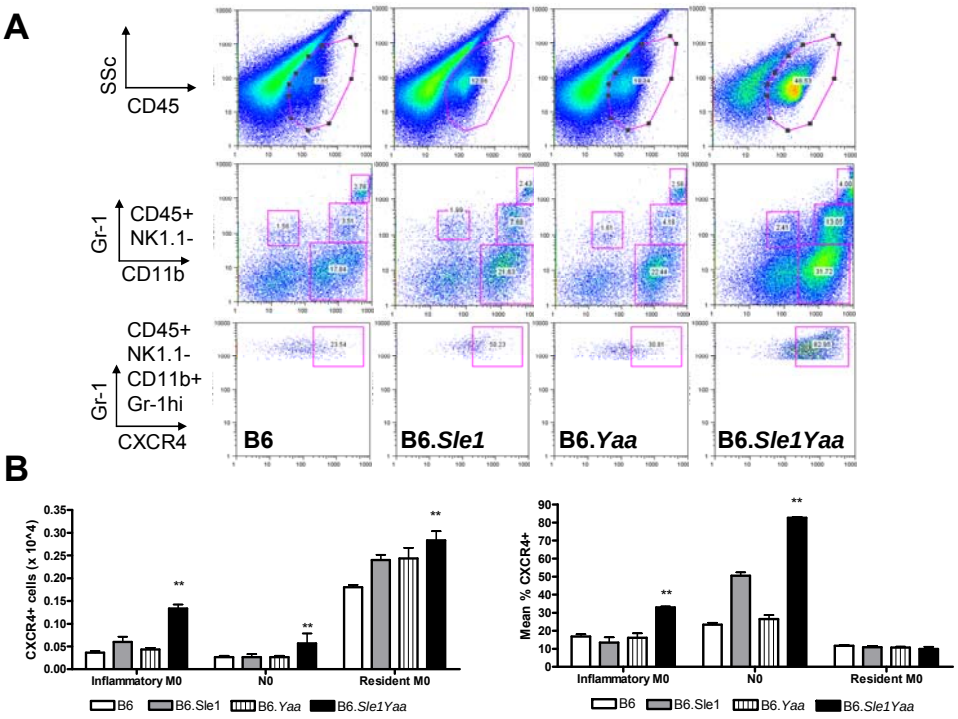

Figure 26. Accumulation of CXCR4$^+$ leukocytes in lupus kidneys.
Whole kidneys were subjected to digestion and percoll density centrifugation, as detailed in Materials and Methods. The fraction enriched for leukocytes (as shown in top row of 2D-plots) was enumerated using trypan blue exclusion and subjected to flow cytometric analyses. Plotted in (B) are the numbers of CXCR4+ cells and the percentage of cells with CXCR4 expression on B6.Sle1Yaa cells and cells from the relevant monocongenic strains and B6 control. Shown P values pertain to comparisons of the B6.Sle1Yaa levels against that of B6.Sle1 and B6.Yaa by ANOVA (Bonferroni post-hoc test, *, $P < 0.05$; **, $P < 0.01$; ***, $P < 0.001$).

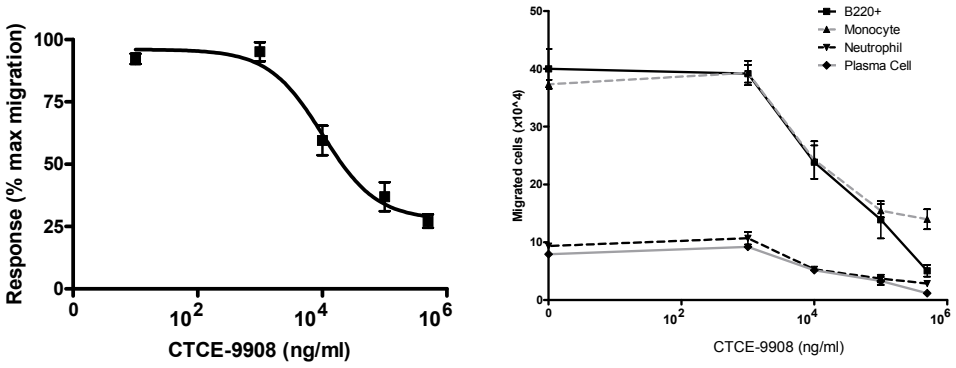

Figure 27. Pharmacodynamic analyses of the effect of CTCE-9908 on leukocyte migration to positive SDF-1 gradients.
Splenocytes from 9 month old B6.*Sle1Yaa* mice were pre-incubated with various doses of CTCE-9908 for 30 minutes at 37^0C and subjected to transwell migration assays towards 50 ng/ml CXCL12 placed in the bottom chamber. Percentage of maximum migration was calculated by dividing the number of CTCE-9908-treated cells which migrated to the lower chamber by the number of untreated migrated cells. Cells that had extravasated into the bottom chamber were enumerated and phenotyped by flow cytometric analyses.

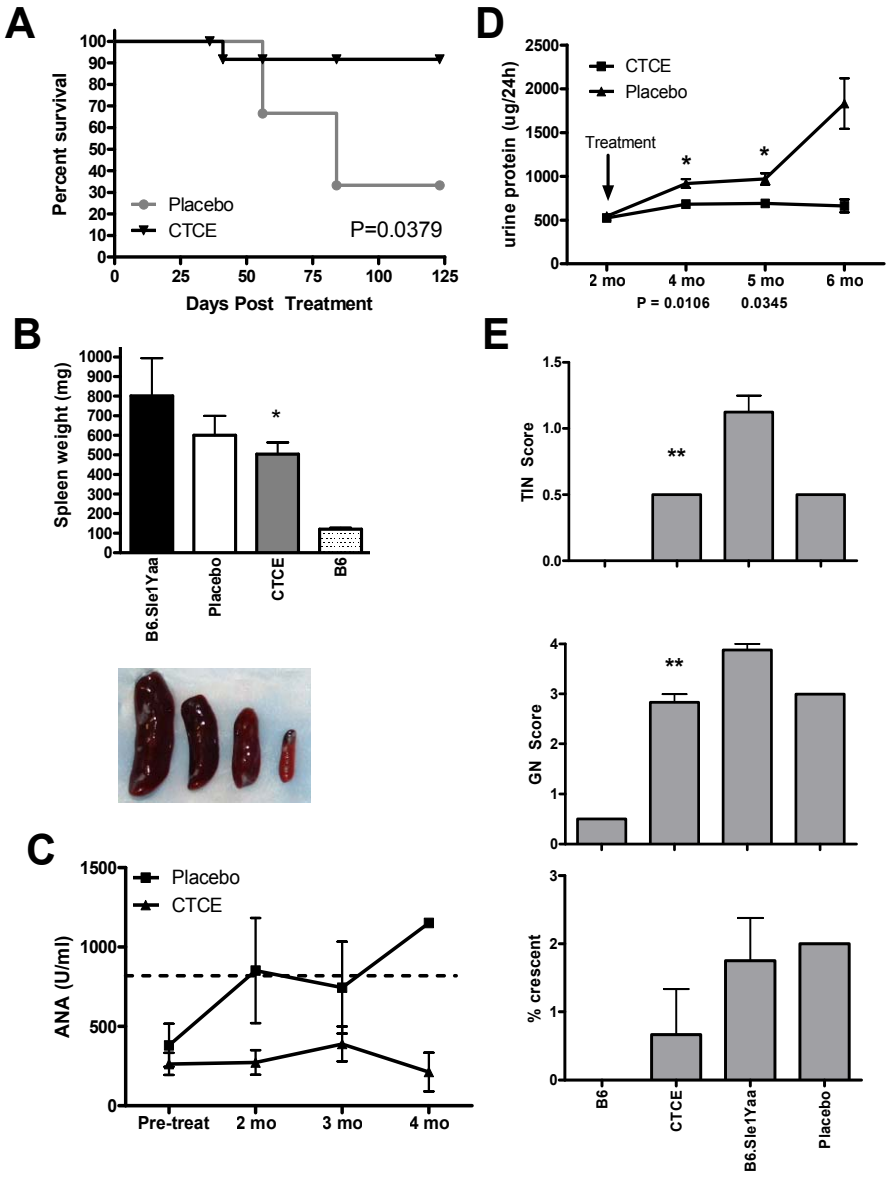

Figure 28. In vivo "prevention" studies with a CXCR4 peptide antagonist.
2 mo old B6.Sle1Yaa males ('Cohort I') were injected with CTCE-9908 (n=11) or vehicle placebo (N = 5). All mice were sacrificed at the age of 5 - 6 mo. 100 µl of CTCE-9908 at 50 mg/kg or vehicle placebo were injected intraperitoneally three times a week for the course of study. Plotted in (A) is the survival curve for mice in the "prevention" study ('Cohort I'). Indicated in (B) are the spleen sizes upon sacrifice of the mice; examples of spleens from the respective strains are aligned below. Displayed in (C) are the anti-chromatin ANA levels (as assayed by ELISA) over the course of the treatment regime. Shown in (D) are the total proteinuria levels detected in 24 hour urine collections, at the indicated ages. Plotted in (E) are the renal histopathological findings, upon

sacrifice at 6 mo. Due to the early mortality of placebo control mice, 5 mo. old B6.Sle1Yaa mice, which were not statistically different when compared placebo controls, were used as disease controls in these experiments and were pooled with surviving placebo controls in subsequent statistical analyses. *, $P < 0.05$; **, $P < 0.01$; ***, $P < 0.001$, by log-rank Mantel-Cox test, Welch-corrected t-test, or the Mann-Whitney u-test, where appropriate.

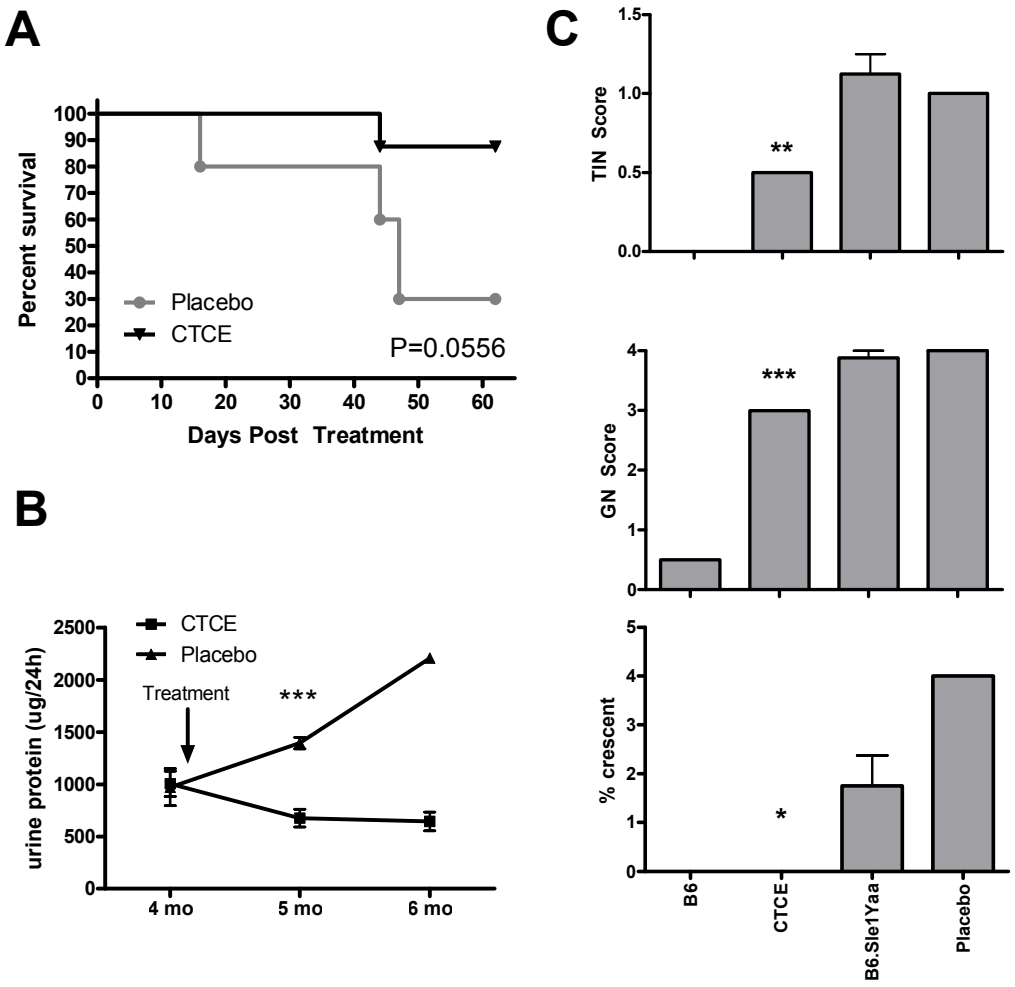

Figure 29. Use of the CXCR4 peptide antagonist dampens lupus nephritis even when administered after disease onset.
4 mo old ANA-seropositive B6.Sle1Yaa males ('Cohort II') were injected with CTCE-9908 (n=8) or vehicle placebo (n=5). 100 µl of CTCE-9908 at 50 mg/kg or vehicle placebo were injected intraperitoneally three times a week for the course of study. Plotted in (A) is the survival curve for mice in the "treatment" study ('Cohort II'). Indicated in (B) are the total proteinuria levels detected in 24 hour urine collections, at the indicated ages. Indicated in (C) are the glomerulonephritis scores, tubulointerstitial disease scores, and extent of glomerular crescent formation in kidneys obtained from the different groups of mice studied, upon sacrifice at 6 mo. Due to the early mortality of placebo control mice, 5 mo. old B6.Sle1Yaa mice, which were not statistically different when compared placebo controls, were used as disease controls in these experiments and were pooled with surviving placebo controls in subsequent statistical analyses. *, $P < 0.05$; **, $P < 0.01$; ***, $P < 0.001$, by log-rank Mantel-Cox test, Welch-corrected t-test, or the Mann-Whitney u-test, where appropriate.

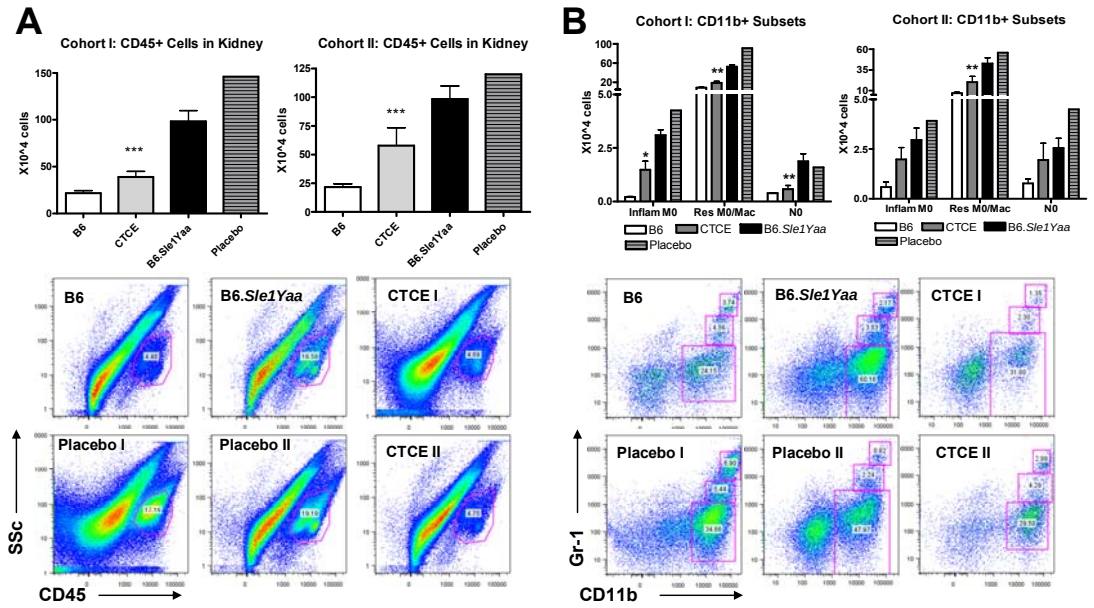

Figure 30. CXCR4 blockade reduces renal leukocyte infiltration in murine lupus nephritis.

Two cohorts of B6.Sle1Yaa male mice were subjected to "prevention" or "treatment" studies, using the CXCR4 peptide antagonist, CTCE-9908, as detailed above in to Figure 6 and 7. Shown in (A) are the absolute numbers of CD45+ cells in the kidneys of the indicated mice upon sacrifice at 6 mo.; indicated below are representative 2D plots demonstrating reduced percentage of leukocytes in the renal cell preparation. Shown in (B) is the Gr-1 / CD11b staining profiles of myeloid cell subsets within the kidneys in the different groups of mice upon sacrifice at 6 mo., and the absolute numbers of various myeloid cell subsets in the kidneys of mice from the different study groups, as further detailed in Supplemental Table S2. Due to the early mortality of placebo control mice, 5 mo. old B6.Sle1Yaa mice, which were not statistically different when compared placebo controls, were used as disease controls in these experiments and were pooled with surviving placebo controls in subsequent statistical analyses. *, $P < 0.05$; **, $P < 0.01$; ***, $P < 0.001$, by log-rank Mantel-Cox test, Welch-corrected t-test, or the Mann-Whitney u-test, where appropriate.

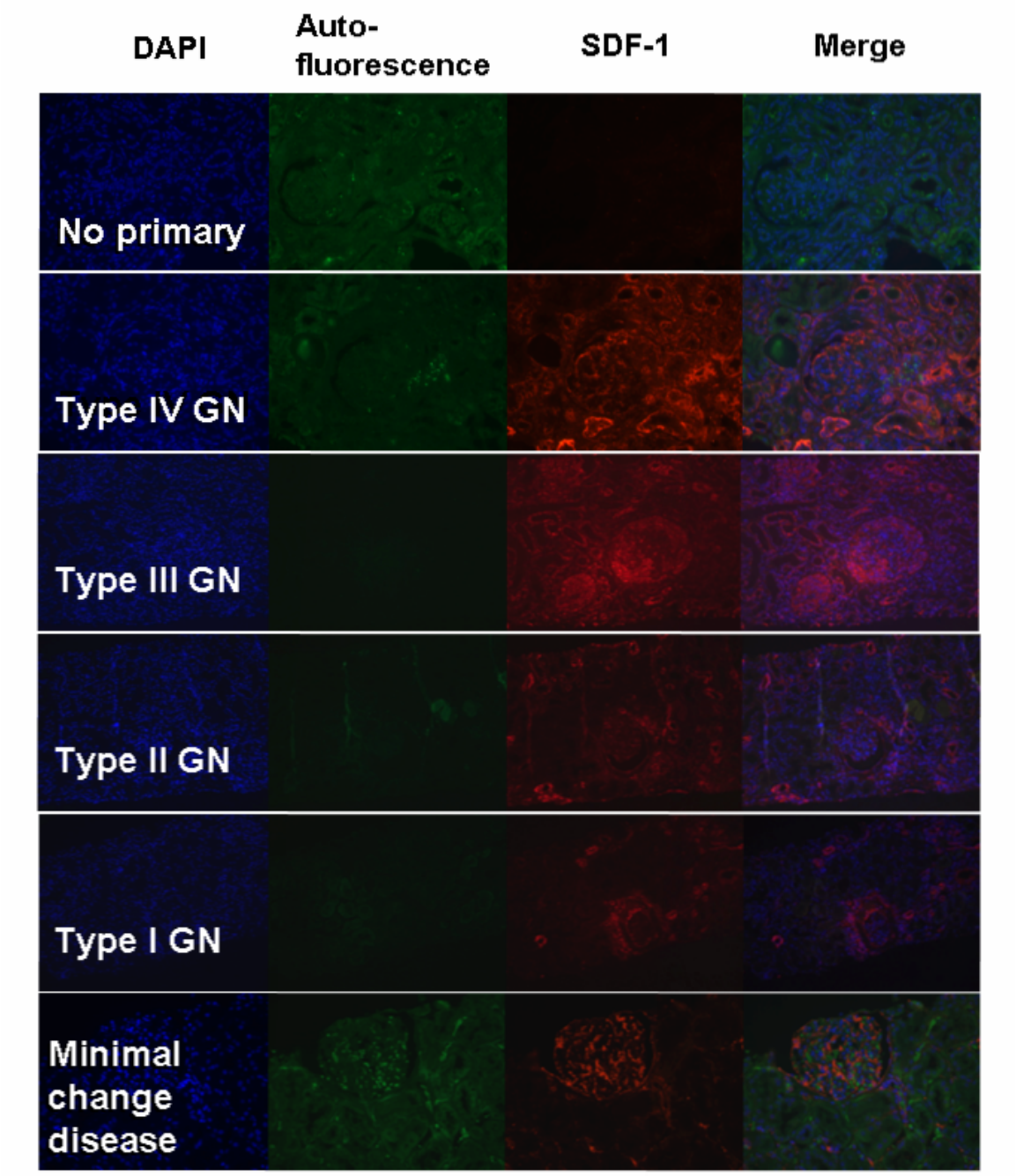

Figure 31. Increased CXCL12 expression in human lupus kidney biopsies. Paraffin-fixed sections of renal biopsies obtained from SLE patients were stained for CXCL12 in a blinded fashion. Displayed are representative images of N = 2 - 3 independent patient kidneys with various WHO-classes of GN. Samples obtained from patients with minimal change disease were used as a non-inflammatory control. When no primary antibody or competitive substrate to the primary antibody was added, no non-specific staining was detected (data not shown).

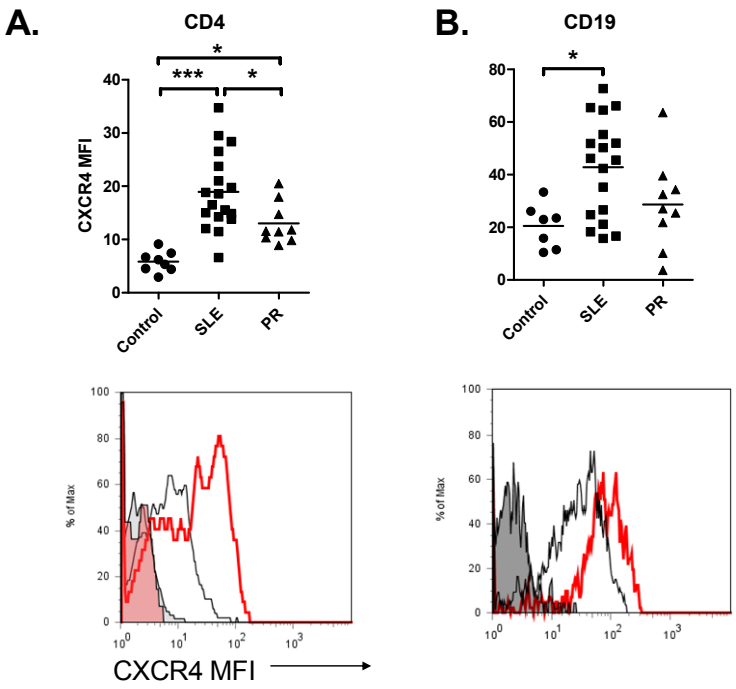

Figure 32. Increased CXCR4 expression in human lupus PBLs.
CXCR4 expression was assessed in healthy controls, SLE patients, and rheumatoid arthritis patients (PR). Shown in (A) are CXCR4 MFIs on CD4 T-cells and in (B) CD19 B-cells with representative histograms below. (*, $P < 0.05$; **, $P < 0.01$; ***, $P < 0.001$, by ANOVA with Bonferroni ad-hoc test)

CHAPTER SIX: General Considerations

Systemic Lupus Erythematosus (SLE) is a complex chronic autoimmune disease. The corpus of studies utilizing congenic dissection in spontaneous murine lupus models, such as NZM2410, has revealed that lesions in two primary pathways, acting in concert, are required for the development of fatal autoimmunity. The first lesion is a dysregulation in humoral tolerance checkpoints that results in production of anti-nuclear autoantibodies (ANA) in the absence of visceral pathologies, while the second involves aberrations of the innate immune system. The epistatic interaction between these lesions on certain backgrounds in the mouse mediates pathologic autoimmunity characterized by lymphadenopathy, splenomegaly, cellular hyperactivation, and renal failure subsequent to glomuerulonephritis (GN).

What follows is a general discussion and critique on the logic behind the work that was presented in this dissertation.

THE MODEL: B6.*Sle1yaa* and CXCR4 revisited

The first question that must be asked when studying animal models of human diseases is whether or not the animal model is an accurate model of the disease. If this question is not posed earnestly and critically, all conclusions drawn from the animal model are irrelevant. Aside from the logical inquiry of the validity of the claim on reality concluded from inductive processes, from the prospective of science as an enterprise—and in translational research in particular—an inquiry on the *a priori* is of the utmost importance, as conclusions drawn from animal models are often applied directly to human disease.

The BXSB.*yaa* and subsequent *yaa*-derived substrains present particular problems with regards to its claim as a *bona fide* model of SLE. The *yaa* models all share characteristics inconsistent with human SLE. At the level of casual observation, *Yaa*, or *Tlr7*, is carried on the Y-chromosome, and, as such, affects uniquely the males, whereas human SLE is known to affect predominantly females with a female to male ratio of 8:1. Although one can envision a scenario in which a problem in X-inactivation in females can cause an inappropriate expression of *Tlr7*, this has not been found in human SLE. Indeed, despite the fact that the conclusions drawn from the discovery of *yaa* point likely to a generalized dysregulation of the innate immune system—and likely in MyD88-associated pathways—rather than a dysregulation in TLR7 *per se*, the questioning of a male model of lupus remains valid, especially because of the known roles of sex hormones in human SLE.

Moreover, TLR7 and RNA-associated antigens are not well-associated with human SLE. In the clinical setting, the immunological hallmark of SLE patients is anti-dsDNA ANA, and serum titers of anti-dsDNA are used clinically, along with serum complement and general signs of inflammation (ESR and fibrinogen), as markers of disease activity. Anti-Sm, present in 25% of SLE patients, but highly specific for SLE, is an autoantibody against a polypeptide in the snRNP complex. All of the antibodies directed against RNA-containing antigens, such as anti-RNP antibody, are used as diagnostic markers of mixed connective tissue disorders, in the case of anti-RNP, such as Sharp's Syndrome. Other RNA-specific antibodies clinically associated with SLE are usually secondary manifestations of autoimmunity that are co-morbid with SLE. Anti-

SSA/SSB antibodies are usually present in SLE patients with associated Sjogren's Syndrome, in cutaneous lupus, or in a neonatal form of lupus. Indeed, SLE patients usually present with tissue-specific autoantibodies in addition to anti-dsDNA or anti-Sm ANAs, such as anti-RBC antibodies responsible for hemolytic anemia, anti-platelet antibodies observed in Evan's Syndrome, anti-phospholipid autoantibodies responsible for anti-phospholipid syndrome and false-positive VDRL tests (ACR criteria), and rheumatoid factor.

At the same time, however, drugs such as hydroxycloroquine are very effective in controlling "mild" SLE. The action of hydroxycloroquine is on the acidification of vesicles in the intracellular transport apparatus. Since TLR recognition of antigens occurs within vesicles, it has been postulated that hydroxycloroquine is effective in controlling the clinical severity of SLE, and, in particular the dermatologic manifestations, because it dysregulates intra-vesicular TLR signaling. TLR7 is one of these intra-vesicular receptors. However, it is clear that in patients with systemic involvement—notably kidney, connective tissue, and CNS involvement—hydroxychloroquine treatment in conjunction with NSAIDs are often not sufficient to control disease activity, and corticotherapy and DMARDs are often required. It is interesting to note here that anti-Ro antibody, theoretically TLR7-dependant, is retrieved in 30% of discoid lupus whereas anti-dsDNA antibody, theoretically TLR9 dependant, is associated with patients with multi-organ involvement, suggesting that, in fact, in humans, it is rather the dysregulation of TLR9 which contributes to disease pathogenesis.

In addition, the *yaa* derived mouse models all share hematologic features inconsistent with human SLE, notably chronic monocytosis, quantitative medullary

insufficiency, and likely myelofibrosis. Analyses of the peripheral blood show general pancytopoenia associated with a flagrant monocytosis (Figure 33 and Figure 34). SLE patients do not present with such pancytopoenia and monocytosis. Whereas anemia (anemia as a result of chronic inflammatory syndrome, pernicious anemia, or autoimmune hemolytic anemia) and Evan's Syndrome are well-associated with SLE, and whereas patients have been found to be lymphopoenic especially during periods of flair, this particular constellation of hematologic features is generally not observed in human SLE patients. Although histological analyses of bone marrow biopsies remain to be done on B6.*Sle1yaa* mice to demonstrate reticular densification and increased collagen content and blood smears need to be done to visualize the presence of dacryocytes, macroscopic observation of the femurs of these mice show that they are extremely hard and brittle. Moreover, the peripheral pancytopoenia and myelemia are together nonetheless very evocative of myelofibrosis.

In addition, neither hepatosplenamegalie nor flagrant lymphadenopathy is well-associated with SLE. In the *yaa*-derived strains, there is massive lymphadenopathies (cervical, axillary, inguinal, and mesenteric) and massive splenomegaly. Taken all together, these particular "symptoms" of the *yaa* mouse—chronic monocytosis, medullary insufficiency, myelofibrosis, lymphadenopathy, splenamegaly—are evocative of chronic myelomonocytic leukemia (CMML).

Analyses of the bone marrow show an accumulation of monomyelocytic precursors with total blasts greater than 5% of the bone marrow content (Figure 35). Coupled with flow cytometric analyses of the peripheral blood, which demonstrates an accumulation of medullary monocytes and medullary insufficiency, and the

lymphadenopathy and splenomegaly observed, the overall clinical picture is suggestive of type II CMML with a tendency towards acutisation towards type IV acute myeoloblastic leukemia (AML), given the accumulation of blasts in the periphery. Histological analyses of bone marrow biopsies need to be performed to ascertain the presence of Auer bodies and the overall architecture of the bone marrow. Bone marrow cultures testing proliferation of these blasts also remain to be done.

Interestingly, in patients with CMML and AML4, there is an association with rearrangements of chromosome 11, and especially 11q23. MyD88 sits in the center of this region. Thus, it is interesting to entertain the possibility that *yaa*, TLR7, actually is an oncogene responsible ultimately for not lupus, but rather for CMML and AML.

Although it is certain that *Sle1* mediates a breach in humoral tolerance and that B6.*Sle1yaa* certainly has aspects of SLE (ANA, anti-dsDNA, glomerulonephritis), it is interesting to consider B6.*Sle1yaa* as a model of cancer. From the viewpoint of a cancer paradigm, we can think of the loss of tolerance, which yields a pro-proliferative and anti-apoptotic phenotype leading to clonal expansions of cells that later are able to mutate further (affinity mature and isotype switch) leading to unchecked polyclonal expansion, much like the loss of checkpoints in the evolution of tumor cells.

Furthermore, the type of kidney pathology seen in the *yaa* strains is also by no means a lupus-specific phenomenon. In B6.*Sle1yaa*, there is an associated tubulopathy, which is evidenced histologically by dilation, destruction, and necrosis of both distal and proximal tubules in addition to the glomerulonephritis expected in a model of SLE. Incidentally, necrotic tubulopathies are a well-known complication of acute leukemias.

Finally, the aggressive nature of the disease in B6.*Sle1yaa* (90% mortality by 6 months of age as compared to 90% mortality in the classic NZBxNZW/F1 model at12 months of age) is also less compatible with the chronic and evolutive nature of SLE and more compatible with CMML with acutisation towards AML.

Thus, perhaps we could re-think of *Sle1*, which results in the loss of humeral tolerance, as another "hit" dysregulating lymphoproliferation in a cancer paradigm because it is clear that *yaa* by itself does not result in the massive hematologic dysregulations seen in B6.*Sle1yaa*, and thus it will be interesting to understand the epistasis between the genes in *Sle1*, and specifically the SLAM family, and the Toll-receptor pathway, in cancer as opposed to SLE.

And if we consider B6.*Sle1yaa* as a model of cancer, it is not surprising that CXCR4 inhibition would ameliorate disease. As discussed previously, CXCR4 is well-associated with cancer, and in addition to being associated with cancer tropism, it is an anti-apoptotic receptor. The fact that CXCR4 inhibition substantially improved all elements of disease in the B6.*Sle1yaa* model is thus, at the end, difficult to interpret because, for me, it is unclear which was more important, treatment of the hematologic disorder present in the B6.*Sle1yaa* mice or treatment of the autoimmune disorder.

Carefully characterizing the *yaa* models from the standpoint of cancer and the eventual link between causative genetic events in autoimmunity and cancer will be a subject that I plan on pursuing while I finish my medical studies in the next two years.

THE LOSS OF TOLERANCE AND ACUTISATION: Ly108, TLRs, (and KLF13) revisited

The loss of tolerance is extremely difficult to understand because the phenomenon of tolerance is a highly sophisticated process involving multiple immune and non-immune actors. From first principles, the loss of tolerance should be expected in a substantial percentage of the general population simply because of the cost-benefit balance of maintaining enough immune diversity to continue our co-existence with an entire universe of potentially fatal infectious entities and the eventual development of autoimmunity. Rephrased, the autoimmune consequences of alleles that act in tolerance maintenance and immune diversity generation would be a relatively rare side effect and only occur in specific genotypes and thus allelic variants in the population would be selectively maintained. It is thus in our best interest as a species in a constantly world of extremely rapidly evolving microbes to maximize our TCR and BCR diversity. The fact that roughly 5% of the population has "benign" autoimmunity characterized by the non-pathological presence of ANAs, and the fact that allelic variants in genes such as the SLAM/CD2 family are selectively maintained in wild mouse populations, strongly supports this evolutionary perspective.

The maximization of the TCR and BCR repertoire was a major evolutionary hurdle in terms of generating diversity. The entire mechanism of generating junctional diversity in permutable VDJ combinations and heavy and light chain combinations in the central lymph organs accounts for the virtual totality of all immune diversity—refined only lightly but indispensably by the further diversity endowed by affinity maturation and isotype switching. But in the scheme of the immune system, it is in fact tolerance which

is the ultimate spigot in determining which immune cells have the right to exit into the periphery, and thus, it is, from this perspective, perhaps more important than the entire VDJ machinery for the simple fact that central tolerance controls the purse strings through risk management.

The elaborate game of tolerance can be boiled down to the selection of shades of gray within a very narrow cut of the pallet. The minority of cells that escape the tolerance machinery are cells that are between reactive and non-reactive. In biophysical terms, this is a precise kinetic and thermodynamic receptor profile that is selected, and indeed, work on K_d ranges and on/off kinetics in positive and negative selection have demonstrated this. The obvious implication this has on tolerance from an immunological perspective is that very slight tweaks in the parameters of tolerance can have huge global impacts on the immune system. A great example of this idea can be found in the work of Barton et al, where they show that positive selection can occur with normal peripheral T-cell population with but 5% of the MHC saturated by a single peptide [199]. However, touch that 5% and peripheral T-cell population is completely impaired. The SLAM/CD2 family is one of these gene families capable of small tweaks in the central organs that could lead to the difference between autoimmunity and healthy immune diversity.

Subsequently, differences observed between the autoimmune and non-autoimmune alleles of Ly108 from the microscopic level should not be that impressive. One of the main critiques of the work on Ly108 is that differences were subtle—within the 5-10% range between a mouse which does and does not have ANAs. Differences in thymic cellularity, Vβ distribution of newly emigrating SPCD4 cells, calcium flux, etc. were admittedly not the black and white differences observed in the CXCR4 study, for

example, but this is precisely the language of tolerance. It is easy to overlook that 5-10% differences do, after all, lead incontrovertibly to the presence or not of ANAs. The experiments using the BAC-transgenic approach to rescue the autoimmune varieties of Ly108 and CD84 show clearly that when Ly108 and CD84 are of B6-origin, there is no autoimmunity. Coupled with the experiments using the OTII system showing that old B6.Sle1b.OTII mice have significant IgM ANAs but little IgG ANAs demonstrates the indispensability of an antigen-specific autoimmune T-cell component. Together with the wealth of Ly108-mediated defects noted in the thymic compartment, it seems fairly clear that it is indeed the 5-10% margin in the thymic compartment that ultimately decides the state of tolerance of the whole organism—in this case with the subtle tweaking of intracellular calcium levels that ultimately lead to tweaks in the cell-cycle progression of developing thymocytes.

If the SLAM/CD2 family is thus crucial to murine lupus, and murine lupus is an adequate model of human lupus, it is then interesting to understand why the SLAM/CD2 family has been problematic in terms of the level of association with ANAs, which many have attributed to technical problems related to the potency of the MHC, and to the effects of the environment—the latter being the conceptually more interesting line of argument to consider. The problem at the base of this observation is in fact the incomplete penetrance of SLE—indeed, the concordance rate of monozygotic twins is less than 50%. There are two possibilities to explain this incomplete penetrance. The first is that there is an external stochastic force, in this case the environment, which randomly skews the immune system. With the recent burgeoning of the TLR field, which has directly linked the outside world to the immune processes, this argument is quite

compelling, and will be discussed later. The second is that there is an internally stochastic process at the level of the TCR/BCR because of random junctional diversity and then at the level of tolerance education which renders even monozygotic twins not genetically or phenotypically identical. Obviously the two possibilities are not mutually exclusive, but it is interesting to consider which is more important because understanding this could help clarify the eventual diagnostic power of SLE genes discovered.

The murine models of lupus are quite useful in this discussion, especially the NZW-derived lines behave very similarly to humans, and because the environment for these laboratory animals is fixed. In B6.*Sle1b* mice, there is also incomplete penetrance with a percentage that varies as a function of age. At 9 months of age, equivalent to roughly 50 human years assuming a median life expectancy of Western countries of around 80, the penetrance in females is still only 80%. I think this simple observation demonstrates that perhaps there is enough internal stochasticity to account for incomplete penetrance in lupus and that the effects of the environment which serve to skew, accelerate or decelerate the eventual development of autoimmunity conferred by susceptibility genes linked to ANAs are less important than the genes themselves, which is not to say that they are irrelevant but to say rather that polymorphisms or haplotypes discovered in association studies have a relevant diagnostic valor that should not be discounted as they are in the current politic of the field.

The other pressing question which plagued me during my years in the lab was why autoantibodies were generated towards nucleic-acid antigens and not other antigens—a question which ultimately tied very closely into TLRs. In fact, the distribution of the antigenic specificity of autoantibodies is skewed heavily towards those

that contain nucleic acids. The argument has been made that because DNA is such a promiscuously available antigen from the massive cell-death endogenous to the tolerance process and to all cellular processes in the periphery as well, it is because of the gross availability of the antigen that leads to ANAs as an eventuality of the highly favorable probability of receptor-antigen recognition. For me, one question which has not been addressed is what is the source of the DNA, human or bacterial/viral? If we consider the very simple biological fact that the entire immune system of a human develops at the same time of our exposure to the bacterial and viral worlds, whose total population outnumbers—on a cell to cell comparison—all cells in our body, and not before, suggests that it is not entirely clear what the source of the autoantigen is. Interestingly, TLRs are expressed both in cells of the myeloid lineage of the bone marrow and thymus, and presumably have had contact to the environment through TLRs and other sensors of pathogen motifs. And due to the structural similarity between DNA between species, it is thus not hard to envision that TLRs might play an important role in making available nucleic-acid-derived antigens for the eventual selection of immune cells, which, in the context of faulty selection, may lead to the inappropriate misrecognition of self nucleic acid. Thus, to understand if the phenomena of ANAs might begin as a sort of molecular mimicry of misrecognition of pathogen-derived nucleic-acid-containing antigens which is exacerbated in the periphery given the availability of both pathogen and host-derived antigen or if it is simply a lack of central education to self nucleic-acid antigens, more work needs to be done. Of course, the other possibility is that TLRs act at the level of the periphery by tipping the delicate peripheral tolerance achieved with the non-trivial percentage of cells that naturally escape central tolerance which happen to be specific for

nucleic-acid antigens. However, this fact still does not change the original question of the source of DNA in the central organs.

Taken altogether, whereas internal stochastic processes might be predominantly responsible for regulating TCR and BCR generation and selection, the selective forces might very well be externally driven through the action of TLRs. I will be pursuing these issues with the role of TLRs in tolerance to nucleic acids in central and peripheral tolerance in the near future.

If TLRs end up playing a minor role in tolerance towards nucleic-acid antigens—which is unlikely given the elegant work of Marshak-Rothstein, Shlomchik, and others—it seems almost certain that TLRs play a major role at the level of disease acutisation. That is, TLR ligands as adjuvants might sufficiently dysregulate peripheral tolerance to a state where tolerance is breached and then hyper-activated. It is thus from a therapeutic context that it is important to identify and understand all innate genes discovered from association studies in the mouse and man, whereas it is important from a diagnostic standpoint to identify and understand genes involved in breach of tolerance. Indeed, drugs like hydroxychloroquine highlight this principle, and a whole new field of translational research in the manipulation of innate processes at the molecular level will surely change the management of clinically severe cases of SLE. It is from this perspective that it is crucial that the work on KLF13 and RANTES as a possible acutisation gene be completed, especially given the extremely promising linkage data with Asian SLE patients (data not shown).

FINAL WORDS

As for the work earnestly presented in this dissertation, Darwin said it best—I have only begun to dent the enormous body of knowledge that is. As such, what I have described in this dissertation is utterly lacking. In a system where Heisenburg principle of uncertainty plays an enormous role, and where the immune system is plastic and responds to a disease process which is also plastic and in so doing renders a virtually unobservable process—it is often frustrating to continue work. There have been times where it seems that real processes are unobservable, or at best, partially observable, and thus inaccurate. There is an infinite amount of work that remains to be done, and what little was done could not have been done without the tremendous help of a whole industry of minds.

As for the writing of the thesis, I am reminded that Emily Dickinson often spent all morning editing a poem removing a period, and then in the afternoon, added it back in. I have concluded from this 6 month writing period, working with Drs. Mohan and Wakeland on the writing and rewriting of the articles, that a piece of scientific work cannot be well-written because its content is always changing and the scientific revolution of paradigms, as Kuhn calls it, is always in a state of revolt. In the course of editing this thesis, the CXCR4 paper went through four versions, the Ly108 paper underwent three major rewritings with major plot developments, the developments in the human CXCR4 story underwent massive plot-twists, and other research projects and ideas flourished and perished. Thus, the writing of this thesis is also quite lacking.

I take faith in that this is just the beginning, and that my best work awaits me still.

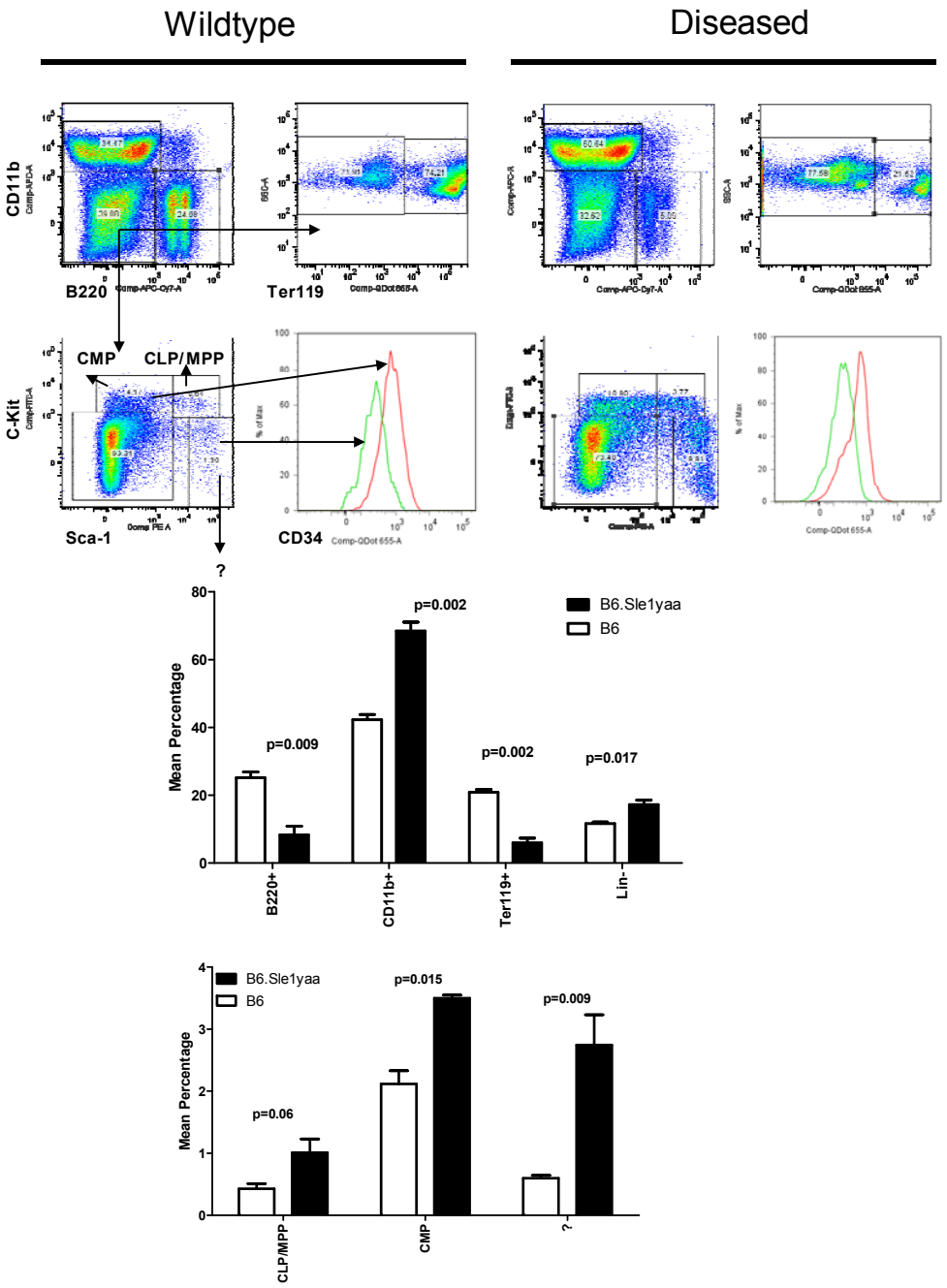

Figure 33. Analyses of peripheral blood leukocyte populations of B6.*Sle1yaa* mice.

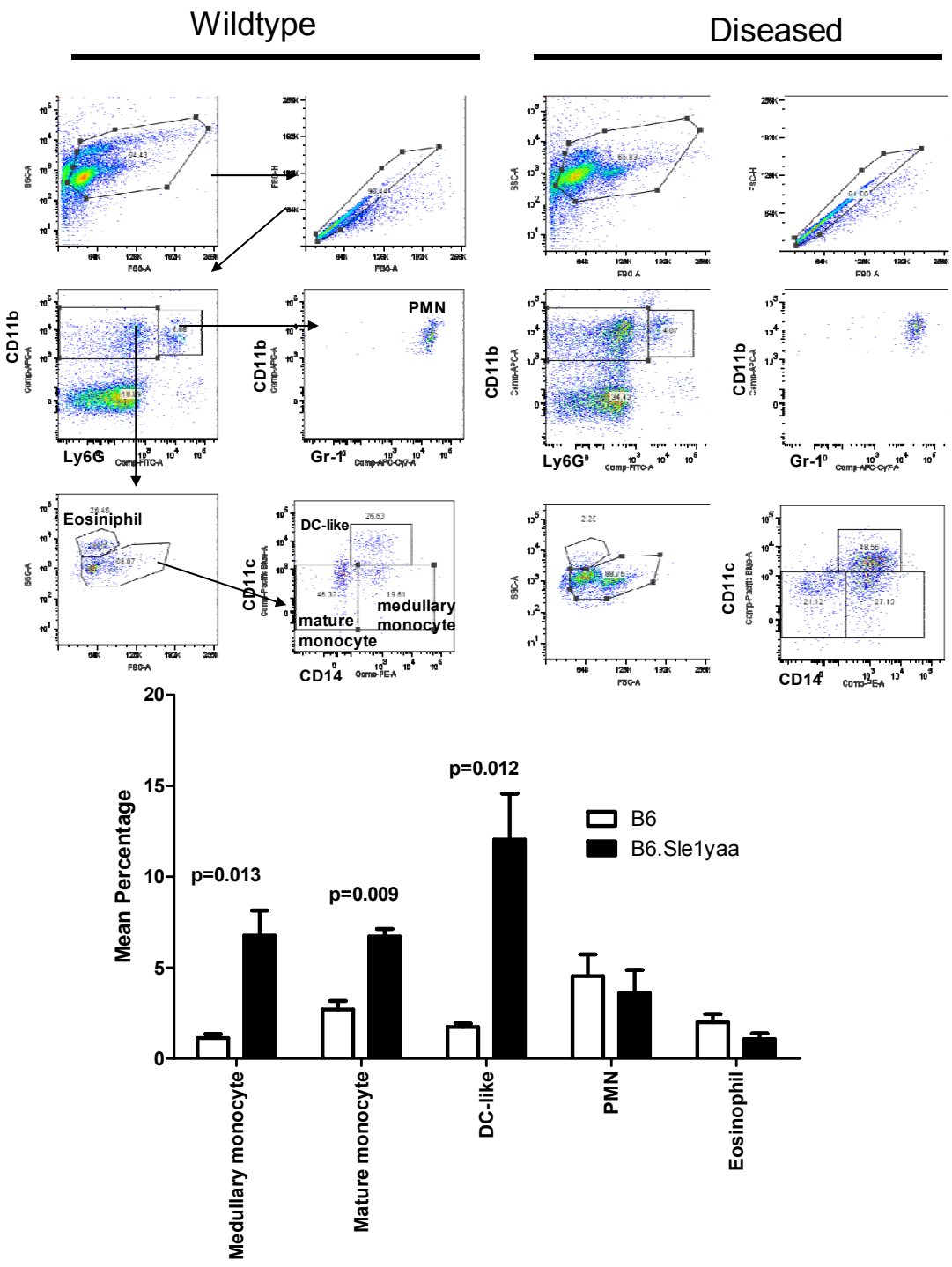

Figure 34. Analyses of myelomonocytic sublineages in the peripheral blood of B6.*Sle1yaa* mice.

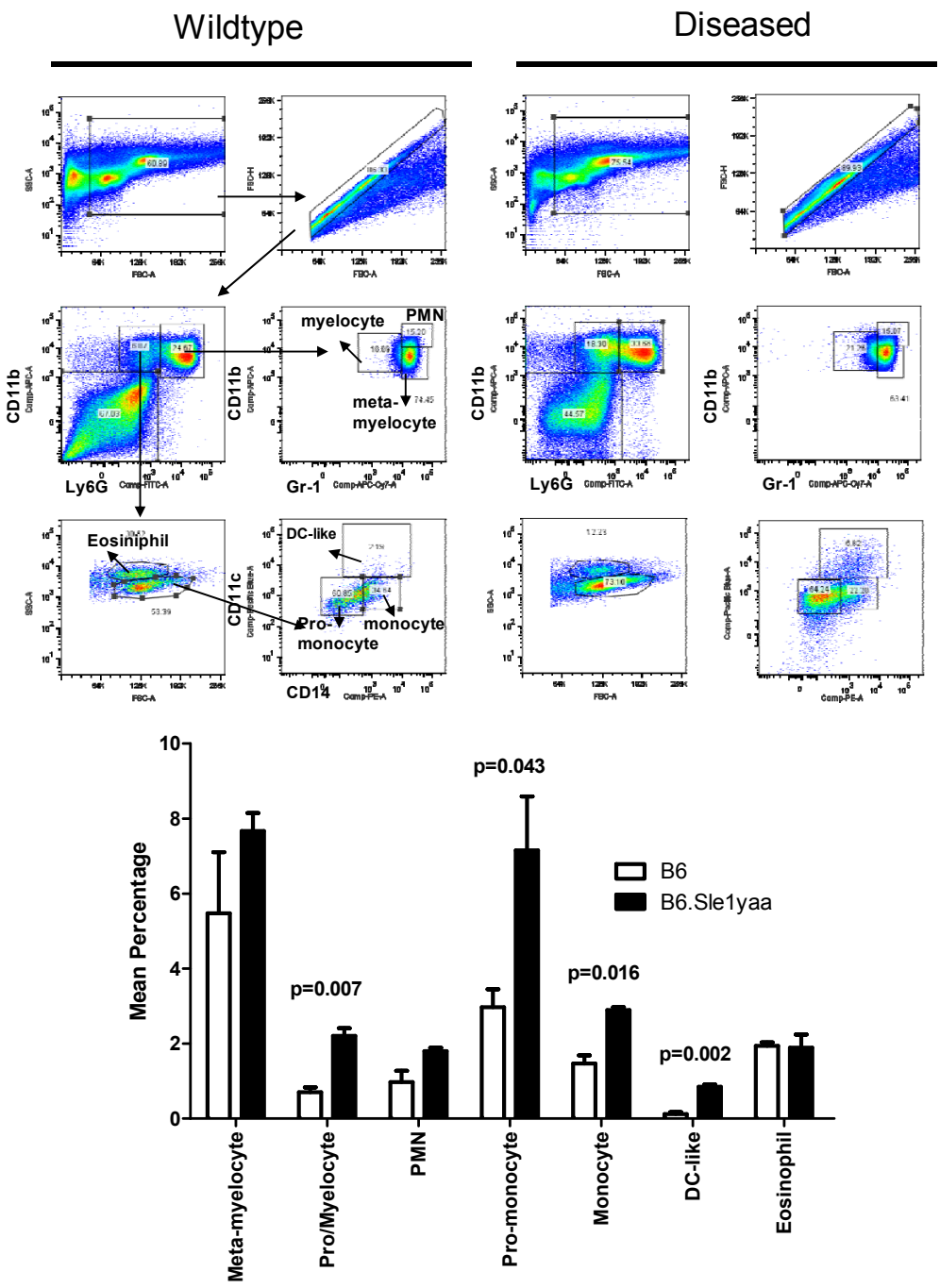

Figure 35. Bone marrow populations in B6.*Sle1yaa* mice.

VITAE

Andrew Wang was born in Miami, Florida, on April 20, 1982, the son of Jui-Jean Chow and Chia Hui Wang. He received his AB with Distinction from Harvard College in May 2004 with a degree in Biochemistry. His Honors thesis focused on the role of complement in B-cell tolerance. In August, 2004 he began his M.D./Ph.D training at the Medical and Graduate Schools at the University of Texas at Southwestern Medical Center at Dallas. He has four children: his 1865 Vuillaume violin, his work in international health and development, BeeFreed LLC, and mountaineering.

Permanent Address: None

LITERATURE CITED

1. Fairhurst, A., et al., *Systemic Lupus Erythematosus: Multiple Immunological Phenotypes in a Complex Genetic Disease*, in *Advances in Immunology*. 2006, Academic Press. p. 1-69.
2. Theofilopoulos, A.N. and D.H. Kono, *Genetics of systemic autoimmunity and glomerulonephritis in mouse models of lupus.* Nephrol. Dial. Transplant., 2001. **16**(suppl_6): p. 65-67.
3. Banchereau, J. and V. Pascual, *Type I Interferon in Systemic Lupus Erythematosus and Other Autoimmune Diseases.* Immunity, 2006. **25**(3): p. 383-392.
4. Cameron, J.S., *Lupus Nephritis.* J Am Soc Nephrol, 1999. **10**(2): p. 413-424.
5. Davis, J.C., I.O. Tassiulas, and D.T. Boumpas, *Lupus nephritis.* Curr Opin Rheumatol., 1996. **8**(5): p. 415-23.
6. Deshmukh, U.S., H. Bagavant, and S.M. Fu, *Role of anti-DNA antibodies in the pathogenesis of lupus nephritis.* Autoimmunity Reviews, 2006. **5**(6): p. 414-418.
7. Churg, J., Sobin LH, *Renal disease: classification and atlas of glomerular disease*, ed. W.H. Organization. 1982, Tokyo: Igaku-Shoin.
8. D'Agati, V.D., *Systemic Lupus Erythematosus*, in *Renal Biopsy Interpretation*, V.D.D.A. Fred G. Silva, Tibor Nadasdy, Editor. 1997, Churchill Livingstone, Inc: New York. p. 181-220.
9. Nguyen, C., N. Limaye, and E.K. Wakeland, *Susceptibility genes in the pathogenesis of murine lupus.* Arthritis Res., 2002. **4**(Suppl 3): p. S255-63. Epub 2002 May 9.
10. Arbuckle, M.R., et al., *Development of Autoantibodies before the Clinical Onset of Systemic Lupus Erythematosus.* N Engl J Med, 2003. **349**(16): p. 1526-1533.
11. Wandstrat, A.E., et al., *Autoantibody profiling to identify individuals at risk for systemic lupus erythematosus.* Journal of Autoimmunity, 2006. **27**(3): p. 153-160.
12. Shmerling, R.H., *Autoantibodies in Systemic Lupus Erythematosus -- There before You Know It.* N Engl J Med, 2003. **349**(16): p. 1499-1500.
13. Deapen, D., et al., *A revised estimate of twin concordance in systemic lupus erythematosus.* Arthritis Rheum., 1992. **35**(3): p. 311-8.
14. Wanstrat, A. and E. Wakeland, *The genetics of complex autoimmune diseases: non-MHC susceptibility genes.* Nat Immunol, 2001. **2**(9): p. 802-809.
15. Manderson, A.P., M. Botto, and M.J. Walport, *The Role of Complement in the Development of Systemic Lupus Erythematosus.* Annual Review Of Immunology, 2004. **22**(1): p. 431-456.
16. Agnello, V., *Association of systemic lupus erythematosus and SLE-like syndromes with hereditary and acquired complement deficiency states.* Arthritis Rheum., 1978. **21**(5 Suppl): p. S146-52.
17. Morgan, B.P. and M.J. Walport, *Complement deficiency and disease.* Immunology Today, 1991. **12**(9): p. 301-306.

18. Nelson, R.A., Jr., *The immune-adherence phenomenon; an immunologically specific reaction between microorganisms and erythrocytes leading to enhanced phagocytosis.* Science., 1953. **118**(3077): p. 733-7.
19. Casciola-Rosen, L.A., G. Anhalt, and A. Rosen, *Autoantigens targeted in systemic lupus erythematosus are clustered in two populations of surface structures on apoptotic keratinocytes.* J. Exp. Med., 1994. **179**(4): p. 1317-1330.
20. Schur, P.H., et al., *Associations between systemic lupus erythematosus and the major histocompatibility complex: clinical and immunological considerations.* Clin Immunol Immunopathol., 1982. **24**(2): p. 263-75.
21. Prokunina, L., et al., *A regulatory polymorphism in PDCD1 is associated with susceptibility to systemic lupus erythematosus in humans.* Nat Genet, 2002. **32**(4): p. 666-669.
22. Kyogoku, C., *Genetic Association of the R620W Polymorphism of Protein Tyrosine Phosphatase PTPN22 with Human SLE.* Am J Hum Genet. , 2004. **75**(3): p. 504-507.
23. Jeffrey C. Edberg, C.D.L.J.W.K.L.M.K.M.K.J.K.V.B.W.M.B.J.E.S.S.S.R.J., *Genetic linkage and association of Fc? receptor IIIA (CD16A) on chromosome 1q23 with human systemic lupus erythematosus.* Arthritis & Rheumatism, 2002. **46**(8): p. 2132-2140.
24. Salmon, J.E., et al., *Fcgamma RIIA Alleles Are Heritable Risk Factors for Lupus Nephritis in African Americans.* J. Clin. Invest., 1996. **97**(5): p. 1348-1354.
25. Graham, R.R., et al., *A common haplotype of interferon regulatory factor 5 (IRF5) regulates splicing and expression and is associated with increased risk of systemic lupus erythematosus.* Nat Genet, 2006. **38**(5): p. 550-555.
26. Wakeland, E.K., et al., *Delineating the Genetic Basis of Systemic Lupus Erythematosus.* Immunity, 2001. **15**(3): p. 397-408.
27. Snell, G., *Methods for the study of histocompatibility genes.* J. Genetics, 1948. **49**(87).
28. Bolland, S. and J.V. Ravetch, *Spontaneous Autoimmune Disease in Fc[gamma]RIIB-Deficient Mice Results from Strain-Specific Epistasis.* Immunity, 2000. **13**(2): p. 277-285.
29. Botto, M., et al., *Homozygous C1q deficiency causes glomerulonephritis associated with multiple apoptotic bodies.* Nat Genet, 1998. **19**(1): p. 56-59.
30. Cohen, P.L. and R.A. Eisenberg, *Lpr and gld: single gene models of systemic autoimmunity and lymphoproliferative disease.* Annual Review Of Immunology, 1991. **9**: p. 243-269.
31. Wandstrat, A.E., et al., *Association of Extensive Polymorphisms in the SLAM/CD2 Gene Cluster with Murine Lupus.* Immunity, 2004. **21**(6): p. 769-780.
32. Subramanian, S., et al., *From the Cover: A Tlr7 translocation accelerates systemic autoimmunity in murine lupus.* PNAS, 2006. **103**(26): p. 9970-9975.
33. Pisitkun, P., et al., *Autoreactive B Cell Responses to RNA-Related Antigens Due to TLR7 Gene Duplication.* Science, 2006. **312**(5780): p. 1669-1672.
34. Christensen, S.R., et al., *Toll-like receptor 9 controls anti-DNA autoantibody production in murine lupus.* J. Exp. Med., 2005. **202**(2): p. 321-331.
35. Kumar, K.R., et al., *Regulation of B Cell Tolerance by the Lupus Susceptibility Gene Ly108.* Science, 2006. **312**(5780): p. 1665-1669.

36. Mohan, C., et al., *Genetic dissection of systemic lupus erythematosus pathogenesis: Sle2 on murine chromosome 4 leads to B cell hyperactivity.* J Immunol, 1997. **159**(1): p. 454-465.
37. Mohan, C., et al., *Genetic Dissection of SLE Pathogenesis . Sle1 on Murine Chromosome 1 Leads to a Selective Loss of Tolerance to H2A/H2B/DNA Subnucleosomes.* J. Clin. Invest., 1998. **101**(6): p. 1362-1372.
38. Mohan, C., et al., *Genetic dissection of lupus pathogenesis: a recipe for nephrophilic autoantibodies.* J. Clin. Invest., 1999. **103**(12): p. 1685-1695.
39. Mohan, C., et al., *Genetic Dissection of Sle Pathogenesis: Sle3 on Murine Chromosome 7 Impacts T Cell Activation, Differentiation, and Cell Death.* J Immunol, 1999. **162**(11): p. 6492-6502.
40. Morel, L., et al., *Functional dissection of systemic lupus erythematosus using congenic mouse strains.* J Immunol, 1997. **158**(12): p. 6019-6028.
41. Morel, L., et al., *Epistatic Modifiers of Autoimmunity in a Murine Model of Lupus Nephritis.* Immunity, 1999. **11**(2): p. 131-139.
42. Morel, L., et al., *Genetic reconstitution of systemic lupus erythematosus immunopathology with polycongenic murine strains.* Proceedings of the National Academy of Sciences, 2000. **97**(12): p. 6670-6675.
43. Morel, L., et al., *The major murine systemic lupus erythematosus susceptibility locus, Sle1, is a cluster of functionally related genes.* PNAS, 2001. **98**(4): p. 1787-1792.
44. Pasare C, M.R., *Toll-like receptors: linking innate and adaptive immunity.* Adv Exp Med Biol, 2005. **560**(11-8).
45. Hargreaves DC, M.R., *Innate sensors of microbial infection.* J Clin Immunol. , 2005. **25**(6): p. 503-10.
46. Marshak-Rothstein, A., *Toll-like receptors in systemic autoimmune disease.* Nat Rev Immunol, 2006. **6**(11): p. 823-835.
47. Zhu, J., et al., *T cell hyperactivity in lupus as a consequence of hyperstimulatory antigen-presenting cells.* J. Clin. Invest., 2005. **115**(7): p. 1869-1878.
48. Molina, H., et al., *Analysis of C3b/C3d binding sites and factor I cofactor regions within mouse complement receptors 1 and 2.* J Immunol, 1994. **153**(2): p. 789-795.
49. Carter, R.H. and D.T. Fearon, *CD19: lowering the threshold for antigen receptor stimulation of B lymphocytes.* Science., 1992. **256**(5053): p. 105-7.
50. Fang, Y., et al., *Expression of Complement Receptors 1 and 2 on Follicular Dendritic Cells Is Necessary for the Generation of a Strong Antigen-Specific IgG Response.* J Immunol, 1998. **160**(11): p. 5273-5279.
51. Schmiedeke, T.M., et al., *Histones have high affinity for the glomerular basement membrane. Relevance for immune complex formation in lupus nephritis.* J. Exp. Med., 1989. **169**(6): p. 1879-1894.
52. Winfield, J.B., I. Faiferman, and D. Koffler, *Avidity of anti-DNA antibodies in serum and IgG glomerular eluates from patients with systemic lupus erythematosus. Association of high avidity antinative DNA antibody with glomerulonephritis.* J Clin Invest., 1977. **59**(1): p. 90-6.

53. Manar Kalaaji, G.S.J.E.M.H.N.O.P.R., *Critical comparative analyses of anti-?-actinin and glomerulus-bound antibodies in human and murine lupus nephritis.* Arthritis & Rheumatism, 2006. **54**(3): p. 914-926.
54. Siegert, C., et al., *IgG autoantibodies against C1q are correlated with nephritis, hypocomplementemia, and dsDNA antibodies in systemic lupus erythematosus.* J Rheumatol., 1991. **18**(2): p. 230-4.
55. Moroni, G., et al., *Anti-C1q antibodies may help in diagnosing a renal flare in lupus nephritis.* Am J Kidney Dis., 2001. **37**(3): p. 490-8.
56. Mannik, M., et al., *Multiple autoantibodies form the glomerular immune deposits in patients with systemic lupus erythematosus.* J Rheumatol., 2003. **30**(7): p. 1495-504.
57. Mannik, M. and M.H. Wener, *Deposition of antibodies to the collagen-like region of C1q in renal glomeruli of patients with proliferative lupus glomerulonephritis.* Arthritis Rheum., 1997. **40**(8): p. 1504-11.
58. Trouw, L.A., et al., *Anti-C1q autoantibodies deposit in glomeruli but are only pathogenic in combination with glomerular C1q-containing immune complexes.* J. Clin. Invest., 2004. **114**(5): p. 679-688.
59. Li, Q.Z., et al., *Protein array autoantibody profiles for insights into systemic lupus erythematosus and incomplete lupus syndromes.* Clinical & Experimental Immunology, 2007. **147**(1): p. 60-70.
60. Turnberg, D., et al., *Complement Activation Contributes to Both Glomerular and Tubulointerstitial Damage in Adriamycin Nephropathy in Mice.* J Immunol, 2006. **177**(6): p. 4094-4102.
61. Chowdhury, P., S.H. Sacks, and N.S. Sheerin, *Toll-like receptors TLR2 and TLR4 initiate the innate immune response of the renal tubular epithelium to bacterial products.* Clinical & Experimental Immunology, 2006. **145**(2): p. 346-356.
62. Tsuboi, N., et al., *Roles of Toll-Like Receptors in C-C Chemokine Production by Renal Tubular Epithelial Cells.* J Immunol, 2002. **169**(4): p. 2026-2033.
63. Patole, P.S., et al., *Viral Double-Stranded RNA Aggravates Lupus Nephritis through Toll-Like Receptor 3 on Glomerular Mesangial Cells and Antigen-Presenting Cells.* J Am Soc Nephrol, 2005. **16**(5): p. 1326-1338.
64. Li, S., et al., *Major Histocompatibility Complex Class II Expression by Intrinsic Renal Cells Is Required for Crescentic Glomerulonephritis.* J. Exp. Med., 1998. **188**(3): p. 597-602.
65. Timoshanko, J.R., et al., *IFN-{gamma} Production by Intrinsic Renal Cells and Bone Marrow-Derived Cells Is Required for Full Expression of Crescentic Glomerulonephritis in Mice.* J Immunol, 2002. **168**(8): p. 4135-4141.
66. Timoshanko, J.R., et al., *Interleukin-12 from Intrinsic Cells Is an Effector of Renal Injury in Crescentic Glomerulonephritis.* J Am Soc Nephrol, 2001. **12**(3): p. 464-471.
67. Timoshanko, J.R., et al., *Leukocyte-Derived Interleukin-1{beta} Interacts with Renal Interleukin-1 Receptor I to Promote Renal Tumor Necrosis Factor and Glomerular Injury in Murine Crescentic Glomerulonephritis.* Am J Pathol, 2004. **164**(6): p. 1967-1977.

68. Timoshanko, J.R., et al., *Intrinsic Renal Cells Are the Major Source of Tumor Necrosis Factor Contributing to Renal Injury in Murine Crescentic Glomerulonephritis.* J Am Soc Nephrol, 2003. **14**(7): p. 1785-1793.
69. Bergtold, A., et al., *FcR-Bearing Myeloid Cells Are Responsible for Triggering Murine Lupus Nephritis.* J Immunol, 2006. **177**(10): p. 7287-7295.
70. Morel, L., et al., *Polygenic control of susceptibility to murine systemic lupus erythematosus.* Immunity, 1994. **1**(3): p. 219-229.
71. Michelle E. K. Haywood, M.B.H.J.H.S.S.J.R.P.J.A.E.M.T.M.A.M.P.C.K.A.D., *Identification of intervals on chromosomes 1, 3, and 13 linked to the development of lupus in BXSB mice.* Arthritis & Rheumatism, 2000. **43**(2): p. 349-355.
72. Drake, C.G., et al., *Analysis of the New Zealand Black contribution to lupus-like renal disease. Multiple genes that operate in a threshold manner.* Journal Of Immunology (Baltimore, Md.: 1950), 1995. **154**(5): p. 2441-2447.
73. Hogarth, M.B., et al., *Multiple lupus susceptibility loci map to chromosome 1 in BXSB mice.* Journal Of Immunology (Baltimore, Md.: 1950), 1998. **161**(6): p. 2753-2761.
74. Vyse, T.J., et al., *Genetic linkage of IgG autoantibody production in relation to lupus nephritis in New Zealand hybrid mice.* The Journal Of Clinical Investigation, 1996. **98**(8): p. 1762-1772.
75. Xie, S., et al., *Genetic contributions of nonautoimmune SWR mice toward lupus nephritis.* Journal Of Immunology (Baltimore, Md.: 1950), 2001. **167**(12): p. 7141-7149.
76. Kono, D.H., et al., *Lupus Susceptibility Loci in New Zealand Mice.* PNAS, 1994. **91**(21): p. 10168-10172.
77. Rahman, Z.S.M., et al., *A novel susceptibility locus on chromosome 2 in the (New Zealand Black x New Zealand White)F1 hybrid mouse model of systemic lupus erythematosus.* Journal Of Immunology (Baltimore, Md.: 1950), 2002. **168**(6): p. 3042-3049.
78. Gu, L., et al., *Genetic determinants of autoimmune disease and coronary vasculitis in the MRL-lpr/lpr mouse model of systemic lupus erythematosus.* Journal Of Immunology (Baltimore, Md.: 1950), 1998. **161**(12): p. 6999-7006.
79. Wang, Y., et al., *Host modifier genes affect mouse autoimmunity induced by the lpr gene.* The American Journal Of Pathology, 1997. **151**(6): p. 1791-1798.
80. Vidal, S., D.H. Kono, and A.N. Theofilopoulos, *Loci predisposing to autoimmunity in MRL-Fas lpr and C57BL/6-Faslpr mice.* The Journal Of Clinical Investigation, 1998. **101**(3): p. 696-702.
81. Drake, C.G., et al., *Genetic analysis of the NZB contribution to lupus-like autoimmune disease in (NZB x NZW)F1 mice.* Proceedings Of The National Academy Of Sciences Of The United States Of America, 1994. **91**(9): p. 4062-4066.
82. Laurence Morel *, C.M., et al., *Multiplex inheritance of component phenotypes in a murine model of lupus.* Mammalian Genome, 1999. **V10**(2): p. 176-181.
83. Watson, M.L., et al., *Genetic analysis of MRL-lpr mice: relationship of the Fas apoptosis gene to disease manifestations and renal disease-modifying loci.* The Journal Of Experimental Medicine, 1992. **176**(6): p. 1645-1656.

84. Santiago, M.L., et al., *Linkage of a major quantitative trait locus to Yaa gene-induced lupus-like nephritis in (NZW x C57BL/6)F1 mice.* European Journal Of Immunology, 1998. **28**(12): p. 4257-4267.
85. Vyse, T.J., et al., *Backcross analysis of genes linked to autoantibody production in New Zealand White mice.* Journal Of Immunology (Baltimore, Md.: 1950), 1996. **157**(6): p. 2719-2727.
86. Waters, S.T., et al., *NZM2328: A New Mouse Model of Systemic Lupus Erythematosus with Unique Genetic Susceptibility Loci.* Clinical Immunology, 2001. **100**(3): p. 372-383.
87. Rozzo, S., et al., *Effect of genetic background on the contribution of New Zealand Black loci to autoimmune lupus慸ephritis.* PNAS, 1996. **93**(26): p. 15164-15168.
88. Tucker, R.M., et al., *Genetic Control of Glycoprotein 70 Autoantigen Production and Its Influence on Immune Complex Levels and Nephritis in Murine Lupus.* J Immunol, 2000. **165**(3): p. 1665-1672.
89. Vyse, T.J., et al., *Control of multiple autoantibodies linked with a lupus nephritis susceptibility locus in New Zealand black mice.* J Immunol, 1997. **158**(11): p. 5566-5574.
90. Rigby, R.J., et al., *New Loci from New Zealand Black and New Zealand White on Chromosomes 4 and 12 Contribute to Lupus-Like Disease in the Context of BALB/c.* J Immunol, 2004. **172**(7): p. 4609-4617.
91. Shangkui Xie, L.L.S.C.R.S.A.K.S.K.D.C.M., *Genetic origin of lupus in NZB/SWR hybrids: Lessons from an intercross study.* Arthritis & Rheumatism, 2005. **52**(2): p. 659-667.
92. Kono, D.H., M.S. Park, and A.N. Theofilopoulos, *Genetic Complementation in Female (BXSB x NZW)F2 Mice.* J Immunol, 2003. **171**(12): p. 6442-6447.
93. Nakatsuru, S., et al., *Genetic dissection of the complex pathological manifestations of collagen disease in MRL/lpr mice.* Pathology International, 1999. **49**(11): p. 974-982.
94. Haywood, M.E., et al., *Autoantigen glycoprotein 70 expression is regulated by a single locus, which acts as a checkpoint for pathogenic anti-glycoprotein 70 autoantibody production and hence for the corresponding development of severe nephritis, in lupus-prone PXSB mice.* Journal Of Immunology (Baltimore, Md.: 1950), 2001. **167**(3): p. 1728-1733.
95. Vyse, T.J. and B.L. Kotzin, *Genetic basis of systemic lupus erythematosus.* Current Opinion in Immunology, 1996. **8**(6): p. 843-851.
96. Rozzo, S.J., et al., *Enhanced Susceptibility to Lupus Contributed from the Nonautoimmune C57BL/10, But Not C57BL/6, Genome.* J Immunol, 2000. **164**(10): p. 5515-5521.
97. Wither, J.E., et al., *Functional Dissection of Lupus Susceptibility Loci on the New Zealand Black Mouse Chromosome 1: Evidence for Independent Genetic Loci Affecting T and B Cell Activation.* J Immunol, 2003. **171**(4): p. 1697-1706.
98. Kong, P.L., et al., *The Centromeric Region of Chromosome 7 from MRL Mice (Lmb3) Is an Epistatic Modifier of Fas for Autoimmune Disease Expression.* J Immunol, 2004. **172**(5): p. 2785-2794.

99. Waters, S.T., et al., *Breaking Tolerance to Double Stranded DNA, Nucleosome, and Other Nuclear Antigens Is Not Required for the Pathogenesis of Lupus Glomerulonephritis.* J. Exp. Med., 2004. **199**(2): p. 255-264.
100. Quintero-del-Rio, A.I., et al., *SLEN2 (2q34-35) and SLEN1 (10q22.3) replication in systemic lupus erythematosus stratified by nephritis.* Am J Hum Genet., 2004. **75**(2): p. 346-8.
101. Quintero-Del-Rio, A.I., et al., *The genetics of systemic lupus erythematosus stratified by renal disease: linkage at 10q22.3 (SLEN1), 2q34-35 (SLEN2), and 11p15.6 (SLEN3).* Genes Immun., 2002. **3**(Suppl 1): p. S57-62.
102. Gillett, C.D., et al., *Fine mapping chromosome 16q12 in a collection of 231 systemic lupus erythematosus sibpair and multiplex families.* Genes Immun., 2005. **6**(1): p. 19-23.
103. Behrens TW, G.R., Kyogoku C, Baechler EC, Ramos PS, Gillett C, Bauer J, Ortmann WA, Hippen KL, Peterson E, Langefeld CD, Moser KL, Gaffney PM, Gregersen PK., *Progress towards understanding the genetic pathogenesis of systemic lupus erythematosus.* Novartis Found Symp., 2005. **267**: p. 145-60; discussion 160-4.
104. Bazilio, A.P., et al., *Fc{gamma}RIIa polymorphism: a susceptibility factor for immune complex-mediated lupus nephritis in Brazilian patients.* Nephrol. Dial. Transplant., 2004. **19**(6): p. 1427-1431.
105. Salmon, J.E., et al., *Altered distribution of Fcgamma receptor IIIA alleles in a cohort of Korean patients with lupus nephritis.* Arthritis Rheum., 1999. **42**(4): p. 818-9.
106. Karassa, F.B., T.A. Trikalinos, and J.P. Ioannidis, *The Fc gamma RIIIA-F158 allele is a risk factor for the development of lupus nephritis: a meta-analysis.* Kidney Int., 2003. **63**(4): p. 1475-82.
107. Hur, J.W., et al., *Poly(ADP-ribose) polymerase (PARP) polymorphisms associated with nephritis and arthritis in systemic lupus erythematosus.* Rheumatology, 2006. **45**(6): p. 711-717.
108. Ludmila Prokunina, I.G.G.S.L.T.V.A.S.J.L.O.M.F.S.L.A.C.M.E.A.-R., *The systemic lupus erythematosus-associated <I>PDCD1</I> polymorphism PD1.3A in lupus nephritis.* Arthritis & Rheumatism, 2004. **50**(1): p. 327-328.
109. Kim, T.-G., et al., *Systemic lupus erythematosus with nephritis is strongly associated with the TNFB*2 homozygote in the Korean population.* Human Immunology, 1996. **46**(1): p. 10-17.
110. Parsa, A., et al., *Association of angiotensin-converting enzyme polymorphisms with systemic lupus erythematosus and nephritis: analysis of 644 SLE families.* Genes Immun., 2002. **3**(Suppl 1): p. S42-6.
111. Shin, H.D., et al., *DNase II polymorphisms associated with risk of renal disorder among systemic lupus erythematosus patients.* J Hum Genet., 2005. **50**(3): p. 107-11. Epub 2005 Feb 19.
112. Duits, A.J., et al., *Skewed distribution of IgG Fc receptor IIa (CD32) polymorphism is associated with renal disease in systemic lupus erythematosus patients.* Arthritis Rheum., 1995. **38**(12): p. 1832-6.

113. Zuniga, R., et al., *Low-binding alleles of Fcgamma receptor types IIA and IIIA are inherited independently and are associated with systemic lupus erythematosus in Hispanic patients.* Arthritis Rheum., 2001. **44**(2): p. 361-7.
114. Song, Y.W., et al., *Abnormal distribution of Fc gamma receptor type IIa polymorphisms in Korean patients with systemic lupus erythematosus.* Arthritis Rheum., 1998. **41**(3): p. 421-6.
115. Alice Y Chan, N.L., Quan Li, Xiang-Hong Tian, Chaoying Liang, Zhiqun Zeng, Ken Kaufman, Jennifer A. Kelly, Shizhong Han, Swapan Nath, Nancy Olsen, Joan Merrill, Judith James, John Harley, David Karp, Amy E Wandstrat, Edward K Wakeland, *Multiple members of the SLAM/CD2 gene cluster mediate susceptibility to systemic autoimmunity in mice and humans.* Submitted., 2008.
116. Liang, Z., et al., *Pathogenic Profiles and Molecular Signatures of Antinuclear Autoantibodies Rescued from NZM2410 Lupus Mice.* J. Exp. Med., 2004. **199**(3): p. 381-398.
117. Tan EM, C.A., Fries JF, Masi AT, McShane DJ, Rothfield NF, et al, *The 1982 revised criteria for the classification of systemic lupus erythematosus.* Arthritis Rheum, 1982. **25**: p. 1271-7.
118. Arnett FC, E.S., Bloch DA, McShane DJ, Fries JF, Cooper NS, Healey LA, Kaplan SR, Liang MH, Luthra HS, et al, *The American Rheumatism Association 1987 revised criteria for the classification of rheumatoid arthritis.* Arthritis Rheum, 1988. **31**(3): p. 315-24.
119. Fu, Y., Y. Du, and C. Mohan, *Experimental anti-GBM disease as a tool for studying spontaneous lupus nephritis.* Clinical Immunology, 2007. **124**(2): p. 109-118.
120. Anders, H.-J., et al., *A chemokine receptor CCR-1 antagonist reduces renal fibrosis after unilateral ureter ligation.* J. Clin. Invest., 2002. **109**(2): p. 251-259.
121. Feng, L., et al., *Prevention of crescentic glomerulonephritis by immunoneutralization of the fractalkine receptor CX3CR1.* Kidney Int, 1999. **56**(2): p. 612-620.
122. Vielhauer, V., et al., *Obstructive Nephropathy in the Mouse: Progressive Fibrosis Correlates with Tubulointerstitial Chemokine Expression and Accumulation of CC Chemokine Receptor 2- and 5-Positive Leukocytes.* J Am Soc Nephrol, 2001. **12**(6): p. 1173-1187.
123. Xie, C., et al., *Strain Distribution Pattern of Susceptibility to Immune-Mediated Nephritis.* J Immunol, 2004. **172**(8): p. 5047-5055.
124. Xie, C., et al., *Enhanced susceptibility to immune nephritis in DBA/1 mice is contingent upon IL-1 expression.* Clinical Immunology, 2007. **124**(1): p. 49-56.
125. Chun Xie, X.J.Z.X.L.C.M., *Enhanced susceptibility to end-organ disease in the lupus-facilitating NZW mouse strain.* Arthritis & Rheumatism, 2003. **48**(4): p. 1080-1092.
126. P. G. Tipping, X.R.H., M. Qi, G. Y. Van, and W. W. Tang, *Crescentic glomerulonephritis in CD4- and CD8-deficient mice. Requirement for CD4 but not CD8 cells.* Am J Pathol., 1998. **152**(6): p. 1541-1548.
127. Bagavant, H., et al., *Role for Nephritogenic T Cells in Lupus Glomerulonephritis: Progression to Renal Failure Is Accompanied by T Cell Activation and Expansion in Regional Lymph Nodes.* J Immunol, 2006. **177**(11): p. 8258-8265.

128. Nolasco, F., et al, *Intraglomerular T cells and monocytes in nephritis: Study with monoclonal antibodies.* Kidney International, 1987. **31**: p. 1160-1166.
129. Takeuchi, T., et al., *T cell abnormalities in systemic lupus erythematosus.* Autoimmunity, 2005. **38**(5): p. 339 - 346.
130. Weening, J.J., et al., *The Classification of Glomerulonephritis in Systemic Lupus Erythematosus Revisited.* J Am Soc Nephrol, 2004. **15**(2): p. 241-250.
131. Morel, L., et al., *The major murine systemic lupus erythematosus susceptibility locus, Sle1, is a cluster of functionally related genes.* Proc Natl Acad Sci U S A, 2001. **98**(4): p. 1787-92.
132. Mohan, C., Alas, E., Morel, L., Yang, P., Wakeland, E.K., *Genetic dissection of SLE pathogenesis. Sle1 on murine chromsome 1 leads to a selective loss of tolerance to H2A/H2B/DNA subnucleosomes.* J Clin Invest, 1998. **101**(6): p. 1362-1372.
133. Howie, D., et al., *Cutting Edge: The SLAM Family Receptor Ly108 Controls T Cell and Neutrophil Functions.* J Immunol, 2005. **174**(10): p. 5931-5935.
134. Craft, J., et al., *Autoreactive T cells in murine lupus: origins and roles in autoantibody production.* Immunol Res, 1999. **19**(2-3): p. 245-57.
135. Datta, S.K., et al., *T helper cells driving pathogenic anti-DNA autoantibody production in lupus: nucleosomal epitopes and CD40 ligand signals.* Lupus, 1997. **6**(3): p. 333-6.
136. Yamada, M., et al., *Selective accumulation of CCR4+ T lymphocytes into renal tissue of patients with lupus nephritis.* Arthritis Rheum, 2002. **46**(3): p. 735-40.
137. Diaz Gallo C, J.A., Brennan DC, Florquin S, Pacheco-Silva A, Kelley VR, *Autoreactive kidney-infiltrating T-cell clones in murine lupus nephritis.* Kidney International, 1992. **42**(4): p. 851-9.
138. Chen, S.Y., et al., *The natural history of disease expression in CD4 and CD8 gene-deleted New Zealand black (NZB) mice.* J Immunol, 1996. **157**(6): p. 2676-84.
139. Hang, L., et al., *The effect of thymectomy on lupus-prone mice.* J Immunol, 1984. **132**(4): p. 1809-13.
140. Koh, D.R., et al., *Murine lupus in MRL/lpr mice lacking CD4 or CD8 T cells.* Eur J Immunol, 1995. **25**(9): p. 2558-62.
141. Jiang, C., et al., *Abrogation of Lupus Nephritis in Activation-Induced Deaminase-Deficient MRL/lpr Mice.* J Immunol, 2007. **178**(11): p. 7422-7431.
142. Zhong, M.C. and A. Veillette, *Control of T lymphocyte signaling by Ly108, a SLAM family receptor implicated in auto-immunity.* J Biol Chem, 2008.
143. Onoyama, I., et al., *Conditional inactivation of Fbxw7 impairs cell-cycle exit during T cell differentiation and results in lymphomatogenesis.* J Exp Med, 2007. **204**(12): p. 2875-88.
144. Raman, V., et al., *Requirement for Ca2+/Calmodulin-Dependent Kinase Type IV/Gr in Setting the Thymocyte Selection Threshold.* J Immunol, 2001. **167**(11): p. 6270-6278.
145. Freedman, B.D., et al., *Receptor Avidity and Costimulation Specify the Intracellular Ca2+ Signaling Pattern in CD4+CD8+ Thymocytes.* J. Exp. Med., 1999. **190**(7): p. 943-952.

146. Wang, C.R., et al., *T cell receptor-mediated signaling events in CD4+CD8+ thymocytes undergoing thymic selection: requirement of calcineurin activation for thymic positive selection but not negative selection.* J. Exp. Med., 1995. **181**(3): p. 927-941.
147. Onoyama, I., et al., *Conditional inactivation of Fbxw7 impairs cell-cycle exit during T cell differentiation and results in lymphomatogenesis.* J. Exp. Med., 2007: p. jem.20062299.
148. Gil-Gomez, G., A. Berns, and H.J. Brady, *A link between cell cycle and cell death: Bax and Bcl-2 modulate Cdk2 activation during thymocyte apoptosis.* Embo J, 1998. **17**(24): p. 7209-18.
149. Murray, A.W., *Recycling the cell cycle: cyclins revisited.* Cell, 2004. **116**(2): p. 221-34.
150. Kaldis, P., *Another piece of the p27Kip1 puzzle.* Cell, 2007. **128**(2): p. 241-4.
151. Gu, Y., J. Rosenblatt, and D.O. Morgan, *Cell cycle regulation of CDK2 activity by phosphorylation of Thr160 and Tyr15.* EMBO J, 1992. **11**(11): p. 3995-4005.
152. Toyoshima, H. and T. Hunter, *p27, a novel inhibitor of G1 cyclin-Cdk protein kinase activity, is related to p21.* Cell, 1994. **78**(1): p. 67-74.
153. Polyak, K., et al., *p27Kip1, a cyclin-Cdk inhibitor, links transforming growth factor-beta and contact inhibition to cell cycle arrest.* Genes Dev, 1994. **8**(1): p. 9-22.
154. Polyak, K., et al., *Cloning of p27Kip1, a cyclin-dependent kinase inhibitor and a potential mediator of extracellular antimitogenic signals.* Cell, 1994. **78**(1): p. 59-66.
155. Grimmler, M., et al., *Cdk-inhibitory activity and stability of p27Kip1 are directly regulated by oncogenic tyrosine kinases.* Cell, 2007. **128**(2): p. 269-80.
156. Ishida, N., et al., *Phosphorylation at serine 10, a major phosphorylation site of p27(Kip1), increases its protein stability.* J Biol Chem, 2000. **275**(33): p. 25146-54.
157. Veillette, A., *Immune regulation by SLAM family receptors and SAP-related adaptors.* Nat Rev Immunol, 2006. **6**(1): p. 56-66.
158. Li, W., et al., *The SLAM-associated protein signaling pathway is required for development of CD4+ T cells selected by homotypic thymocyte interaction.* Immunity, 2007. **27**(5): p. 763-74.
159. Griewank, K., et al., *Homotypic interactions mediated by Slamf1 and Slamf6 receptors control NKT cell lineage development.* Immunity, 2007. **27**(5): p. 751-62.
160. Veillette, A., Z. Dong, and S. Latour, *Consequence of the SLAM-SAP signaling pathway in innate-like and conventional lymphocytes.* Immunity, 2007. **27**(5): p. 698-710.
161. Latour S, V.A., *Molecular and immunological basis of X-linked lymphoproliferative disease.* Immunological Reviews, 2003. **192**(1): p. 212-224.
162. McGargill, M.A., et al., *Active Ca2+/Calmodulin-Dependent Protein Kinase II{gamma}B Impairs Positive Selection of T Cells by Modulating TCR Signaling.* J Immunol, 2005. **175**(2): p. 656-664.
163. Orrenius, S., B. Zhivotovsky, and P. Nicotera, *Regulation of cell death: the calcium-apoptosis link.* Nat Rev Mol Cell Biol, 2003. **4**(7): p. 552-65.

164. Bernardi, P., *Mitochondrial Transport of Cations: Channels, Exchangers, and Permeability Transition.* Physiol. Rev., 1999. **79**(4): p. 1127-1155.
165. Nutt, L.K., et al., *Bax and Bak promote apoptosis by modulating endoplasmic reticular and mitochondrial Ca2+ stores.* J Biol Chem, 2002. **277**(11): p. 9219-25.
166. Scorrano, L., et al., *BAX and BAK Regulation of Endoplasmic Reticulum Ca2+: A Control Point for Apoptosis.* Science, 2003. **300**(5616): p. 135-139.
167. Rathmell, J.C., et al., *Deficiency in Bak and Bax perturbs thymic selection and lymphoid homeostasis.* Nat Immunol, 2002. **3**(10): p. 932-9.
168. Morgan, D.O., *CYCLIN-DEPENDENT KINASES: Engines, Clocks, and Microprocessors.* Annual Review of Cell and Developmental Biology, 1997. **13**(1): p. 261-291.
169. Williams, O., et al., *Activation of Cdk2 is a requirement for antigen-mediated thymic negative selection.* Eur J Immunol, 2000. **30**(2): p. 709-13.
170. Hakem, A., et al., *The cyclin-dependent kinase Cdk2 regulates thymocyte apoptosis.* J Exp Med, 1999. **189**(6): p. 957-68.
171. Liu, K., et al., *Sle3 and Sle5 can independently couple with Sle1 to mediate severe lupus nephritis.* Genes Immun, 2007.
172. Deane, J.A., et al., *Control of Toll-like Receptor 7 Expression Is Essential to Restrict Autoimmunity and Dendritic Cell Proliferation.* Immunity. **In Press, Corrected Proof**.
173. Song, A., et al., *RFLAT-1: A New Zinc Finger Transcription Factor that Activates RANTES Gene Expression in T Lymphocytes.* Immunity, 1999. **10**(1): p. 93-103.
174. Cathleen J. Ciesielski, E.A.Brian M.J.F.M.F., *TNF&agr;-induced macrophage chemokine secretion is more dependent on NF-&kgr;B expression than lipopolysaccharides-induced macrophage chemokine secretion.* European Journal Of Immunology, 2002. **32**(7): p. 2037-2045.
175. Tachibana, K., et al., *The chemokine receptor CXCR4 is essential for vascularization of the gastrointestinal tract.* Nature, 1998. **393**(6685): p. 591-594.
176. Zou, Y.-R., et al., *Function of the chemokine receptor CXCR4 in haematopoiesis and in cerebellar development.* Nature, 1998. **393**(6685): p. 595-599.
177. Allen, C.D.C., et al., *Germinal center dark and light zone organization is mediated by CXCR4 and CXCR5.* Nat Immunol, 2004. **5**(9): p. 943-952.
178. Sugiyama, T., et al., *Maintenance of the Hematopoietic Stem Cell Pool by CXCL12-CXCR4 Chemokine Signaling in Bone Marrow Stromal Cell Niches.* Immunity, 2006. **25**(6): p. 977-988.
179. Nagasawa, T., et al., *Defects of B-cell lymphopoiesis and bone-marrow myelopoiesis in mice lacking the CXC chemokine PBSF/SDF-1.* Nature, 1996. **382**(6592): p. 635-638.
180. Scarlatti, G., et al., *In vivo evolution of HIV-1 co-receptor usage and sensitivity to chemokine-mediated suppression.* Nat Med, 1997. **3**(11): p. 1259-1265.
181. Connor, R.I., et al., *Change in Coreceptor Use Correlates with Disease Progression in HIV-1-Infected Individuals.* J. Exp. Med., 1997. **185**(4): p. 621-628.
182. Muller, A., et al., *Involvement of chemokine receptors in breast cancer metastasis.* Nature, 2001. **410**(6824): p. 50-56.

183. Hernandez, P.A., et al., *Mutations in the chemokine receptor gene CXCR4 are associated with WHIM syndrome, a combined immunodeficiency disease.* Nat Genet, 2003. **34**(1): p. 70-74.
184. Tashiro, K., et al., *Signal sequence trap: a cloning strategy for secreted proteins and type I membrane proteins.* Science, 1993. **261**(5121): p. 600-603.
185. Togel, F., et al., *Renal SDF-1 signals mobilization and homing of CXCR4-positive cells to the kidney after ischemic injury.* Kidney Int, 2005. **67**(5): p. 1772-1784.
186. Ueda, Y., M. Kondo, and G. Kelsoe, *Inflammation and the reciprocal production of granulocytes and lymphocytes in bone marrow.* J. Exp. Med., 2005. **201**(11): p. 1771-1780.
187. Nie, Y., et al., *The Role of CXCR4 in Maintaining Peripheral B Cell Compartments and Humoral Immunity.* J. Exp. Med., 2004. **200**(9): p. 1145-1156.
188. Ding, M., et al., *Loss of the tumor suppressor Vhlh leads to upregulation of Cxcr4 and rapidly progressive glomerulonephritis in mice.* Nat Med, 2006. **12**(9): p. 1081-1087.
189. Hauser, A.E., et al., *Chemotactic Responsiveness Toward Ligands for CXCR3 and CXCR4 Is Regulated on Plasma Blasts During the Time Course of a Memory Immune Response.* J Immunol, 2002. **169**(3): p. 1277-1282.
190. Moser, K., et al., *Long-lived plasma cells in immunity and immunopathology.* Immunology Letters, 2006. **103**(2): p. 83-85.
191. Muehlinghaus, G., et al., *Regulation of CXCR3 and CXCR4 expression during terminal differentiation of memory B cells into plasma cells.* Blood, 2005. **105**(10): p. 3965-3971.
192. Balabanian, K., et al., *Role of the Chemokine Stromal Cell-Derived Factor 1 in Autoantibody Production and Nephritis in Murine Lupus.* J Immunol, 2003. **170**(6): p. 3392-3400.
193. Abraham, M., et al., *Enhanced Unique Pattern of Hematopoietic Cell Mobilization Induced by the CXCR4 Antagonist 4F-benzoyl-TN14003.* Stem Cells, 2007: p. 2007-0161.
194. Takenaga, M., et al., *A single treatment with microcapsules containing a CXCR4 antagonist suppresses pulmonary metastasis of murine melanoma.* Biochemical and Biophysical Research Communications, 2004. **320**(1): p. 226-232.
195. Schols, D., et al., *Inhibition of T-tropic HIV Strains by Selective Antagonization of the Chemokine Receptor CXCR4.* J. Exp. Med., 1997. **186**(8): p. 1383-1388.
196. Arakaki, R., et al., *T134, a Small-Molecule CXCR4 Inhibitor, Has No Cross-Drug Resistance with AMD3100, a CXCR4 Antagonist with a Different Structure.* J. Virol., 1999. **73**(2): p. 1719-1723.
197. Kim, S., Midura, BV., Mendoza, A., *In vitro and in vivo effects of CXCR4 inhibition in osteosarcoma.* Proceedings of the American Association of Cancer Research, 2006. **Abstract 285**.
198. Wong, D., Merzouk A., Salari H., *A peptide antagonist of chemokine receptor CXCR4 reduces tumor metastasis in a murine orthotopic model of human prostate cancer.* Proceedings of the American Association of Cancer Research, 2006. **Abstract 2162**.
199. Barton, G.M. and A.Y. Rudensky, *Requirement for Diverse, Low-Abundance Peptides in Positive Selection of T Cells.* Science, 1999. **283**(5398): p. 67-70.